Modelling of Multiphasic Behavior of Biodiesel Transesterification Operating Below Critical Conditions Using CO2 as a Co-solvent with PC-SAFT EoS

by

Gianfranco Rodriguez

Chemical Engineering, Universidad Simon Bolivar, 2012

Submitted to the Graduate Faculty of

Swanson School of Engineering in partial fulfillment

of the requirements for the degree of

Doctor of Philosophy

University of Pittsburgh

2019

UNIVERSITY OF PITTSBURGH

SWANSON SCHOOL OF ENGINEERING

This dissertation was presented

by

Gianfranco Rodriguez

It was defended on

September 6, 2019

and Approved by

Robert Enick, PhD., Assistant Chair of Research Professor, Department of Chemical & Petroleum Engineering

Vikas Khanna, PhD., Associate Professor, Department of Civil and Environmental Engineering

James McKone, PhD., Assistant Professor, Department of Chemical & Petroleum Engineering

Dissertation Director: Eric Beckman, Ph.D., Distinguished Service Professor, Co-Director of the Mascaro Center for Sustainable Innovation, Department of Chemical & Petroleum Engineering

Modelling of Multiphasic Behavior of Biodiesel Transesterification Operating Below Critical Conditions Using CO2 as a Co-solvent with PC-SAFT EoS

Gianfranco Rodriguez, PhD

University of Pittsburgh, 2019

Two major obstacles to effective transesterification of triglycerides to form biodiesel are the initial immiscibility of the reactants and the depletion of the short chain alcohol used throughout the reaction progress due to formation of the glycerol phase. Traditionally, to deal with such problems, high temperatures and pressures are employed to enhance the kinetics of the reaction. Co-solvents can also be introduced as means to promote mixing and lower the energetic requirements of the process. Amongst the multiple proposed co-solvents in the literature carbon dioxide is the one with the highest vapor pressure of all, which provides multiple benefits in the downstream separation process of the biodiesel products and excess reactants. Biodiesel yield's dependence on pressure, temperature (P-T) and methanol to oil molar ratio has been extensively explored but these variables do not only influence the process kinetics but also greatly affect the phase equilibria.

Modelling results achieved accurate phase behavior representations for pure components, plus binary and ternary mixtures that include carbon dioxide by using a polar version of PC-SAFT. Group contribution methods were employed to predict pure component parameters for a range of fatty acid methyl- and ethyl-esters, simplifying the modelling while minimizing the number of parameters. Small errors were obtained using very low values of binary interaction coefficients (below 0.12) for the binary mixtures. In this work the presence of an optimal content of CO_2 for each set of PT conditions is demonstrated for a system containing CO_2, methanol and triglycerides

(transesterification reactants) and a full map depicting optimal conditions for every set of pressure and temperature conditions is provided. That approach has also been extended looking into the quaternary system of CO_2, methanol, glycerol and biodiesel. Optimal values of carbon dioxide content in terms of enhancing the solubility of the phases are hereby investigated. Variation of the phase separation in a range of pressures (10-40 MPa) temperatures (40-200 °C) and different methanol to glycerol ratios (2-30:1) and the influence on the optimal conditions are reported using a polar version of PC-SAFT that can easily be extended to multiple substances and process conditions.

Table of Contents

List of Tables

List of Figures

Preface

I will like to offer this work to Our Lady of the Miraculous Medal for constant intercession throughout so many years of challenges.

I will like to say a word of thank you for:

My friends Megan, Jenna, Flo and Mike for making Pittsburgh home (and also being my wedding party)

My parents for constant support,

My siblings for non-ending laughter

My wife and children for been the source of love and motivation

And my advisor Dr. Eric Beckman who supported me through my research and taught me about this topic and many others. All, while taking care of my parents, taking care of my siblings, getting married with my wife and having my children. Thank you

I will also like to express my gratitude for support via the Heinz graduate student fellowship at the University of Pittsburgh and the National Science Foundation for the support provided through award number 1437595.

1.0 Introduction

Depletion of natural oil, coal and natural gas reserves and the search for fuels with reduced environmental impact has driven interest in biodiesel production. Biofuels and the process involved in their production have proven to lower greenhouse gas emissions up to 41% when compared to standard fossil fuels [1], and to use up to 76% less fossil energy than traditional diesel fuel [2]. Biodiesel is a renewable fuel, is biodegradable, performs similarly in engines as compared to traditional fuel, and improves air quality by reducing emissions of carbon monoxide and sulfur oxides (SO_x) [3]–[6].

The production of biodiesel uses up to 76% less fossil energy than traditional diesel fuel.[2] Biodiesel production and consumption in the US has risen steadily over the last 20 years, and since 2006 the market has experienced a ten-fold increase in consumption.[7] Life cycle assessments show that the energy required to grow the triglyceride feedstock is the most significant portion of the energy input for biodiesel. However, the processing stage (extraction and conversion), does consume approximately one fourth of the total required energy, opening a window for improvement of the energy demand of the process [1]. Over several years, both industry and academia have produced improvements to the biodiesel process that seek to lower the cost of feedstock growth or that try to identify optimal reaction conditions that would reduce such energy requirements [8], [9]

The preferred method for biodiesel production is transesterification of triglycerides with methanol or ethanol. The reaction proceeds with two intermediaries: diglycerides and monoglycerides, and usually involves high temperature, pressure, and alcohol-to-oil ratio to promote the miscibility of the reactants, as well as high-intensity mixing to enhance transport

between the immiscible phases [10]–[12]. **Figure 1** shows the reaction scheme for transesterification of trilaurin with methanol.[13]–[19]

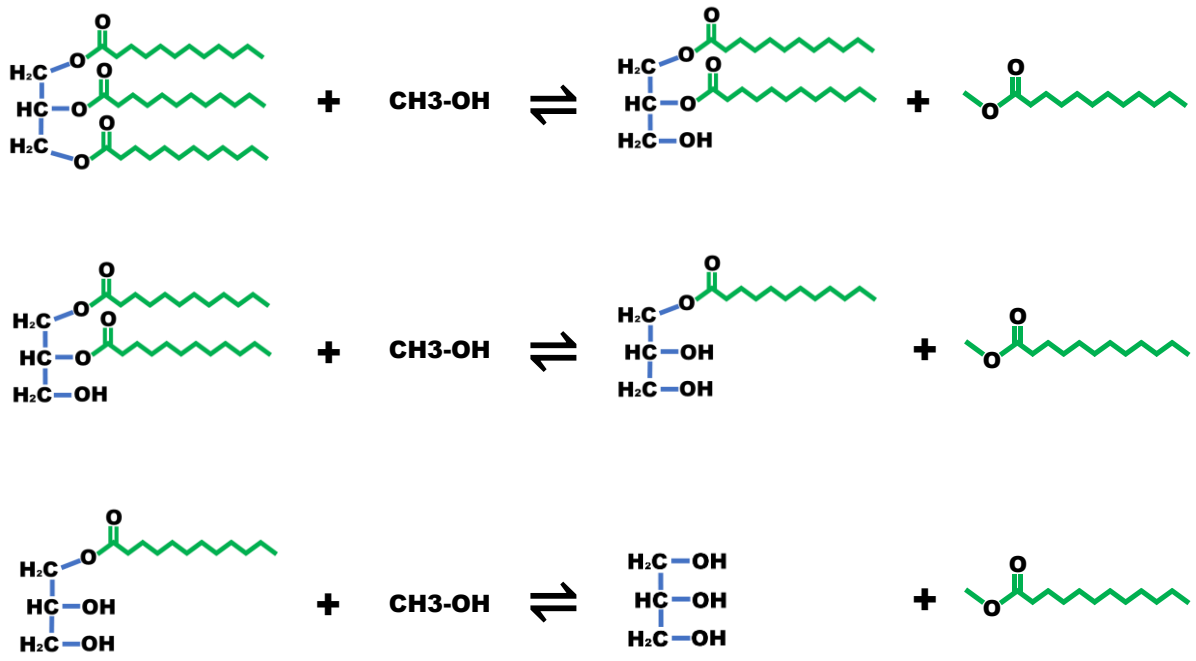

Figure 1 Reaction diagram for biodiesel production through triglycerides transesterification.

This reaction can be performed with or without a catalyst. The catalyzed transesterification process includes both acidic and basic homogeneous catalysts and is currently the preferred commercial route to biodiesel [3]. However, the presence of water and free fatty acid impurities contained in the feedstock used in commercial processes, and extra cost associated with the separation of the biodiesel from the byproduct glycerol detract from the overall efficiency [3], [20]. The transesterification process has also been performed uncatalyzed at supercritical conditions, namely temperatures of 250 - 400 °C, pressures of 19- 24 MPa, and with methanol/ethanol to oil molar ratios of 40:1 -- these conditions are employed to guarantee the

formation of a single phase in the reactor at the onset of the reaction. This process presents challenges due to high energy requirements and downstream separation of products from excess reactants and byproducts [13]–[17], [21]. Heterogeneous catalysts have also been investigated; the viable reaction rates and ease of separation of catalyst from product promote favorable economics [22]. The catalysts employed vary in nature from alkaline earth, titanium silicates, anion exchange resins to polymers [18], [23]–[26].

1.1 Phase Equilibria in Biodiesel Production

Csernica et al. showed that the phase behavior plays a critical role in the rate of production of biodiesel. Not surprisingly, they noted that the reaction proceeds slowly when the concentration of triglycerides (TG) in the reactive phase is low and increases dramatically when this concentration increases [27]. Other authors have reported measurements that suggest that observed slow reaction rates are due to the poor mutual miscibility of the reactants and consequently focused on exploring the importance of agitation (and naturally its impact on mass transport between phases) in biodiesel production processes. These researchers proposed different numerical models to predict reaction outcomes, such as correlation of kinetic constants to the Reynolds number of the system [28], correlating total conversion of fatty-acid alkyl esters to droplet size during agitation [29], incorporating an interfacial mass transfer term in the kinetic model [30], [31], relating conversion to impeller speeds[32], or by considering the influence of the area of the interfacial boundary to account for mass transfer limitations [33].

Other research teams created improvements to the traditional biodiesel process by attempting to improve the poor mutual miscibility of the alcohols and triglycerides in the initial

mixture. For example, one can choose the initial reactants to be more mutually miscible using either longer chain alcohols such as butanol[34], [35] or shorter chain triglycerides[36] that are entropically favored to blend more easily with methanol or ethanol. Transesterification performed at high pressures (19 - 45 MPa) and temperatures (250 - 400 °C) allows biodiesel production without the need of a catalyst and in shorter times than any other method; not surprisingly, this process starts with a homogeneous mixture of the reactants [13]–[16], [19], [21], [37].

A common way to reduce the energy input in the processing of triglycerides is by the use of co-solvents during the reaction[19] to promote mixing of the reactants. Co-solvents enhance the miscibility of the heavy oils with the alcohol-rich phase and hence mitigate the severity of the thermodynamic conditions necessary to drive the reaction to completion.[38] A wide variety of co-solvents have been explored, including tetrahydrofuran, hexane, propane, dimethyl-ether, diethyl-ether, chlorobenzene, acetone, and carbon dioxide [12], [19], [35], [38]–[40]. Kuramochi et al. [41], for example, have achieved high yield of fatty acid methyl ester (FAME, the major component of biodiesel) at short reaction times using dimethyl-ether as a co-solvent to promote the mixing of methanol and triolein. Patil et al. [38]compared supercritical biodiesel production from camelina sativa oil with hexane to form a single phase versus a subcritical process using KOH and showed similar results in terms of yield in comparable times. This suggests that the improvement obtained through use of supercritical conditions is strongly connected to a thermodynamic effect (enhancing miscibility) rather than through enhancing the reaction kinetics alone. The influence of the concentration of different co-solvents was explored by Alhassan and colleagues; they obtained optimal conversions at particular co-solvent concentrations suggesting that there are thermodynamically optimal conditions when using co-solvents [40].

Carbon dioxide has been suggested as a potentially useful co-solvent for biodiesel transesterification at supercritical conditions because CO_2 is naturally abundant, it has been widely used in vegetable oil extraction, it has rather mild critical parameters (31.1 °C and 7.39 MPa), and it enhances the miscibility between alcohols and triglycerides significantly [42], [43]. Using carbon dioxide as a co-solvent, Soh et al. [44] showed that triglyceride transesterification does not need to be conducted at supercritical conditions to achieve high rate of reaction, and can be coupled with heterogeneous catalysis. The addition of CO_2 increased the concentration of triglycerides in the alcohol-rich phase, which consequently enhanced the rate of the transesterification reaction. Essentially complete conversion was obtained in moderate reaction times (< 2 hr.). Comparatively mild temperatures and pressures (95 °C, 9.5 MPa) were sufficient to achieve 98% methyl oleate yield in a tri-phasic catalyzed process. Given the apparent advantage to using CO_2 as a cosolvent during biodiesel generation, it would be useful to understand the phase behavior of the system throughout the reaction, in order to identify those conditions that provide the best reaction outcomes.

Phase equilibria also influences the later stages of the transesterification reaction when most of the triglycerides have been consumed due to the formation of two distinct phases: the biodiesel-rich phase, and the glycerol-rich phase. Freedman et al. [45] proposed that the reaction rates have three distinct stages starting with a comparatively slow regime, then an acceleration, and finally another slow phase at higher conversions -- however they attributed these effects to the reverse reactions of the transesterification's chemical equilibria. Boocock et al.[34] investigated the positive effect of THF on increasing the miscibility of the initial reactants and noted as an unexpected effect that separation of the glycerol byproduct occurred faster than in the THF-free system. Maeda et al. [46] later explained these two effects by verifying that the reverse reactions

of the biodiesel transesterification could not be playing a relevant role in the process since the formation of products from transesterification reactants is negligible, even when using a catalyst at different temperatures and for an extended time period, and concluded the delay had to be attributed to the depletion of the methanol reactant by its migration into the newly formed glycerol phase. They also investigated the use of acetone as a co-solvent for the initial reactants but a poor solvent for glycerol and obtained comparatively faster FAME production than with other solvents. Glisic and Skala. [47] were able to observe and quantify the effect that a multiphase reactor has over the concentration of reactants and products and particularly the influence a glycerol-rich phase has over the methanol concentration in the triglyceride-rich phase. Research such as that performed by Yin et al. [48] suggests that addition of carbon dioxide results in beneficial reduction on necessary reaction conditions and increases on overall biodiesel yield similar to the effects observed by Boocok et al. but the effect of CO_2 in the transesterification process has not been fully explained. Thus, a better understanding of CO2 influence on the phase separation is required as a potential explanation for such improvements.

1.2 Literature Experimental Data on Phase Behavior of Biodiesel-relevant mixtures

The phase behavior of mixtures of CO_2 with biodiesel esters and triglycerides has been explored experimentally, confirming limited miscibility at supercritical conditions [49]–[53]. Binary vapor- liquid equilibria data of CO_2 + alkyl ester mixtures [54]–[58], CO_2 + alcohol mixtures [59], and for both CO_2 and alcohol + glycerol [60], [61] are available in the literature, providing a solid basis from which to develop a predictive model. So far, the focus of most of the literature has been high pressure and temperature conditions aiming to characterize the behavior

of the supercritical regime and consequently does not focus on moderate to low pressures and temperatures where ethanol or methanol are below their critical temperatures. The sources of relevant data for mixtures of FAMES with CO_2 are shown in **Table 1**.

Table 1 FAMES and FAEES with CO_2 binary Vapor-Liquid Equilibria literature.

Methyl esters-CO_2	Reference	Ethyl Ester/CO_2	Reference	Chain length: Unsat.
Methyl-Caproate	[-]	Ethyl-Caproate	Hwu et al. [58]	C6:0
Methyl-Caprylate	[-]	Ethyl-Caprylate	Hwu et al. [58]	C8:0
Methyl-Caprate	[-]	Ethyl-Caprate	Hwu et al. [58]	C10:0
Methyl-myristate	Inomata et al. [54] Lockeman [62]	Ethyl-myristate	[-]	C14:0
Methyl-palmitate	Inomata et al. [54] Lockeman [62]	Ethyl-palmitate	[-]	C16:0
Methyl-stearate	Inomata et al. [54]	Ethyl-stearate	Bharath et al. [57]	C18:0
Methyl-oleate	Inomata et al. [54] Chang et al. [56] Zou et al. [55]	Ethyl-oleate	Bharath et al. [57]	C18:1
Methyl-linoleate	Chang et al. [56] Zou et al. [55]	Ethyl-linoleate	Bharath et al. [57]	C18:2

Measurements of the phase equilibrium of triglycerides (TG) in mixtures that contain alcohols and/or alkyl esters are also needed to describe biodiesel production systems such as the one we evaluated in this work. Binary and ternary data are more abundant than pure component TG measurements for such systems. Various authors have explored the phase behavior of TG's with methanol [11], [27], [63], [64], alkanes [10], supercritical carbon dioxide [51]–[53], [65], [66] and sub-critical CO_2 [67]–[70]. Ternary systems comprising TG- CO_2-FAME [71], and TG - CO_2 - Alcohol [72] have also been explored experimentally. Experimental work showing interaction with carbon dioxide is particularly relevant for this work and highlighted in **Table 2.**

Table 2 Triglycerides with CO2 binary Vapor-Liquid Equilibria literature.

Triglyceride-CO_2	Avail lit.	Chain length: insaturations
Triolein	Bharath et al. [68] Fernandez-Ronco et al. [73] Weber et al. [74] Chen et al. [70]	C18:1
Tristearin	Weber et al. [74]	C18:0
Trilaurin	Bahrath et al. [68]	C12:0
Tripalmitin	Bahrath et al. [68] Weber et al. [74] Chrastill et al. [65] Munuklu et al. [75]	C16:0
tricaproin	Florusse et al. [67]	C6:0
tricaprilyn	Florusse et al. [67]	C8:0

Diglycerides (DG) and monoglycerides (MG) are intermediates of the conversion of TG's to the fatty acid esters that comprise biodiesel. These compounds are somewhat more hydrophilic than the original triglycerides given their hydroxyl groups, and hence may help to increase triglyceride content in the polar reactive phase. Thermophysical data for these compounds are scarce and are generally associated with results for multi-component systems that contain some mono- or di-glycerides [76]–[78], or measurements performed in supercritical carbon dioxide [51], [52].

1.3 Previous modelling efforts

Despite the system's apparent simplicity, the species present during transesterification of triglycerides with alcohols using CO_2 as co-solvent exhibit multiple types of molecular interactions, including hydrogen bonding and relevant polar forces, which complicate modeling efforts. Triglycerides have the potential to form weak hydrogen bonds through their carbonyl oxygens, and also exhibit dispersion forces. Carbon dioxide presents a strong quadrupolar moment and the possibility of forming weak hydrogen-bond cross-associations by acting as an electron donor with active hydrogen compounds.[79] Given this, plus the large number of components present during the creation of biodiesel from triglycerides and methanol in the presence of CO_2 (CO_2, methanol, triglycerides, fatty acid methyl esters, glycerol, di- and mono-glycerides), modeling of the phase behavior of this system is far from straightforward.

1.3.1 Modelling of alcohol, glycerol and FAAEs mixtures

Phase equilibria predictions of the behavior of ternary CO_2 + alcohol + glycerol mixtures, or quaternary mixtures of these + biodiesel esters have not been extensively explored. Initial attempts have been made with cubic equations of state, obtaining overall good results with respect to errors in phase behavior representation, but with very limited predictability, and little ability to be expanded to mixtures with similar components outside the ones that are used in each particular case [59], [61], [64], [80]. Ferreira et al. and Andreatta et al. have modelled alcohol-ester and alcohol-glycerol-ester systems using the Group Contribution Equation of State (GC-EoS) successfully, however due to the nature of this equation a wide range of binary interaction parameters are required each time a new component is added, since correlation is calculated group

by group [81], [82]. Cubic Plus Association (CPA) has been used by Oliveira et al. to model glycerol containing systems with excellent results. [83] Alcohols-esters and ternary systems including glycerol were modelled by this same group using two binary interaction coefficients that could be generalized to multiple components depending solely on the carbon chain length.[84]

Perturbed Chain Statistical Association Fluid Theory (PC-SAFT) [85], [86] has become a widely used engineering resource for modeling complex mixtures due to its ability to describe chain-like molecules, highly compressible mixtures, strong molecular associations, and more recently polar compounds [87]–[91]. Corazza et al. [92], and NguyenHuynh et al. [93], [94], used PC-SAFT to model biodiesel related phase equilibria, parametrizing pure methyl- and ethyl-esters at different conditions and obtaining promising results for methanol, ethanol, glycerol, and biodiesel binary and ternary systems – these researchers, however, did not examine the impact of a CO_2 co-solvent on the phase behavior of these biodiesel-related systems. PC-SAFT has been used previously to understand carbon dioxide interactions with short alcohols but never specifically employed to predict CO_2-methanol/ethanol-biodiesel ternary systems [95]–[97]. Similarly, methanol/ethanol-glycerol-biodiesel ternary system predictions can be found in the literature where polar and non-polar versions of PC-SAFT have been used, but descriptions of such systems where carbon dioxide is also present remain unexplored [92], [98].

1.3.2 Modelling the Behavior of Acylglycerols

Accurate modelling of the thermodynamic behavior of triglycerides depends upon parametrization via fits to experimental data; these are unfortunately relatively scarce due to extremely low triglyceride vapor pressures and experimentally unattainable critical properties. In particular, vapor pressure measurements for triglycerides are present in only a few papers [74],

[99], and models designed to predict thermophysical properties reduce to a small set of group contribution approaches as proposed by Ceriani and Meirelles [100], or a segmental approach as proposed by Zong et al. [101].

Modelling of binary mixtures that include triglycerides has also been explored previously. Bamberger et al. used a lattice equation of state to obtain good results and reasonable binary interaction coefficients (less than 13%) that correlate the solubility of different TG's in supercritical carbon dioxide [53]. Well known cubic equations of state show high accuracy predicting the behavior of *some* binary mixtures of triglycerides and CO_2 [11], [72], [74], [75], [102] although most require temperature dependent binary interaction coefficients. Similarly, the triglyceride-methanol system has been analyzed with cubic equations of state and non-idealities have been considered using UNIFAC and UNIQUAC activity coefficient models; these also require temperature dependent binary coefficients to produce accurate descriptions of the phase behavior [63], [103].

A number of researchers have employed the Group Contribution Equation of State (GC EoS) to model the phase behavior of mixtures that include TG's. Bottini et al. modelled triglyceride + alkane binary mixtures [104], Fornari et al. analyzed the solubility of tri-, di- and monoglycerides in supercritical carbon dioxide [105], Fernandez-Ronco et al. described CO_2-triglycerides vapor-liquid equilibria behavior [73], and Espinosa et al. modelled the mixture data of fatty oils with various near-critical and supercritical solvents [106]. Temperature dependent binary interaction coefficients were required in these systems in order to obtain a reasonable representation of the phase behavior.

Modelling of the behavior of DG's and MG's has previously been performed using traditional cubic equations of state [52], [107], however challenges arise for these EoS's when

considering multicomponent systems where both multiple associations and polar forces are present. Other thermodynamic models, such as UNIFAC, UNIQUAC and NRTL excess Gibb's models, as well as the GC EoS have been tested [105], [107]. These systems require fitting a large number of binary parameters, and little to no binary data was considered on isolated MG or DG systems during parameter optimization.

The Perturbed Chain Statistical Association Fluid Theory Equation of State (PC-SAFT EoS) [85] has been used successfully to model biodiesel related systems, mostly those containing mixtures of FAMES and/or FAEES with lower molecular weight components such as alcohols and carbon dioxide. PC-SAFT EoS has yet to be used to model triglyceride mixture behavior (with reactants and products of the biodiesel reaction), possibly because triglycerides do not entirely fit the description of a chain of Lennard-Jones spheres employed during the initial derivation of PC-SAFT. However, the model has been applied to systems such as highly branched alkanes, crosslinked compounds and aromatics with considerable success [108]–[111].

2.0 Objectives

Phase equilibria plays a significant role governing the transesterification outcomes in the biodiesel manufacturing process. Carbon dioxide appears to be a promising co-solvent to improve the overall energy demand and yield of the reaction process, but its effect in the phase separation of biodiesel reactants and products is still widely unexplored. Thermodynamic modelling of the phase separation can resolve important issues regarding component-phase-distribution and the effect of the cosolvents. Modelling the phase equilibria of this complex systems using a robust EoS that accounts for all the intra- and intermolecular forces like PC-SAFT has not been done before. Therefore, the following aims are proposed to deepen the comprehension of carbon dioxide potential benefits on the biodiesel transesterification process:

1. Fully characterize the phase behavior of biodiesel-related compounds (methanol/ethanol, glycerol and FAMES/FAEES) with carbon dioxide as a co-solvent using the PC-SAFT EoS, subsequently predicting supercritical and sub-critical phase behavior, ultimately generating binary and ternary diagrams that are relevant to the biodiesel formation process.
    a. Understand the multiple association configuration glycerol can assume and obtain the best pure component parameters using the PC-SAFT EoS.
    b. Derive binary interaction coefficients from extant binary data.
2. Collect experimental data regarding the phase behavior of monoglycerides in CO_2 to supplement the current relatively scant literature data set on these compounds.
    a. Obtain experimental validation of multiphasic systems with liquid phases expanded by carbon dioxide.

b. Collect valuable binary data of carbon dioxide with monoglycerides in vapor liquid equilibria.
c. Collect ternary data of carbon dioxide with methanol and monoglycerides in vapor liquid equilibria.

3. Provide a method to systematically model tri-, di- and monoglycerides in mixtures with other common biodiesel components where carbon dioxide is employed as a co-solvent.
   a. Obtaining reusable parameters for the intermediaries of the biodiesel reaction for pure and mixed phase behavior prediction, that will enlarge a basis of existing parameters for the PC-SAFT equation of state.
   b. Provide trends and correlations amongst the parameters of triglycerides and their corresponding diglycerides and monoglycerides to favor a predictable approach that can be used in more complex blends of triglycerides as raw material for biodiesel production.
4. Employ the PPC-SAFT model, with the derived binary parameters to predict the phase behavior of the biodiesel initial reactants represented by methanol and triolein using CO_2 as a co-solvent.
   a. Understand the influence that carbon dioxide to triglyceride ratios as well as methanol to triglyceride ratios in presence of CO_2 have in the reaction.
   b. Propose pressure and temperature (P-T) conditions that promote higher ratios of methanol to triglycerides in the oil-rich phase of the system, which would likely represent useful conditions to conduct the transesterification reaction.
5. Employ the PPC-SAFT EoS, to predict the phase behavior of the biodiesel products (represented by methanol, methyl oleate, and glycerol) using CO_2 as a co-solvent.

a. Understand the influence that carbon dioxide to FMA/FAEE ratios as have in the phase equilibria of biodiesel transesterification.

b. Explain the partition of methanol in a multiphasic biodiesel transesterification reactor using CO_2 as a co-solvent, as compared to a reactor without carbon dioxide.

c. Identify favorable thermodynamic (P-T conditions, CO_2 content, etc.) by minimizing the glycerol content and increasing methanol content in the reactive phase in order to obtain optimal reaction outcomes of biodiesel transesterification, based solely on the phase separation of the reactants and products.

3.0 Methods

3.1 Theory: The equation of State

Statistical Association Fluid Theory (SAFT) as proposed by Chapman et al.[112] has been designed to capture non-idealities and molecular interaction at different levels. Based on Wertheim's first-order perturbation theory [113]–[116], the Helmholtz free energy of a fluid is an expansion dependent on the Helmholtz free energy of a reference system perturbed by the residual free energy due to association. Each term is expressed as a nonlinear expansion dependent on the packing fraction and its derivatives as well as the reduced temperature, calculated using the Lennard-Jones Parameters for a mixture of LJ chains with spherical segments. Unlike the cubic equations of state, the phase behavior is not based on critical properties but rather on statistical mechanical quantities fitted to pure component behavior. As such:

$$A = A^{hc} + A^{disp} + A^{Assoc} + A^{Multipolar} \qquad 3\text{-}1$$

Where A refers to the Helmholtz free energy of the fluid and the superscripts make reference to Helmholtz free energy due to:

1) A^{hc}: hard chain reference fluid

2) A^{disp}: dispersion forces,

3) A^{Assoc}: association due to hydrogen bonding, and

4) $A^{Multipolar}$: polar and induced polar interactions

Gross and Sadowski [85] modified the original reference fluid to become hard-sphere chain molecules in the development of PC-SAFT:

$$A^{hc} = RT\left(\overline{m}A^{hs} + \sum_i x_i(1 - m_i) \cdot \ln\left(g_{ii}(d_{ii})^{hs}\right)\right) \quad 3\text{-}2$$

Where x_i is the molar composition, $\overline{m} = \sum_i x_i m_i$ the average segment size, g is the radial distribution function, itself a function of "d" which is the soft diameter of the spherical segment described by equation 3-3:

$$d_i = \sigma_i\left(1 - 0.12e^{-\frac{3\varepsilon_i}{kT}}\right) \quad 3\text{-}3$$

Where: σ_i and ε_i are the Lennar-Jones segment size and potential energy of the spheres.

The dispersion forces are based on the second order perturbation theory of Barker and Henderson [117].

$$A^{disp} = A_1(I_1) + A_2(I_2) \quad 3\text{-}4$$

Where I_1 and I_2 are the overlap integrals approximated by Gross and Sadowski by fitting coefficients to long-chain alkane experimental data, and written as:

$$I_1(\eta, \overline{m}) = \sum_{i=0}^{6} a_i \eta^i \quad 3\text{-}5$$

$$I_2(\eta, \overline{m}) = \sum_{i=0}^{6} b_i \eta^i \quad 3\text{-}6$$

Where η is the packing fraction and a_i and b_i are the fitted coefficients dependent on the average segment number $\overline{m}$. For a detailed review of the perturbation expansion and fitted polynomials please refer to Appendix 1. At this point, 3 parameters entirely describe the model's description of thermodynamic behavior of a molecule (segment number m, diameter σ_i and potential ε_i).

PC-SAFT's perturbation terms included Chapmans original SAFT association term based on a square well potential approximation to calculate the association strength [112]:

$$A^{assoc} = RT\left(\sum_{i} x_i\left[\frac{m_i}{2} + \sum_{A_i} \ln\left(X^{A_i}\right) - \frac{X^{A_i}}{2}\right]\right) \quad 3\text{-}7$$

Where X^{A_i} is the fraction of the of molecules not bonded to a given site *A* in one segment of the chain molecule, as shown in equation 3-8:

$$X^{A_i} = \left(1 + \sum_{j}\sum_{B} \rho_j \cdot X^{B_j} \cdot \Delta^{A_i B_j}\right)^{-1} \quad 3\text{-}8$$

Where ρ_j is the density of the fluid and $\Delta^{A_i B_j}$ is the association strength given by:

$$\Delta^{A_i B_j} = d_{ij}^3 g_{ij}\left(d_{ij}\right)^{seg} \kappa^{A_i B_j}\left(e^{\frac{\varepsilon^{A_i B_j}}{kT}} - 1\right) \quad 3\text{-}9$$

Two more pure components parameters are hereby introduced: κ^{AB} represents a volumetric overlap characterization of site "AB" and a given unique value of energy potential for bonding occurrence ε^{AB}.

Polar forces and induced dipole interactions can be approximated for localized polar forces in certain segments of the chainlike molecule. The inclusion of the polar term contemplates long range interaction of molecules with multiple dipolar or quadrupolar groups versus the short bonding effects that the association term is designed for following the square well potential approximation.

A multipolar term prevents overly increased values for the association energy parameter during pure component parametrization and provides smaller values for binary interaction coefficients [118]. Gross and Vrabec also suggested a polar term contribution using a broader set of data for fitting the values of the overlap integrals [90], [119], [120].

Twu et al. suggested a segment localized polar contribution term based on a Padé approximation of third order perturbation theory expressed as [87]–[89]:

$$A^{pol} = A_2 \left[\frac{1}{1 - \frac{A_3}{A_2}} \right] \qquad 3\text{-}10$$

Where A_2 and A_3 are sums of binary and ternary polar interaction contributions to the free energy respectively, with multiple terms accounting for actual and induced dipole and quadrupole moments. The full expansion equations for each contribution have been designed to deal with chain molecules instead of segments by incorporating a polar fraction of the chain x_{pi}^{μ} and x_{pi}^{Q} for molecules with dipolar and quadrupolar moment respectively, as used by Nguyen et al. [121] and are fully shown in **Appendix A**.

Therefore, up to seven parameters fully describe each substance: segment number (m), segment diameter (σ_i) , and molecule dispersive potential (ε_i) are required for all molecules. If the molecule is associative: volumetric overlap of molecules association sites (κ^{AB}) and energy potential for bonding sites (ε^{AB}) are also needed. If the molecule is polar or quadrupolar: the fraction of the molecule considered polar/quadrupolar (x_p) and the dipole or quadrupole moment (μ/Q) are included.

3.1.1 Group contribution

The central idea of the use for group contribution theory is to be able to estimate component parameters (described in the previous section) using fixed values for molecular sub-groups. For example, long chain alkane parameters can be estimated by combining parameters for (CH_3), (CH_2), (CH), etc. The equations for a homonuclear approach are given by Tamouza et al. [122] and Nguyen et al. [93] and shown below:

$$\sigma = \sum_{k=1}^{n_{groups}} \frac{n_k \sigma_k}{n_g} \quad 3\text{-}11$$

$$\varepsilon = \sqrt[n_G]{\prod_{k=1}^{n_{groups}} {\varepsilon_k}^{nk}} \quad 3\text{-}12$$

$$m = \sum_{k=1}^{n_{groups}} n_k R_k \quad 3\text{-}13$$

$$n_G = \sum_{k=1}^{n_{groups}} n_k \quad 3\text{-}14$$

Where n_k is the number of groups of type k in the molecule, R_k is group contribution to the number of segments, σ_k is the group contribution to the segment diameter, and ε_k is the group contribution to the dispersive energy. Polar moments for methyl and ethyl-esters have been calculated by NguyenHuynh et al. [96]:

$$\mu = \mu_0 - \mu_1 \left(1 - \frac{1}{n}\right) - \mu_1 \left(1 - \frac{1}{n'}\right) \quad 3\text{-}15$$

Where μ is the dipolar moment, μ_0, μ_1, μ_2 are fitted constants in Debyes [D] derived through examination of 35 esters, and *n* and *n'* are the number of carbons adjacent to the carbonyl carbon and the ester oxygen. The molecules considered here always contain one unique type of associating group (alcohols, esters or oxygen groups) thus, no extra equations are needed to find association parameters in this group contribution version of PC-SAFT, as each association site is inherently a segmental attribute rather than a value averaged from all "groups" of the molecule. Moreover, as stated above, group contribution is only applied to long chain alkyl esters since this approach does not correctly predict the behavior of small molecules like methanol or carbon dioxide [97].

3.2 Phase equilibria modelling

Traditional phase equilibria algorithms for the isothermal isobaric flash procedure as, proposed by Henley [123] to predict VLE and VLLE, have been successfully tested for similar systems using the PC-SAFT equation of state. This procedure provides robust convergence for multicomponent systems with simple liquid-vapor equilibria, however it is known to be a slowly convergent flash algorithm that can encounter problems near critical regions of an isotherm.[124] Alternatively, different authors have used Gibbs energy minimization methods in conjunction with PC-SAFT with excellent results in terms of convergence.[109], [125] The algorithm as described by Michelsen [124], [126], [127] is suitable for the system under consideration here. The algorithm is based on regular descent methods and accounts for the possibility of multiple unknown phases with more than two components and verifies the stability of the present phases.

3.3 Fitting methods

3.3.1 Parameter Fitting

The best value for each unknown pure component parameter is identified using experimental data available in the literature or data collected from physicochemical databases, and then minimizing the error in vapor pressure and saturated liquid density at different temperatures using equation **3-16:**

$$\%AAD = \frac{1}{N_{points}} \sum_{i} \frac{\left\| P_i^{exp} - P_i^{calc} \right\|}{P_i^{exp}} + \sum_{j} \frac{\left\| \rho_j^{exp} - \rho_j^{calc} \right\|}{\rho_j^{exp}} \qquad 3\text{-}16$$

Here P_i^{exp} and ρ_j^{exp} are experimental data points of saturated pressure and density respectively and P_i^{calc} and ρ_j^{calc} are the predicted properties from the model.

Similarly, each binary interaction coefficient has been fitted by minimizing error using equation **3-17**

$$\%AAD = \frac{1}{N_{points}} \sum_i \frac{\left\| \Omega_i^{exp} - \Omega_i^{calc} \right\|}{\Omega_i^{exp}} \qquad 3\text{-}17$$

Where: Ω_i^{exp} are the experimental data points of the thermodynamic property of interest and Ω_i^{calc} are the predicted properties from the model.

3.3.2 Optimal conditions search with a P-T flash algorithm

Optimization of the methanol to oil ratio in the triglyceride-rich phase (chapters **6.0 and 7.0)** was performed through brute force substitution methods by incrementing the carbon dioxide mole fraction by a small amount (1%) and then observing the consequential increase or decrease of the value of the ratio. The most significant challenge here derives from the stability of the multiphasic regime in the region being explored. At certain a priori unknown values of pressure, temperature and total molar fraction, the situation changes from liquid-liquid-vapor equilibrium (LLVE) to liquid-liquid equilibrium (LLE). Thus, for each tested set of conditions, phase equilibria modelling was performed sequentially, assuming the presence of three phases at first. If the third phase was proven unstable, the algorithm then performs calculations using a simpler 2-phase flash algorithm which in turn alternated between regular direct substitution and Gibbs minimization methods depending on whether the objective function convergence values were below the assigned tolerance.

When approaching the critical region of instability of the third phase, the probability of the algorithm yielding a false negative for the tri-phase regime (LLVE) increases. In this region several iterations are needed to achieve the assigned tolerance. The possibility of a false positive LLVE equilibrium can also occur by assigning convergence values that are too large. To overcome these challenges, when the critical region was detected step increases of P-T conditions were chosen such that the system will be on either side of the transition to avoid stalling and excessive iteration.

3.4 Experimental Section

3.4.1 Materials

CO_2 was obtained from Matheson (99.9 % bone dry), and methanol (HPLC grade 99.9%) purchased from Sigma Aldrich; each was used without further purification. Food grade monoglycerides with >95% purity as reported by TheScienceKit Store for monostearate and New Directions Australia for monocaprylate were also used as received.

3.4.2 Phase Behavior Measurements

Phase behavior data for mixtures were acquired using a high-pressure variable volume view cell (VVVC) manufactured by D.B. Robinson and Associates. The apparatus consists of a steel casing with aligned front and back sapphire windows that allows for visual inspection of the selected sample. The volume of the sample can be varied using a movable piston which is displaced using silicone oil as the overburden fluid. The internal pressure is monitored and controlled with

the use of two syringe pumps that are operated with a closed loop electronic controller system. One pump corresponds to the silicone oil fluid and a second one controls the CO_2 displaced into the cell. The system is encased in a constant temperature housing [128]. A schematic of the experimental setup is shown in **Figure 2**.

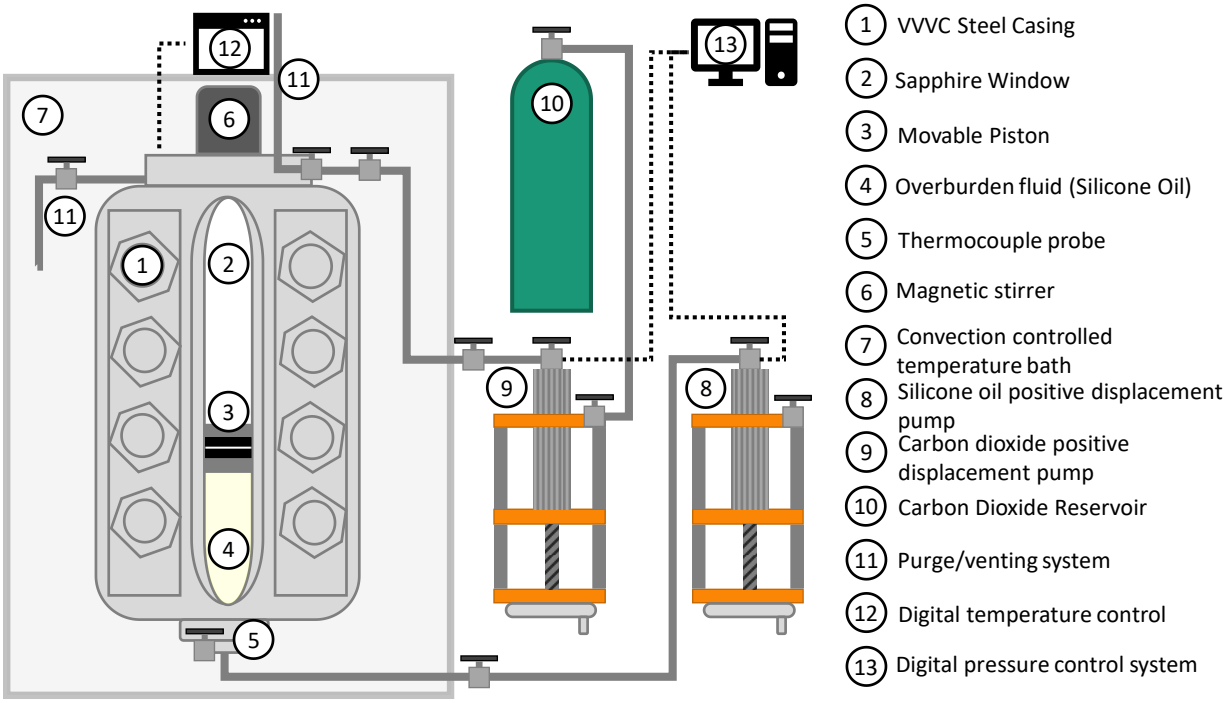

Figure 2. Variable volume view cell (VVVC) experimental setup schematic.

Liquid-vapor and liquid-liquid data were acquired by introducing known amounts of material into the sample cell. The desired temperature was set, and the pressure was increased until a single phase was formed. After allowing for mechanical equilibrium to be reached, the pressure was lowered by expanding the liquid at very slow volumetric rates varying from 20 to 50 cc/hr. When the incipient formation of either a vapor or a second liquid phase was noticed, the pumping

system was stopped, and the system was allowed once more to reach mechanical and chemical equilibrium between the phases. Similar procedures have previously been used and verified [129]–[131]; each data point was performed in duplicate. Errors for pressure measurements were calculated as standard deviation from the two-fold measurements and composition uncertainties were calculated through dispersion error formulas of instruments measuring uncertainty and measurements fluctuation following guidelines from Khu [132].

4.0 Results Part I: Modelling the phase behavior of biodiesel related systems with CO_2 using a polar version of PC-SAFT (published in *Fluid Phase Equilibria* (2019), 485, 32-43)

4.1 CO_2 – Methanol/Ethanol – FAAES pure component modelling

Carbon dioxide, methanol and ethanol pure component parameters were taken from NguyenHuynh et al. [97] and are shown in **Table 3**. CO_2 and methanol parameters were not constructed from segmental group contributions but were rather treated as unique molecules insofar as their parameters were concerned. As shown by Mourah et al. [133] a 2B scheme (one electron donor and one acceptor site) can be used to describe methanol self-association. Carbon dioxide is considered to have two donor sites but does not self-associate. Ethanol is represented with a 3B association scheme (two electron donor and one acceptor site) to accurately reproduce pure and binary data [97].

The apparent contradiction in the association schemes of methanol and ethanol is part of an ongoing literature discussion about lower alcohol parametrization with SAFT-like equations. The 3B model is known to be the most rigorous approach for the association scheme, as established by the work of Huang and Radosz [134], and corresponds to two donor sites present in the oxygen atom due to two lone pairs of electrons and one proton on the OH- group. At the same time, it could be argued that not many molecules will in practice associate with three other molecules. Different authors have concluded that both the 2B and 3B schemes are in fact suitable to correctly model alkanol pure and mixture phase behavior. Wolbach and Sandler suggested using quantum chemistry modelling to determine the association scheme of methanol and obtained inconclusive

results in terms of errors in pure component property prediction [135]. Yarrison and Chapman, as well as Tybjerg et al showed that the optimal association scheme for methanol depends on the range of thermodynamic properties used or the mixture that is being modeled [136], [137]. For PPC-SAFT specifically, Mourah et al. [133] explored all multiple-site association possibilities, and were not able to conclude which methanol association scheme is correct. Finally Nguyen et al. using GC-PPC-SAFT, developed a systematic procedure for alkanols in presence of carbon dioxide using a 3B model but accepted that the rules were not applicable to the first molecule of each series (i.e. in this case methanol) [97]. In this work we have chosen to follow this latter reference in the spirit of been able to assess carbon dioxide interaction with a wide range of biodiesel related systems.

Fatty acid methyl-ester and ethyl-ester pure component parameters were obtained using the values shown in **Table 3** and equations **3-11** to **3-15**. Polar moments were calculated using group contribution values and the esters were considered to have 1 cross-association site with short chain alcohols as developed by NguyenHuynh et al. [97] . Biodiesel parameters were calculated based on the composition of alkyl-esters in the system. Instead of adding multiple components to the mixture, biodiesel was treated as a unique pseudo-component. Parameters for the biodiesel component were calculated using group contribution equations **3-11** to **3-15** using the average number of carbons in the ester chain and the average number of methyl, methylene and methine groups in the chain.

Table 3 Parameters used for GC-PPCSAFT taken from Mourah et al.[133], Hemptinne et al. [138] and NguyenHuynh et al [96], [97].

Component	Assoc.	m	σ (Å)	ε/k (K)	κ^{AB}	ε^{AB}/k(K)	$x_p{}^{\mu}m$	$x_p{}^{Q}m$	μ (D)	Q (B)[e]
CO_2[a]	2 Sites	1.8465	2.9839	139.997	0.0947	449.71		0.5268		4.3
Methanol	2B	2.8271	2.6321	166.875	0.2373	2069.08	0.35		1.7	
Ethanol	3B	2.0050	3.4106	247.992	0.0088	2143.29	0.50		1.83	
-CH_3		0.7866	3.4872	189.962						
-CH_2-		0.3821	3.9307	261.087						
-CH=		0.1953	3.8614	287.400						
-CH<		0.200	4.9350	402.000						
-OH (1)[b]	3B	0.8318	2.8138	307.5094	0.0088	2143.29				
-OH (2)[b]	3B	0.3573	2.8138	307.5094	0.0044	2143.29				
COO (1) [a, b, c]	1 Site	0.8274	3.3448	362.820	0.0088	2143.29	1.15			
COO (2) [a, b, c]		0.8116								
COO (4) [a, b, d]		0.728								

[a] Compounds listed with a number of sites are not self-associating. Association parameters are for cross association only.

[b] Numbers in parenthesis indicate the position in the carbon chain

[b] Parameters change based on ester's group position in the carbon chain.

[c] μ_0=2.0177, μ_1=0.2216, μ_2=0.3425 to be used with equation **3-15**.

[d] Ester group was taken in the 4th position for triglycerides. The position is the most embedded in the carbon chain available and polar moment was assigned.

[e] Buckingham 1 B=10^{-10} D.

4.2 Glycerol Parameters

Glycerol presents a challenge to modelling efforts as it exhibits a molecular weight of only 92 g/mol, yet also exhibits vapor pressures that are extremely low owing to the strong self-associations resulting from its three hydroxyl groups. Glycerol pure component parameters were calculated in this work considering two different association schemes: (1) two donor and two acceptor sites (denoted as the 4C association scheme) and (2) three donor and three acceptor sites (3x2B). Barreau et al. [139] have proposed two different sets of glycerol parameters, employing the two association schemes mentioned above, but also using the polar fraction of the molecule $(x_p \cdot m)$ as a free fitting parameter. They obtained accurate fits of the model to the experimental data, but with a value for the polar fraction that appears unrealistically small (< 0.05). Instead, we considered two values for the polar fraction of the molecule; 0.35 and 0.5 (similar to values used for other polyols [62]); following NguyenHuynh et al.'s development for short chain alcohols, [97] the dipolar moment was set to the experimental value of 2.68 D. A non-polar version has also been fitted to compare these results with those found using the traditional version of PC-SAFT. Results of fitting the various scenarios to glycerol data are shown in **Table 4** – while comparably good results for pure vapor pressure and saturated density are obtained using all set of parameters, significant differences between the performance of the different parameter sets arose during modeling of the binary mixtures. Experimental data for vapor pressure were obtained from the DIPPR 2015 version [140] and saturation density was obtained from McDuffie et al. [141] using temperatures from 298.75 to 535 K

Table 4 Glycerol Pure component parameters and saturation prediction error (in %).

									Av. Errors	
Set	Scheme	m	σ (Å)	ε/k (K)	κ^{AB}	ε^{AB}/k (K)	$x_p \cdot m$	μ (D)	P^{sat}	ρ^{sat}
I[a]	4C[c]	4.597	2.891	294.380	0.1485	1481.38	0.0049	2.68	7.36	2.57
II[a]	3x2B[d]	6.203	2.577	261.340	0.6020	501.87	0.0430	2.68	3.98	1.09
III[b]	4C[c]	1.457	4.400	313.845	0.0121	2411.31	0.5000	2.68	4.36	1.04
IV[b]	3x2B[d]	2.829	3.405	265.278	0.0484	2672.05	0.5000	2.68	4.17	0.08
V[b]	4C[c]	2.833	3.405	291.885	0.0419	2587.89	0.3500	2.68	4.24	0.16
VI[b]	4C[c]	5.156	2.738	247.651	0.3018	1765.47	0	0	3.83	0.89

[a]Glycerol pure component parameters from Barreau et al. [139].
[b]Glycerol pure component parameters from present study.
[c]2 electron donor and 2 electron acceptor sites.
[d]2 electron donor and 2 electron acceptor sites.

4.3 Binary Systems

4.3.1 Methanol/Ethanol-Glycerol

Binary mixture data, including both high pressure data [142] and lower pressure data from [83], [143], of methanol and ethanol with glycerol were fit using the different glycerol parameter sets. All sets of parameters provided comparatively good results, as depicted in **Figure 3**. Increasing the polar fraction parameter ($x_p \cdot m$) from 0.35 to 0.5 shifts the value of the binary interaction coefficient from negative to positive for the methanol case – positive k_{ij}'s would be traditionally expected when using polar versions of PC-SAFT, as negative values would suggest a higher degree of association than would be predicted from the averages [93]. Similarly, for PC-

SAFT with no polar association negative binary interaction coefficients are needed for good data representation; this could be due to an overly increased dispersion interaction owing to lack of polar contribution. The parameters from Barreau et al. [139] generate the lowest errors for the ethanol-glycerol phase behavior, but comparable results can also be obtained using the more realistic higher polar molar fractions, as shown in **Table 5**.

Table 5 Binary interaction parameters and prediction errors (in %) for VLE of Methanol/Ethanol with glycerol binary system.

Binary system		Parameters	Error[a]		NPts
	Glycerol SET	k_{ij}	*P*	*T*	
Methanol-Glycerol	I	-0.0324	7.0	0.8	30
	II	-0.0372	9.8	0.9	
	III	0.0462	6.1	0.7	
	IV	0.0807	8.5	0.9	
	V	0.0439	4.6	0.8	
	VI[b]	-0.0406	8.9	0.9	
Ethanol-Glycerol	I	0.0003	16.2	1.4	36
	II	0.0137	11.0	1.8	
	III	0.0289	17.5	1.3	
	IV	0.0572	36.8	1.1	
	V	0.0274	18.4	1.4	
	VI[b]	-0.0142	20.8	1.5	

[a]Error prediction has been done with two distinct set of data: Pressure prediction at high temperatures from Shimoyama et al.[142] and temperature prediction at lower pressures from Oliveira et al.[83] and Veneral et al.[143]
[b]Parameters for Methanol and ethanol for the non-polar version of PC-SAFT are from Corazza et al. [144]

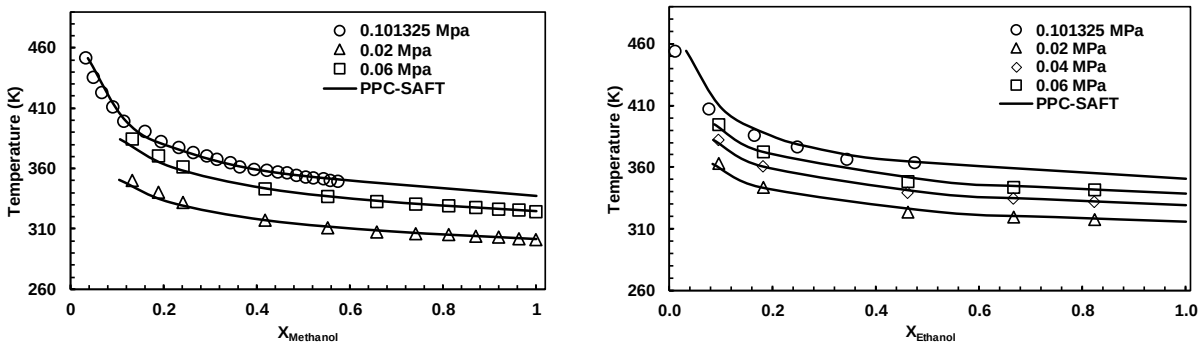

Figure 3 LVE of methanol-glycerol (kij=0.0439) left, and ethanol-glycerol (kij=0.0274) right, using glycerol set V of parameters. Experimental data is from Oliveira et al.[83] and Veneral et al.[143]

4.3.2 CO_2 and Glycerol

Not surprisingly, supercritical carbon dioxide is poorly soluble in glycerol over a wide range of temperatures and pressures. Experimental data for this system have been collected by Medina-Gonzalez et al. [61] and show a maximum solubility of 13% (molar) CO_2 in glycerol. Solubility is only weakly affected by pressure and decays rapidly with increasing temperature. The low values of the CO_2 mole fractions coupled with the very steep slope of the *P-x* diagrams poses a challenge to any thermodynamic model because small changes in calculated parameter values can lead to large errors. For the non-polar version of PC-SAFT CO_2 parameters were obtained from Zubeir et al.[145]

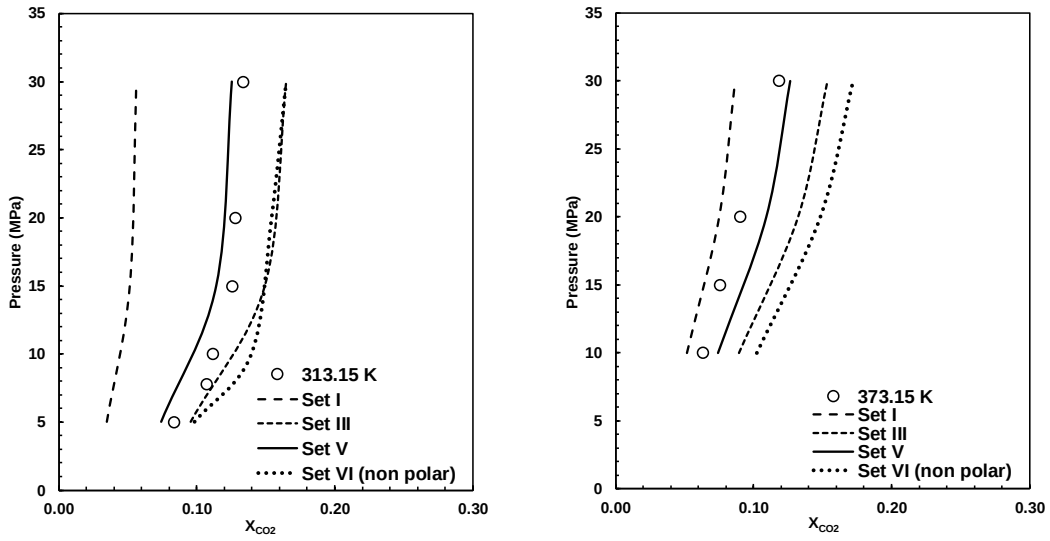

Figure 4 Comparison of Liquid solubility of CO_2 on glycerol with different polar and associative contributions. Set III and V with d_{ij}=1. Experimental data is from Nunes et al. [60].

The inclusion of the polar term allows us to account for quadrupolar-dipolar interactions between CO_2 and glycerol. Parameters obtained by Barreau et al. [139] consistently show lower solubility of CO_2 in glycerol than the experimental values while the parameters obtained in this work predict solubility for supercritical CO_2 in glycerol that is generally higher than the experimental data. Prediction using the non-polar version of PC-SAFT (Set VI in **Table 4**) has small deviations at low temperatures but at higher temperatures larger errors accrue than for any other polar version. This could be because polar effects have been merged into dispersive and associative forces that do not respond to the effect of temperature in the same way. As expected, all sets of parameters predict correctly the composition of the CO_2 rich phase which is almost pure (> 99.9 %) carbon dioxide. The best results for liquid-liquid equilibria (LLE) prediction were obtained using set V (see Table 3) of the glycerol parameters, with a polar fraction of 0.35, and by

setting the binary interaction coefficient d_{ij} in eq 5 to 1.0 for CO_2 and glycerol (see **Figure 4**). The overall average error is 47% in composition; this is primarily due large errors accrued at temperatures above 100 °C. Below this temperature, errors are in the neighborhood of 12% in composition, as shown in **Figure 5**.

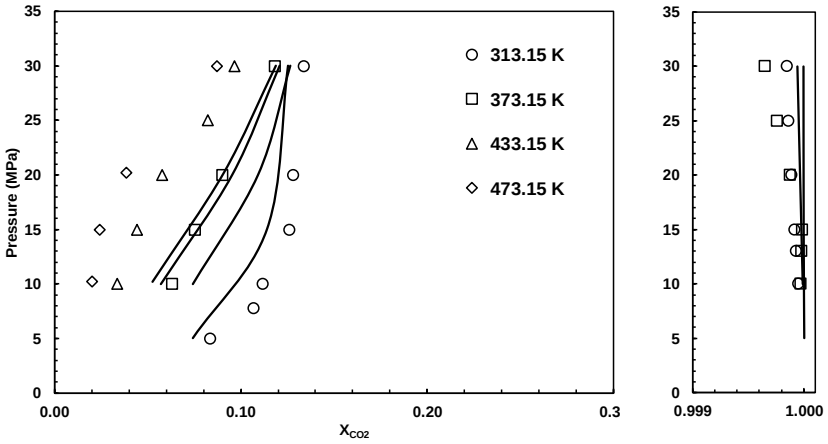

Figure 5 Liquid-Liquid Phase Behavior of CO_2 with Glycerol modelled with PC-SAFT k_{ij}=0 and d_{ij}=1. Experimental data is from Nunes et al. [60].

By setting d_{ij} to one, the association contribution for CO_2-glycerol to the Helmholtz free energy effectively becomes zero. Different authors have treated CO_2 solvation using different approaches and different configurations. Zubeir et al. have employed a varying value of potential association (ε^{AB}/k) depending on the solvent used [145]. Perakis et al. used a simplified version of SAFT and CPA and concluded that in specific cases the association with carbon dioxide might effectively be negligible, for some similar systems like CO_2/water, once accounting for other interactions [146]. For the particular case glycerol-CO_2 with PPC-SAFT, the interaction can be most closely modelled taking into account dipolar-quadrupolar interactions without a need of

fitting associating parameters. However as previously established, modelling at high temperatures cannot be fully reconciled even when applying a temperature dependence to the binary interaction coefficient (see **Appendix B**).

4.3.3 CO_2 with Fatty acid alkyl esters

High pressure phase behavior data (liquid-vapor equilibria) for mixtures of carbon dioxide plus eleven alkyl-esters of interest were modelled using GC-PPC-SAFT where results are shown in **Table 6**. At first, the data was fit allowing the binary interaction parameter, k_{ij}, to vary with each individual methyl ester: CO_2 combination and excellent predictions were obtained. In order to simplify the system, the data were refit using a single binary interaction coefficient for all of the alkyl ester L-V data. A value of k_{ij} = 0.0114 was found to be optimal for CO_2 alkyl ester phase behavior modelling, as shown in **Figure 6**. Pressure prediction error is 7.5% while the error in composition prediction is on average 3.9% through the different alkyl-esters. Employing a single k_{ij} to cover all of the alkyl esters increases the average error a small amount (1.7%) but greatly simplifies the modeling of the system.

Table 6 Individual and generalized binary interaction coefficients and prediction error (in %) in for LVE of CO_2 with alkyl esters binary systems.

Binary System	k_{ij}	Average errors		k_{ij}	Average errors		Data pts.	Ref
		Error P	Error X_{CO2}		Error P	Error X_{CO2}		
CO_2-Methyl Stearate	0.0184	9.7	3.9	0.0114	10.9	4.5	27	[54]
CO_2-Methyl Oleate	0.0146	6.6	3.3		8.9	3.3	38	[54]
CO_2-Methyl Linoleate	0.0085	8.4	3.3		9.0	3.8	26	[55], [56]
CO_2-Methyl Myristate	0.0145	3.7	2.4		4.9	2.7	24	[54]
CO_2-Methyl Palmitate	0.0154	8.3	4.2		10	4.5	38	[54]
CO_2-Ethyl Stearate	0.0158	9.7	4.7		12.4	5.4	27	[57]
CO_2-Ethyl Oleate	0.0137	6.5	3.4		11.3	3.7	38	[57]
CO_2-Ethyl Linoleate	0.0109	6.4	3.4		8.3	3.5	33	[57]
CO_2-Ethyl Caprate	0.0116	1.2	0.9		1.2	0.9	30	[58]
CO_2-Ethyl Caproate	0.0022	1.8	1.5		3.6	6.9	30	[58]
CO_2-Ethyl Caprylate	0.0022	1.4	1.2		2.3	4.5	31	[58]
Total	[-]	5.8	2.9		7.5	3.9	342	[-]

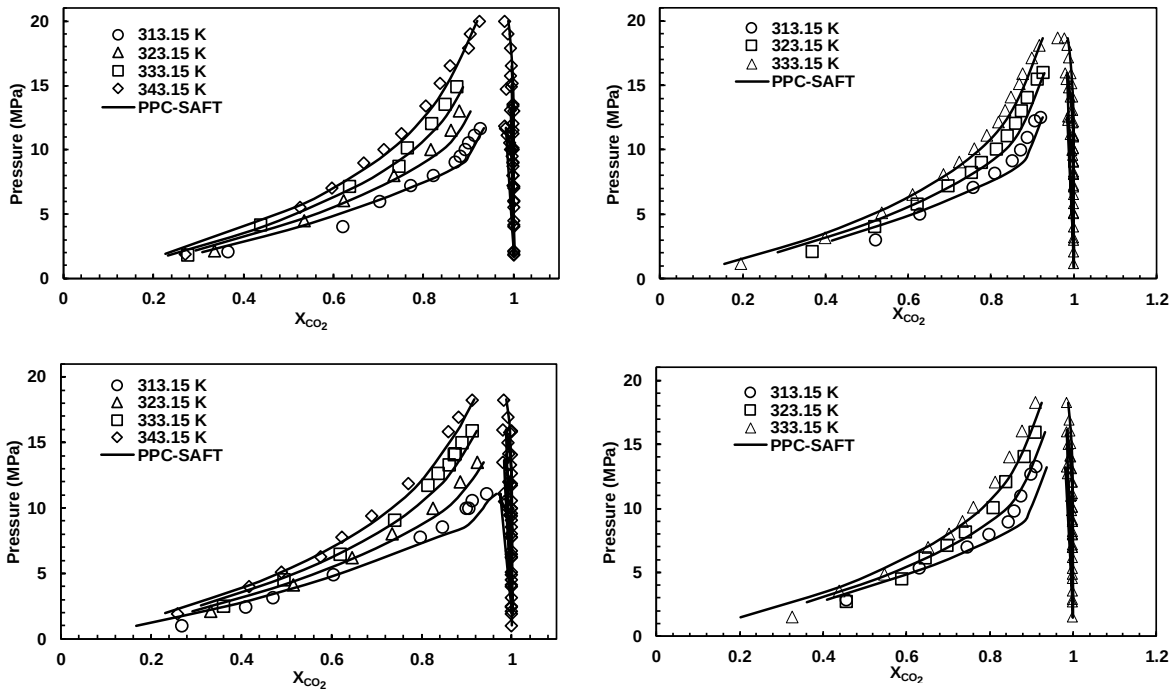

Figure 6 LVE of CO2 with A) methyl oleate B) methyl palmitate C) ethyl oleate D) ethyl stearate using a generalized binary interaction coefficient kij=0.0114.

Carbon dioxide + biodiesel binary LV vapor behavior has been ***predicted without needing any extra parameters*** by using the approach explained in section **3.2** and using the same binary interaction parameter calculated for all alkyl-esters presented in **Table 6**. Excellent agreement has been found between experimental data measured by Araujo [147] and Pinto et al. [130] on ethyl and methyl esters derived from soybean oil and depicted in **Figure 7** As expected LLV equilibria appears at 303.15 K near to carbon dioxide critical conditions, data and predictions are also shown in **Figure 7.**

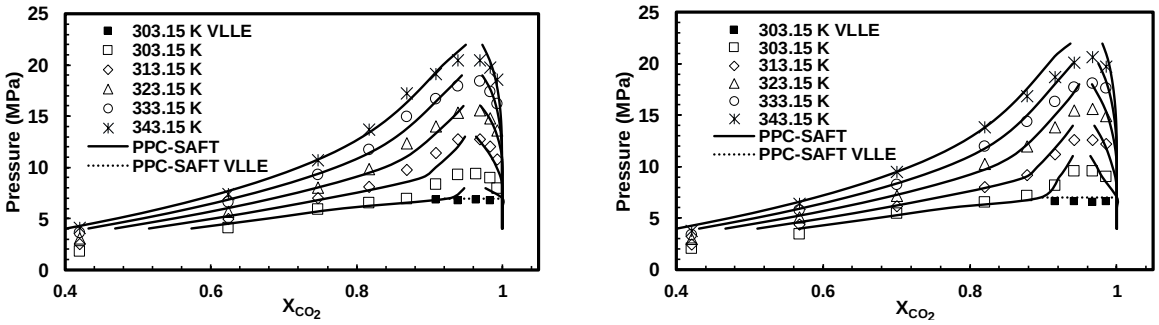

Figure 7 Liquid-Vapor equilibria of CO_2-FAME derived from Soybean Oil experimental data is from Pinto et al. [130] and CO_2-FAEE derived from Soybean Oil experimental data is from Araujo [147].

4.3.4 Methanol/ethanol and Fatty acids alkyl esters

Given the results obtained with the fitting of the carbon dioxide + methyl ester data, a generalized binary interaction parameter for alkyl-esters plus either methanol or ethanol were determined using LVE data of four different methyl esters with methanol and four ethyl esters with ethanol at a range of pressures and temperatures as shown in **Table 7**. Methanol does not follow the group contribution trends developed for alcohols, as it is the first compound of the series the interactions of the carbon chain cannot be really separated from the alcohol group. The association scheme, association strength and polar fraction all differ from the expected values obtained by group contribution [97].

Table 7 Binary interaction coefficients and modelling errors (in %) for LVE of short alcohols and alkyl esters binaries.

Binary System	Parameter	Average errors		Data pts.	Ref
	k_{ij}	Prediction Error	Error in X_{CO2}		
Methanol-Methyl laureate	0.0667	3.2	6.7	35	[84], [148]
Methanol-Methyl myristate	0.0667	2.3	7.4	31	[84], [148]
Methanol-Methyl oleate	0.0667	3.6	13.3	10	[84]
Ethanol-Ethyl laureate	0	5.7	4.0	22	[149]
Ethanol-Ethyl myristate	0	3.6	3.6	19	[149]
Ethanol-Ethyl palmitate	0	1.2	21.6	28	[150]
Ethanol-Ethyl stearate	0	1.8	20.2	22	[150]

Methanol requires a binary interaction coefficient of 0.0667 to represent the L-V phase behavior; similar but slightly lower values were obtained by Barreau et al. [139] in the modelling of methyl oleate with methanol. The relatively higher values of the binary interaction coefficient as opposed to other alcohol containing binaries (i.e. methanol-glycerol, ethanol-glycerol) ensure liquid-liquid phase separation near room temperature between methanol and FAME, as expected experimentally [64]. By contrast, the optimal binary coefficient for ethanol + FAEE mixtures is effectively zero, since the parameters for all of the involved compounds are consistent with the group contribution parameters developed by NguyenHuynh et al. [97] (see **Figure 8**).

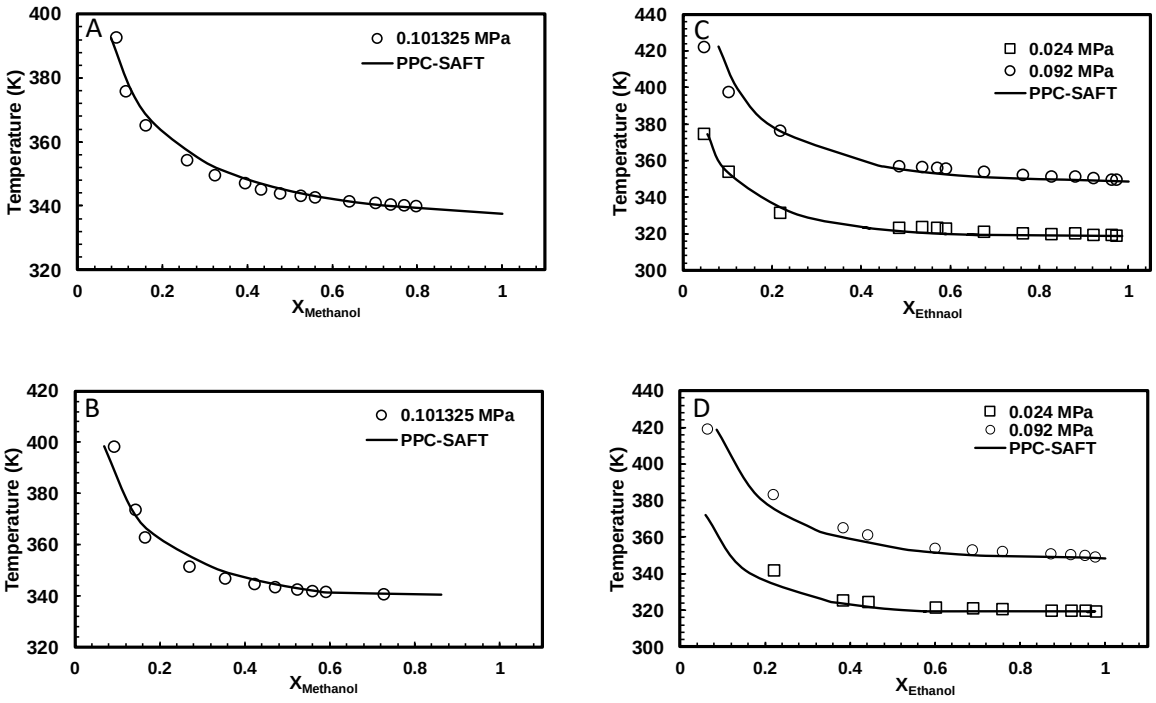

Figure 8 LVE of A) methanol methyl laureate B) methanol methyl myristate with kij=0.0667 C) ethanol ethyl palmitate D) ethanol ethyl stearate with kij=0.

4.3.5 Fatty acids alkyl esters and glycerol

Use of any of the parameter sets for glycerol (as shown in **Table 4**) reproduce the expected liquid-liquid phase behavior with alkyl-esters when binary interaction coefficients are calculated for the specific binary data. Using set V for glycerol allows the best phase behavior representation in a fully predictive approach with a binary interaction coefficient of k_{ij}=0 (see **Figure 9**). The balance of the modelling, the prediction of ternary system phase behavior, was therefore done using set V of the glycerol parameters. Finally, an overall optimization was done using set V of glycerol with all available methyl esters LLE data and an optimal value of k_{ij} = 0.022 was obtained.

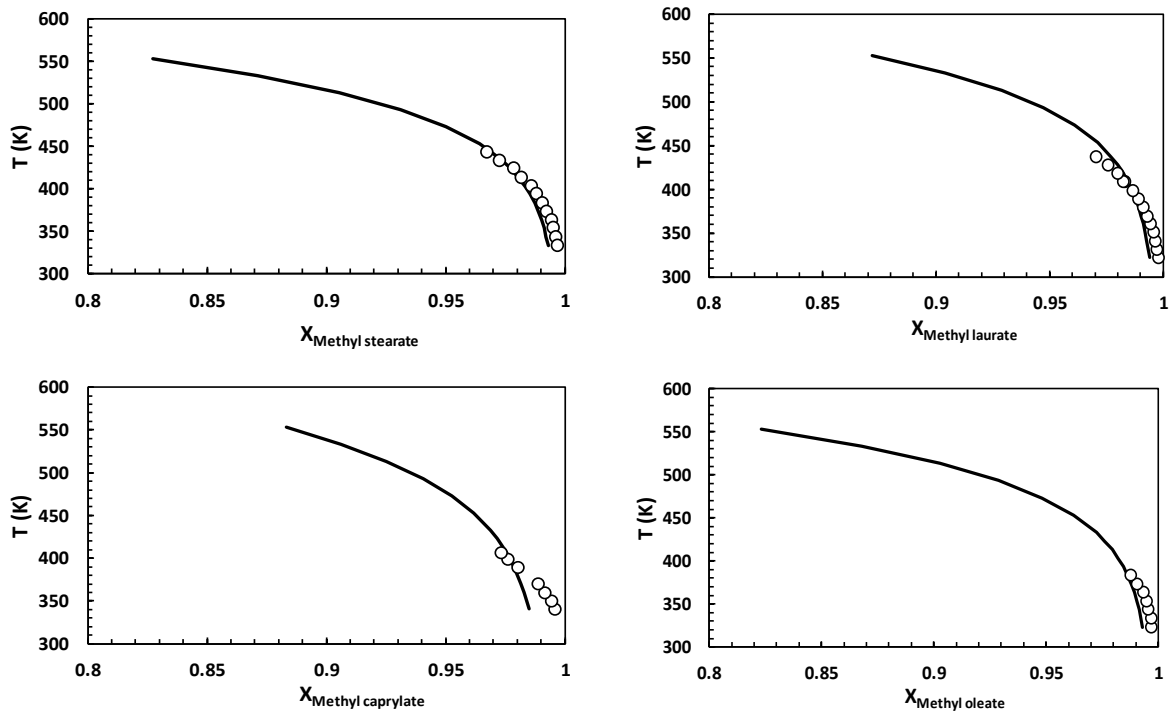

Figure 9 LLE of glycerol and methyl esters with kij=0. Experimental data are from Garrido et al. [151]**, Barreau et al.** [139]**, and Silva et al. [64].**

4.4 Ternary Systems

4.4.1 CO_2-methanol-glycerol.

Ternary systems were modelled to test the predictability of the PC-SAFT using set V of the glycerol parameters (see Table 2) and the ternary mixture CO_2 + glycerol + methanol. The available experimental data shows pressure-CO_2 concentration data with fixed molar ratios of methanol to glycerol, as measured by Pinto et al. [129]; three ratios of interest in biodiesel processing are shown, namely 1:12, 1:20 and 1:30 in **Figure 10**.

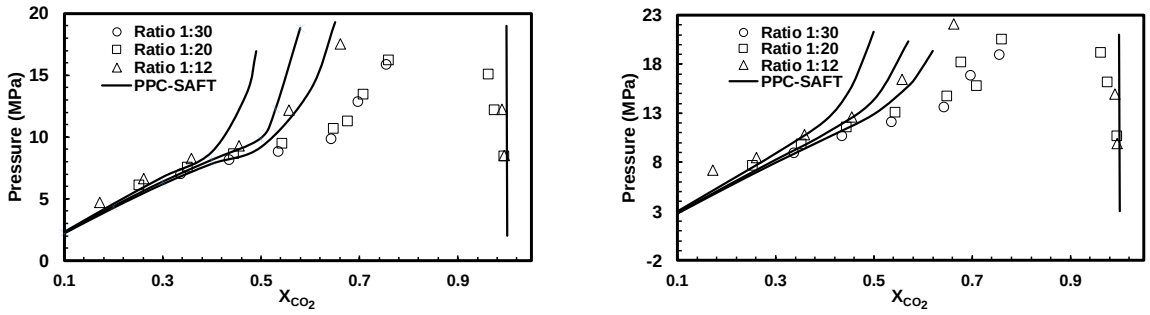

Figure 10 Ternary System CO2-methanol-glycerol, with methanol to glycerol fixed ratios 1:30, 1:20 and 1:12 for temperatures 323.15K (left) and 343.15K (right). Experimental data is from Pinto et al. [129].

At lower concentrations the phase diagram looks remarkably similar to the binary methanol-carbon dioxide LVE, however at higher concentrations glycerol immiscibility with supercritical carbon dioxide (as shown above) dramatically increases the bubble point pressure of the mixture. Modelling with PPC-SAFT was done using binary interaction coefficients calculated from the binary systems; results show excellent accuracy in the low CO_2 concentration region,

while at higher CO_2 concentrations the experimental behavior is only qualitatively represented. The steepness of the *P-x* curve at high CO_2 concentrations presents a challenge from a modelling perspective and is systematically underestimated when using PPC-SAFT, by 15% on average. Similar errors can be observed with the modelling of CO_2 + polyol phase equilibria by NguyenHuynh et al. [97] and could be due to an oversimplification of the association schemes with multiple association sites as well as unaccounted ternary interaction effects.

4.4.2 CO_2-Ethanol-Glycerol

A better representation of the ternary behavior is obtained for the ethanol + CO_2 + glycerol system, as shown in **Figure 11**. The locus of the *P-x* diagram at high CO_2 concentrations is predicted with less error.

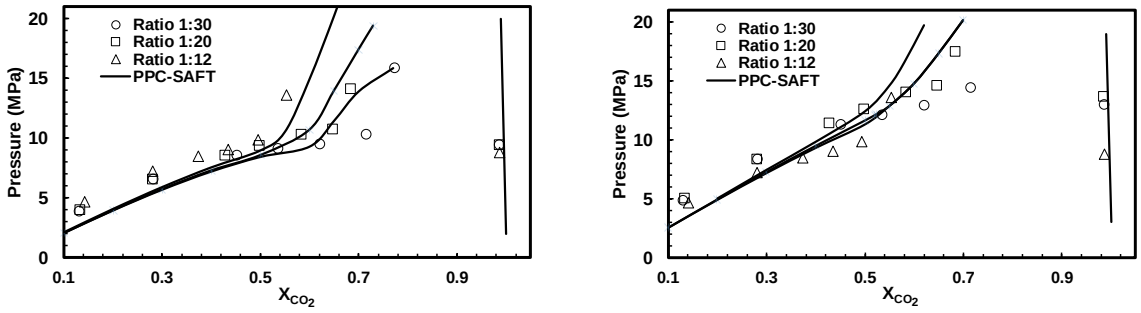

Figure 11 Ternary System CO_2-ethanol-glycerol, with ethanol to glycerol fixed ratios 1:30, 1:20 and 1:12 for temperatures 323.15K and 343.15K. Experimental data is from Araujo et al. [131].

4.4.3 CO_2-Alcohol-Biodiesel.

Ternary systems involving soybean oil derived FAME and FAEE plus ethanol or methanol in the presence of carbon dioxide were also modelled; results are shown in **Figure 12** using parameters from **Table 8**. As above, experimental *P-x* data at constant alcohol to FAMES ratios were predicted by the model and compared to the data by Pinto and Araujo [62, 61]. Small errors were observed which could be due to approximations made in the biodiesel parameter estimations.

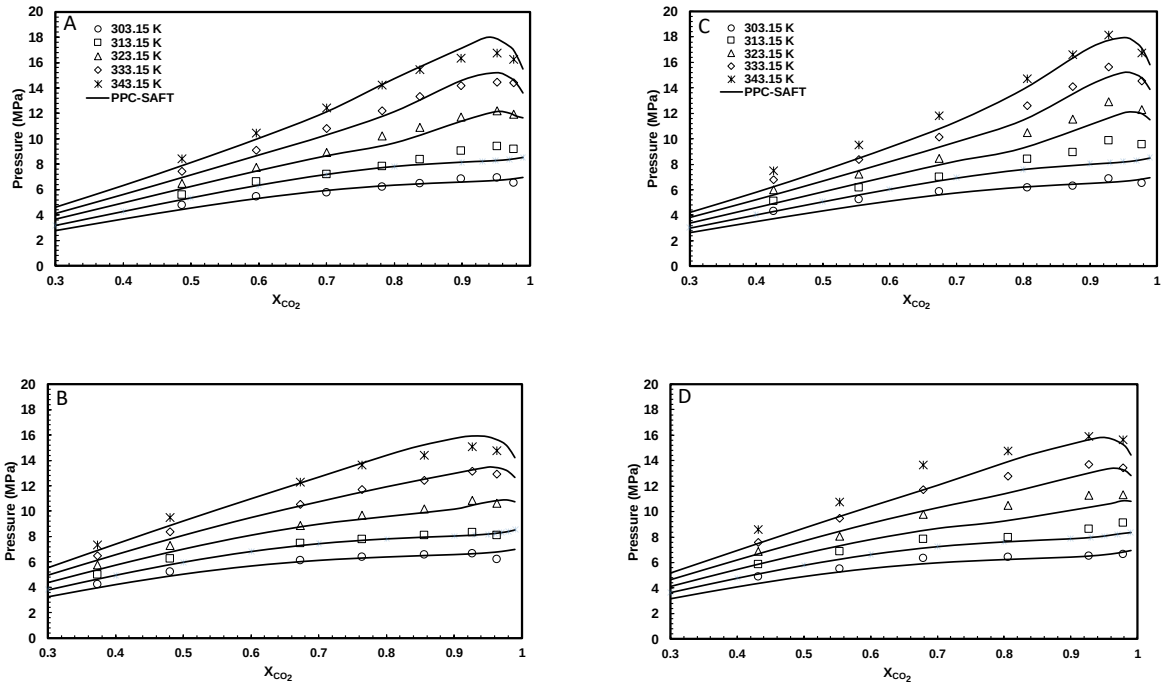

Figure 12 Ternary Systems: CO_2-methanol-FAME derived from soybean oil, with methanol to FAME fixed ratios 1:3 (A) and 1:8 (B). Experimental data is from Pinto et al.[130] CO_2-ethanol-FAEE derived from soybean oil, with ethanol to FAEE fixed ratios 1:3 (C) and 1:8 (D). Experimental data is from Araujo [147].

Table 8 Binary systems with non-zero binary interaction coefficients.

Binary System	k_{ij}	d_{ij}
CO_2-Methanol*	0.0043	0.22979
CO_2-Ethanol*	0.00248	0
CO_2-Glycerol	0	1
CO_2-Ester	0.0114	0
Methanol-Glycerol	0.0439	0
Ethanol-Glycerol	0.0274	0
Methanol-Methyl ester	0.0667	0
Glycerol-Alkylester	0.022	0

* numbers from NguyenHuynh et al.[97]

4.4.4 Alcohol-Glycerol-Biodiesel.

Ternary systems of methanol or ethanol with glycerol and alkyl esters were calculated to test the predictability of the model. In general, good results are achieved for both the binodal curve and the tie lines at high concentrations of alkyl-esters and glycerol. The model does predict an unrealistic LL phase separation at very low concentrations of glycerol due to the profoundly unfavorable interactions between glycerol and the alkyl esters. Also, higher errors are observed for the case with ethanol, probably due to higher errors accrued from the ethanol-glycerol binary system, as can be observed in **Figure 13**.

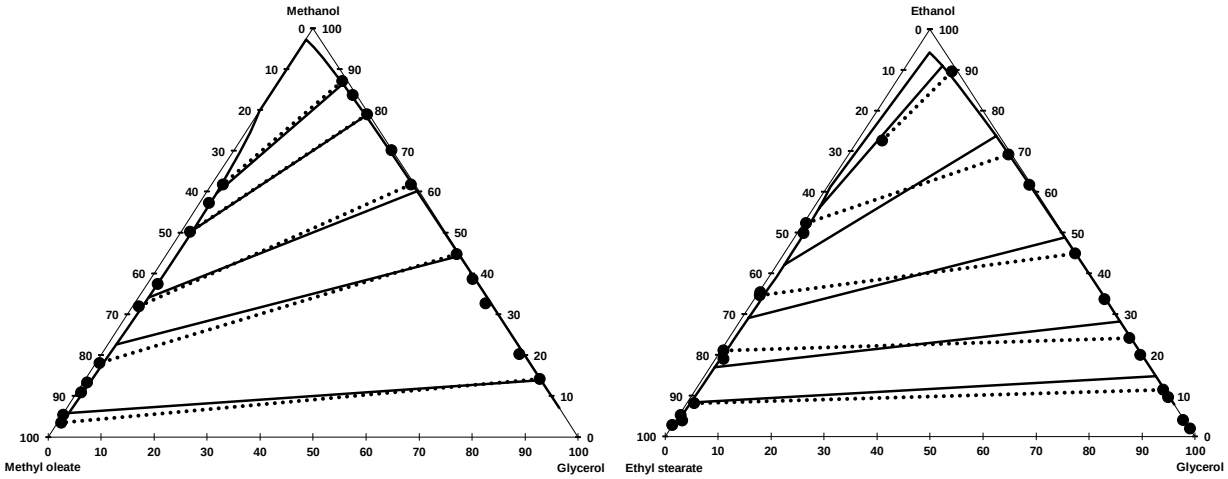

Figure 13 Ternary Systems: methanol-glycerol-methyl oleate at 333.15 K and ethanol-glycerol-ethyl stearate at 323.15 K and atm. pressure. The solid lines are the model predicted tie lines and binodal curve (PPC-SAFT) using parameters from Tables 1,2 and 6. Dotted lines and circles are the experimental measurements. Data is from Andreatta et al. [82] and from Andrade et al. [152].

5.0 Modelling the phase behavior of triglycerides, diglycerides and monoglycerides related to biodiesel transesterification in mixtures of alcohols and CO_2 using a polar version of PC-SAFT [submitted to *Fluid Phase Equilibria,* May 2019; revised and resubmitted, August 2019]

5.1 Pure Component glycerides parameters

The pure component parameters for long chain tri-, di-, and monoglycerides were calculated using a group contribution approach (GC-PPCSAFT) as proposed by Tamouza et al. [122], Hemptinne et al. [138] and NguyenHuynh et al. [96], [97]. The pure component parameters of each chain-like substance were calculated using equations **3-11** to **3-14** and the information in **Table 3** corresponding to basic molecular subgroups present in the molecules of interest. The tri-ester group present in triglycerides could be regarded as a unique molecular subgroup; however, for simplicity the PPC-SAFT parameters of the tri-ester core were calculated as an assembly of 3 ester groups, 2 methylene bridges and 1 methine group for the purposes of this study. Fitting unique parameters for the tri-ester core was explored (see in **Appendix C**), but significant improvement was not observed for any of the binary or ternary systems explored in this work.

The experimental value of the dipole moment (μ) of the molecule is usually inserted directly into the model and then the polar fraction of the molecule ($x_p \cdot m$) found through fitting to pure component phase behavior. The $x_p \cdot m$ value accounts for the fraction of the molecule that contributes to the dipolar moment, which theoretically is the entirety of the molecular structure. However, for practical reasons it has been treated as adjustable parameter ever since PC-SAFT was extended using this polar term [121] . Due to the paucity of existing vapor pressure data from

which to fit the polar parameters, the $x_p \cdot m$ value was fixed to the theoretical value of 1, and the dipole moment was fixed to the value of 2.7 D for saturated glycerides and 3.12 D for any unsaturated glycerides based on data available for triolein, trilaurin and glycerol as well as property estimation databases for other triglycerides [153]–[157]. During this work it was found that inclusion of the polar term is unnecessary to accurately model the behavior of the triglycerides (although very important for small molecules such as methanol and glycerol). Throughout this work, stochastic changes were made to polar parameters in order to measure the impact that the above-mentioned assumptions have over phase behavior predictions and were found to have little to no effect. Nevertheless, the polar term was retained in the description of the glycerides to preserve all model features, particularly because other components of the biodiesel transesterification (methanol, glycerol, etc.) require the inclusion of this term in the EoS for accuracy [158].

5.2 Binary Systems

5.2.1 Triglycerides-CO_2

Binary mixtures of triglycerides and carbon dioxide have been evaluated using the pure component parameters from **Table 3** while fitting binary interaction coefficients to available mixture data. Most of the collected data is LVE or LLE where temperatures are above carbon dioxide's critical value. In the case of triglycerides most data shows that the extent of swelling of the TG's by CO_2 is weakly dependent on both temperature and pressure. Consequentially the modelled phase equilibria of the binary systems exhibit steep slopes in P-T space (see **Figure 13**).

This represents a source for significant prediction error given the form of the objective function (equation **3-17**) and the influence that small changes in the binary parameters have over the composition values. As mentioned earlier, triglycerides are not strictly chain molecules within the context of PC-SAFT (given the "star-like" nature of the TG's), and therefore the use of the model introduces a fundamental problem that translates into higher errors when predicting pressure or temperature of a phase transition. Another relevant source of error relates to the purity of components used to acquire the experimental data since variations in lipid content as well as impurities can shift the phase behavior significantly; high purity glycerides are not always easy to obtain, as noted by a number of experimentalists [57], [69], [70], [74].

Eight binary pairs of CO_2-triglycerides have been considered to generate an overall binary interaction coefficient for TG-CO_2 mixtures. As can be seen in **Figure 14**, shorter chain triglycerides such as tributyrin and tricaproin require negative binary interaction coefficients to produce a reasonable fit -- this is an indication that the group contribution parameters do not fully describe the tri-ester core of these molecules. However, the absolute values of the binary interaction coefficients are small (less than 3% generally), and good descriptions of the binary phase behavior are supported. Naturally, the impact of the triglyceride ester core on the overall fit is somewhat mitigated as the length of the carbon chain increases. A higher number of methylene groups increases the influence that such groups have on dispersive forces as is well captured by the averaging expressions in equations **3-11** to **3-14**.

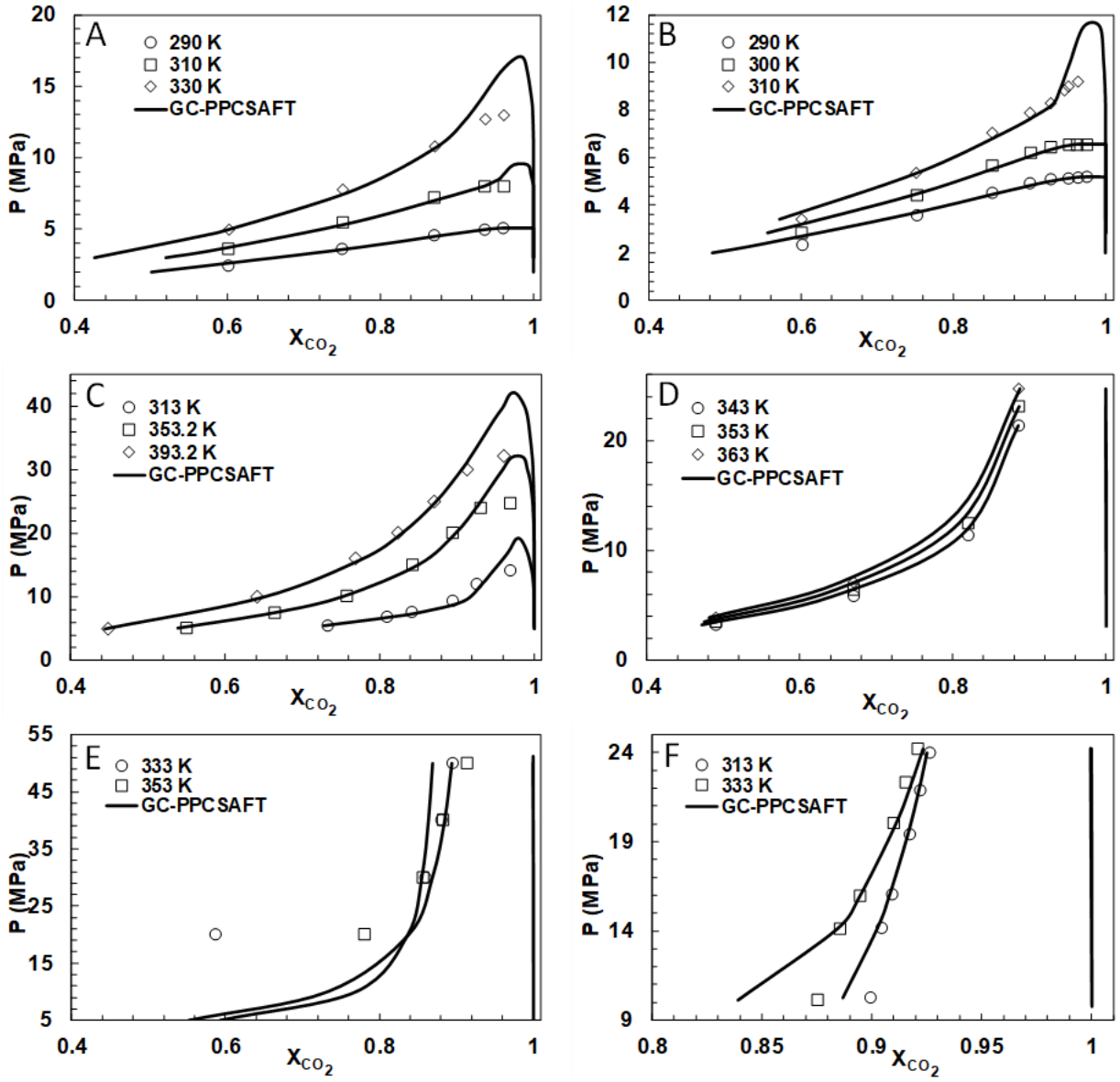

Figure 14 Experimental data and modelling with GC-PPCSAFT for: A) tributyrin, B) tricaproin, C) tricaprylin, D) tripalmitin, E) tristearin, F) triolein. Experimental data specified in Table 9.

The location of the phase boundary of the triglyceride-CO_2 binary where carbon dioxide content is low also presents larger errors, possibly due to the error prediction of pure triglyceride vapor pressure. Overall prediction errors for composition on the liquid phase ranged from 1.2 - 7.3% with an average of 2.5%, as shown below.

Table 9 Binary interaction coefficients and prediction error in % of molar CO_2.

Binary System	k_{ij}	Error X_{CO2}	k_{ij}	Error X_{CO2}	Data pts.	Ref
CO_2-Tributirin	-0.023	1.7	eq (11)	2.0	15	[67]
CO_2-Tricaproin	-0.012	1.9		6.0	24	[67]
CO_2-Tricaprylin	-0.003	1.2		1.3	20	[69]
CO_2-Trilaurin	0.0148	2.1		2.4	5	[68]
CO_2-Tripalmitin	0.0186	2.9		5.8	20	[74], [75]
CO_2-Tristearin	0.0346	7.3		7.4	8	[74]
CO_2-Triolein	0.0098	0.6		2.8	12	[70]
CO_2-Rapeseed oil	0.0054	1.9		1.9	12	[72]
Average		2.5		3.7		

In a fully predictive model k_{ij} should approach zero. However, due to the approximation introduced by the equation of state (mainly geometric and arithmetic averages of the square well and Lennard-Jones spherical segments parameters) the use of a binary interaction coefficient is required (to compensate for these approximation errors). **Figure 15** compares the effect of $k_{ij} = 0$, with the optimized value from the **location** of the phase boundary of the triglyceride-CO_2 binary where carbon dioxide content is low also presents larger errors, possibly due to the error prediction of pure triglyceride vapor pressure. The non-polar version of the EoS (PC-SAFT) has also been included for comparison purposes, showing that higher values of k_{ij} are required if this version is used, but a good description of the phase behavior can still be achieved.

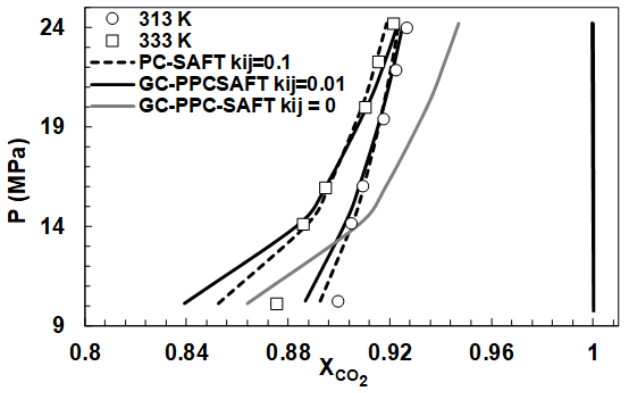

Figure 15 CO_2 – triolein experimental data and modelling with PC-SAFT and GC-PPCSAFT

To strengthen the predictability of the model, the effect of a unique formula to calculate the binary interaction parameter was investigated, so that the model can be easily extended to different types of triglycerides beyond the ones studied in this work. The binary interaction parameters were found to closely correlate with the carbon chain length and the degree of unsaturation of the triglycerides as shown in **Figure 16.** As such, a general binary interaction coefficient was established via fitting against chain length, and, with information from tristearin, triolein and the rapeseed oil, against the number of double bonds in the triglyceride chain. The result is shown in equation **5-1.**

$$k_{ij} = (0.00372 * x - 0.03457) * e^{-0.698*y} \qquad 5\text{-}1$$

Where x is the average number of carbons in the fatty chains and y the average number of double bonded carbons in the fatty chains. The penalty in prediction error for using equation **5-1** can be compared to the substance-particular k_{ij} fitting shown in **Table 9**. The location of the phase boundary of the triglyceride-CO_2 where carbon dioxide content is low also presents larger errors, possibly due to the error prediction of pure triglyceride vapor pressure. Overall prediction errors

for composition on the liquid phase ranged from 1.2 - 7.3% with an average of 2.5%, as shown in **Table 9**. Oils containing multiple types of triglycerides, as is the case for rapeseed oil, have been treated as a single pseudo-component as suggested by different authors [29], [72], [159] and performed in chapter **4.0** for FAMES and FAEES derived from soybean oil, by averaging all of the group contribution parameters of all present groups in the oil.

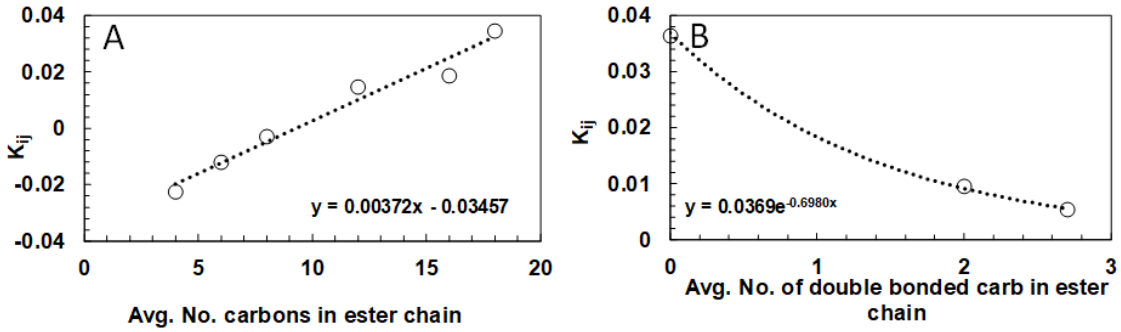

Figure 16 Dependence of binary interaction coefficient on average carbon chain length (A) and average double bonded carbons (B) for GC-PPCSAFT.

5.2.2 Monoglycerides-CO_2

The group contribution approach described above was also used to model mixtures of monoglycerides with carbon dioxide. For the hydroxyl groups in the first and second positions on the carbon chain, a 3B association scheme (two electron donor sites and 1 electron acceptor) was employed, with an additional cross association site due to the ester group. The volumetric overlap of the association term (κ^{AB}) is in general taken as a unique value for the homonuclear approach, thus it was calculated as a geometric mean of the volumetric overlap for each of the hydroxyls and ester groups considered in the group contribution scheme shown in **Table 10**.

Few experimental phase behavior data are available for CO_2 + monoglyceride mixtures. Data from the literature plus experimental data collected in this work were used to estimate binary interaction coefficients. As mentioned before, a weak dependence of CO_2 solubility (in the heavy MG-rich phase) on temperature and pressure is the main source of error. This can be appreciated by noting the marginal difference in CO_2 solubility between two different temperatures as shown in the experimental data collected in **Table 10** and depicted in **Figure 17** for monostearin and monocaprylin. All collected and modelled data shown in **Table 10** correspond to a saturated liquid (the heavy phase) which can be in equilibrium with either a vapor phase (LVE transition) or a second liquid phase (LLE transition), where the second phase is composed mainly of carbon dioxide. Relatively low values (approximately 3%) of binary interaction coefficients were obtained. A generalized parameter using the CO_2-monostearin and CO_2-monocaprylin systems was calculated, although it was difficult to establish the optimal solution because the minimization curve was very flat. Biasing the solution towards the monocaprylin (k_{ij} = 0.0091) or towards the monostearin (k_{ij} = 0.0361) altered the objective function by only 0.3%. Therefore, the midpoint was selected so to have a binary interaction coefficient that is not strongly substance biased. Nonetheless, higher errors relative to those obtained with triglycerides were found for monoglycerides, due to the small number of candidate MG's, the assumptions made during fitting, and the relatively low purity of the monoglyceride samples. It is important to highlight the negative effects of this last-mentioned source of error, since the phase equilibria measurements can be affected by the presence of impurities on the original sample. Some of the potential compounds present have strong associative and dispersive forces (i.e. glycerine and water) that play a role in modifying specially the loci of the CO_2 saturated liquid loci on a liquid-liquid equilibrium.

Table 10 Phase equilibria data for CO_2 – Monoglycerides.

X_{CO2}	P (Mpa)	σ (Mpa)	σ_X	Transition Type	X_{CO2}Predicted	Error X_{CO2}
CO_2-Monostearin						
T = 358.1 ± 0.2						
0.30	6.41	0.08	0.08	LVE	0.43	45
0.40	8.34	0.08	0.11	LVE	0.51	28
0.50	12.34	0.01	0.11	LVE	0.62	25
0.60	15.43	0.01	0.10	LLE	0.68	13
0.70	27.29	0.06	0.07	LLE	0.78	11
0.80	53.72	0.07	0.04	LLE	0.87	9
	Average	0.05	0.08			22
T = 373.1 ± 0.2						
0.30	6.97	0.04	0.08	LVE	0.43	44
0.40	10.24	0.04	0.11	LVE	0.54	36
0.50	15.01	0.03	0.11	LVE	0.65	29
0.60	21.74	0.03	0.10	LLE	0.73	22
0.70	37.39	0.81	0.07	LLE	0.83	18
0.75	48.35	0.06	0.06	LLE	0.87	16
	Average	0.17	0.09			27
CO_2-Monocaprylin						
T = 358.1 ± 0.2						
0.30	5.74	0.07	0.07	LVE	0.26	12
0.40	8.29	0.22	0.10	LVE	0.35	12
0.50	12.51	0.01	0.10	LVE	0.45	9
0.60	18.25	0.04	0.09	LLE	0.53	11
0.70	28.27	0.09	0.06	LLE	0.60	14
0.80	45.41	0.38	0.04	LLE	0.67	16
	Average	0.13	0.08			12
T = 373.1 ± 0.2						
0.30	5.75	0.04	0.07	LVE	0.25	18
0.40	8.90	0.07	0.10	LVE	0.34	14
0.50	12.67	0.06	0.10	LVE	0.43	14
0.60	19.37	0.05	0.09	LLE	0.53	12
0.70	29.11	0.08	0.06	LLE	0.61	13
0.80	45.07	0.61	0.04	LLE	0.69	14
	Average	0.15	0.08			14

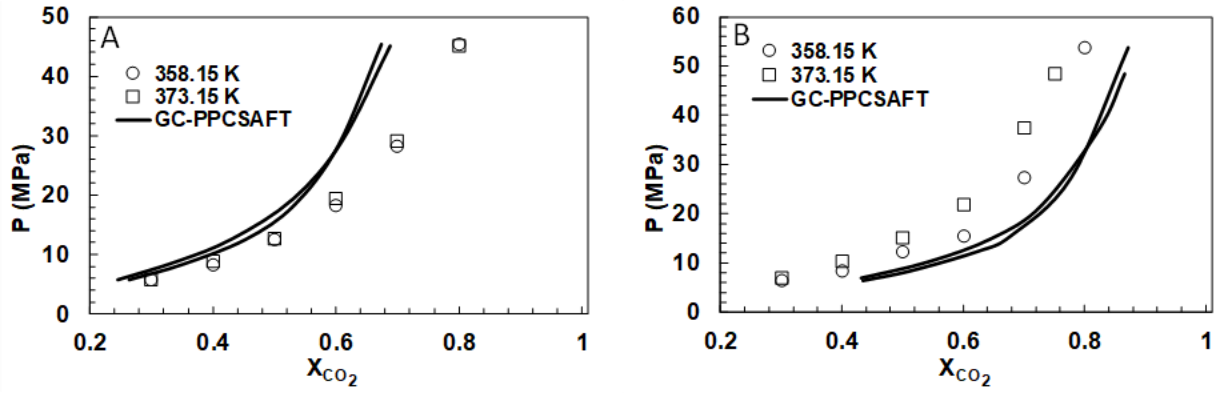

Figure 17 Phase equilibria modelling of CO_2 - monoglycerides using group contribution. A) Monocaprylin. B) Monostearin.

5.2.3 Diglycerides-CO_2

Mixture data for diglycerides and CO_2 are scarce, possibly due to difficulties associated with the separation techniques required to obtain relatively pure DG samples for testing. Two references [51], [52] on supercritical extraction contain information for diglycerides and CO_2 but only the compositions in the light supercritical phase are available (shown in **Figure 18**). All predicted data points using GC-PPC-SAFT correctly show a dew point composition that closely matches the expected experimental values. However, because the compositions of this "light" end of the phase envelope are always above 99% CO_2, the binary interaction parameters obtained using this data (**Table 11**) are not expected to fully match the ones obtained from the glyceride-rich branch of the diagram. Pure component parameters for diglycerides have been calculated using the group contribution technique with one hydroxyl group and two ester groups while maintaining the association schemes shown in **Table 3.**

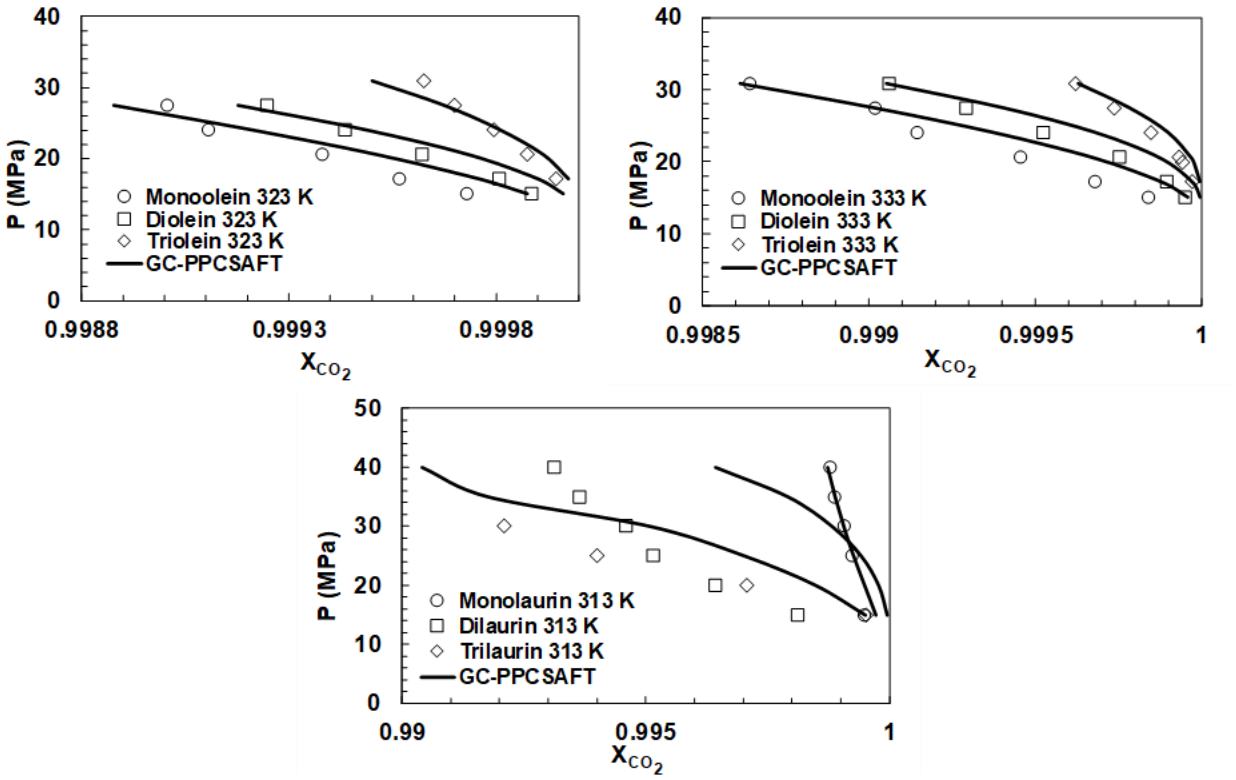

Figure 18 Phase equilibria modelling of supercritical extraction of glycerides with CO_2 Using parameters from Table 11.

Values of the binary interaction coefficients can be adjusted in order to capture the progressive solubility of mono-, di-, and triglycerides extracted with supercritical carbon dioxide, as done previously by other authors [107]. However, parameters obtained in this way are less reliable than desired since they represent the steepest side of the phase envelope, whose locus is more sensitive to small changes. Therefore, only diglyceride-specific information has been incorporated into a generalized parameter for CO_2-diglycerides, obtaining k_{ij} = 0.0144 for both diolein and dilaurin -- no other experimental data are available.

Table 11 Binary interaction parameters fitted to vapor supercritical phase.

Binary System	k_{ij}	Data pts.	Ref
CO_2-Monoolein	0.02356	11	[51]
CO_2-Diolein	0.01703	11	
CO_2-Triolein	0.01294	11	
CO_2-Monolaurin	0.04684	5	[52]
CO_2-Dilaurin	-0.00816	9	
CO_2-Trilaurin	0.0079	16	

5.2.4 Triglycerides-methanol

Despite the importance of this binary system to the overall performance of the transesterification process for biodiesel, there are surprisingly few data available on the phase equilibria of triglycerides and short chain alcohols. These mixtures exhibit large differences in polarity and in carbon chain length, prompting large changes in equilibrium composition upon small changes in temperature or pressure (as bubble and cloud points measured by Tang et al.[11] and the corresponding cloud and bubble points predicted and shown in **Figure 19**). Upon fitting of the available data, these binaries exhibited the largest errors between actual and predicted curves and required one of the higher values for the binary interaction coefficient that we encountered. The lower the values for k_{ij} the more accurate the basic model is, since the averaging approximations used by the combining rules for chains of unlike segments are closer to experimental data. The triolein methanol system has the highest values of binary interaction coefficients amongst all the studied systems, which suggests lower reliability of subsequent predictions as compared to the previous results in this work. However, k_{ij} values below 12% are

sufficient to obtain the best possible phase equilibria representation. Predictions of phase behavior when methanol composition is high are correctly captured by the model in terms of the nominal value of equilibrium composition and a low dependence on pressure and temperature. However, large deviations can be observed at lower methanol mole fractions associated with inaccuracies in predicted pure component properties for triglycerides.

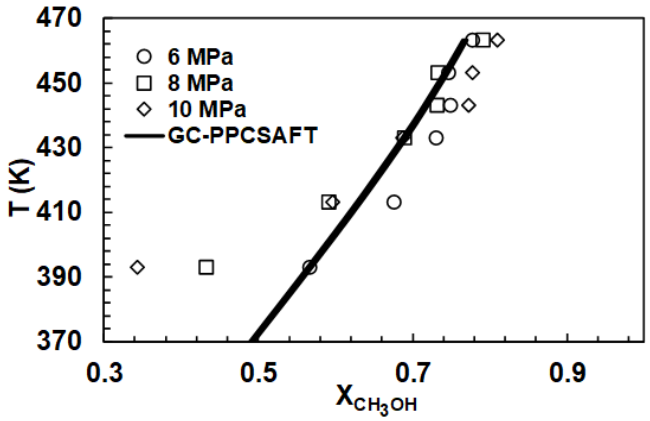

Figure 19 Phase equilibria modelling of methanol – triolein.

5.2.5 Triglycerides-glycerol

Due to the obvious immiscibility of the components involved in this binary system the only data available are liquid-liquid equilibria at low pressure and temperatures collected by Silva et al. [64] that show an average solubility of 0.7% of the triglyceride in the glycerol-rich phase, and 1% glycerol in the non-polar glyceride-rich phase. A binary interaction coefficient has been fitted to the available information, obtaining $k_{ij} = 0.0569$. The model representation is only accurate on the oleic-rich branch of the phase envelope (average error is 0.3%). By contrast, the model is

unable to capture the trace amounts of triglycerides in the glycerol-rich phase, rather predicting a practically pure phase for all conditions.

5.3 Ternary systems

5.3.1 CO_2-Methanol-Monoglyceride

Literature data for mixtures of methanol with di- and monoglycerides could not be located. Instead, experimental ternary phase diagrams containing methanol and monoglycerides with CO_2 were plotted, in **Figure 20** and shown in **Table 12**, following the procedure described in section **3.4.2** (calibration experiments can be found in **Appendix D)**. As explained in section **7.2** the experimental data available correspond to the monoglyceride-rich liquid phase in equilibrium with a CO_2-rich phase**.** These data were then used to fit the missing binary interaction coefficients for the methanol-glyceride pairs. An overall optimization was performed, obtaining k_{ij} = 0.12 for the methanol-monoglyceride pair, which is consistent with values obtained for the methanol-triglyceride system.

As shown in **Figure 20** the model correctly predicts general trends showing higher vapor pressures for higher methanol contents but lower cloud point pressures when supercritical conditions for CO_2 are reached. However, the model shows a large departure from experimental behavior in the steepest region of the phase diagram (LLE) at high CO_2 composition. This behavior has been observed previously in mixtures containing glycerol in section **4.4.1** and **4.4.2** , where the predicted solubility in the LLE regime does not increase with pressure in the same way as the data do.

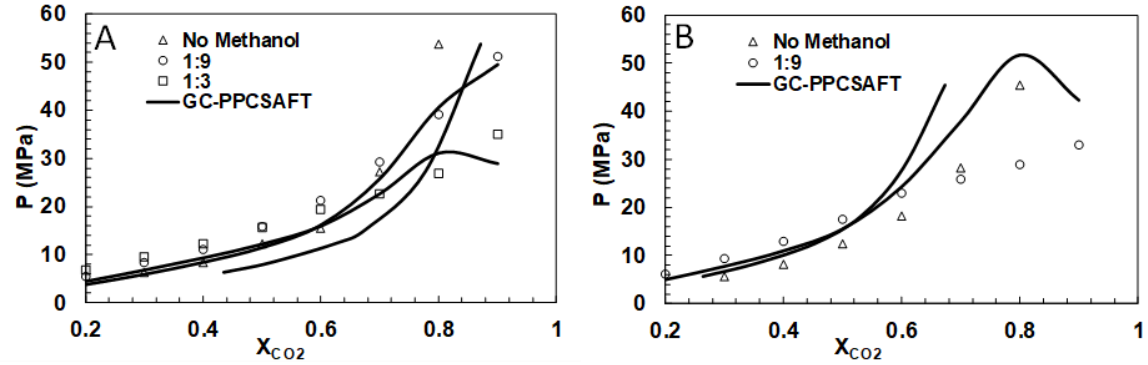

Figure 20 Phase equilibria modelling of: A) CO_2 - methanol - monostearin. B) CO_2 - methanol – monocaprylin.

Table 12 Phase equilibria data for CO_2 (1) - Methanol (2) - Monoglycerides (3) at different methanol to monoglycerides ratios at 358.15 K.

X_1	X_2	P (Mpa)	σ (Mpa)	σ_X	Transition Type	$P_{predicted}$ (Mpa)	Error P
CO_2 (1) - Methanol (2) - Monostearin (3)							
$X_2/X_3 = 9$							
0.20	0.60	5.47	0.01	0.04	LVE	3.81	30
0.30	0.53	8.35	0.19	0.07	LVE	5.97	29
0.40	0.45	11.05	0.02	0.08	LVE	8.46	23
0.50	0.38	15.79	0.03	0.07	LVE	11.53	27
0.60	0.30	21.21	0.10	0.06	LLE	16.25	23
0.70	0.23	29.37	0.03	0.04	LLE	25.90	12
0.80	0.15	39.14	0.10	0.02	LLE	40.74	4
0.90	0.08	51.28	0.04	0.01	LLE	49.59	3
		Average	0.07	0.05			19
$X_2/X_3 = 3$							
0.20	0.72	6.91	0.01	0.02	LVE	4.47	35
0.30	0.63	9.51	0.03	0.04	LVE	6.83	28
0.40	0.54	12.36	0.01	0.04	LVE	9.37	24
0.50	0.45	15.71	0.04	0.04	LVE	12.21	22
0.60	0.36	19.49	0.02	0.03	LLE	15.98	18
0.70	0.27	22.71	0.01	0.02	LLE	22.72	0
0.80	0.18	26.86	0.03	0.01	LLE	31.15	16
0.90	0.09	35.07	0.01	0.00	LLE	28.95	17
		Average	0.02	0.03			20
CO_2 (1) - Methanol (2) - Monocaprylin (3)							
$X_2/X_3 = 9$							
0.20	0.60	6.15	0.13	0.06	LVE	4.95	19
0.30	0.53	9.43	0.06	0.09	LVE	7.71	18
0.40	0.45	12.96	0.03	0.10	LVE	10.94	16
0.50	0.38	17.64	0.02	0.09	LVE	15.49	12
0.60	0.30	22.99	0.01	0.07	LLE	24.25	5
0.70	0.23	25.82	0.03	0.05	LLE	37.81	46
0.80	0.15	29.04	0.03	0.03	LLE	51.65	78
0.90	0.08	33.02	0.08	0.01	LLE	42.26	28
		Average	0.05	0.06			28

5.3.2 Monoglycerides-Glycerol-Fatty Acid Methyl Esters (FAME)

Negi et al. [76] performed measurements of the ternary system containing glycerol, methyl oleate and monoolein that provides valuable information about how the phase behavior of the biodiesel reaction system evolves as intermediates and products are formed. Since long chain molecules closely follow the group contribution approach, the FAME-monoglycerides binary interaction coefficient has been set to 0.0225 for methyloleate, consistent with findings of section **4.3.5** All compositions where the experimental value was below 2% molar were excluded from the minimization function to prevent the optimization from being strongly biased towards these points. It was found that a binary interaction parameter of k_{ij} = 0.0145 for the glycerol-monoolein pair was sufficient to correctly capture the liquid-liquid equilibria at 135 °C (see

Figure 21**)**.

As noted by Negi et al., different variations of the UNIFAC equations of state exhibit large errors predicting the composition of the co-existing phases when significant amounts of monoglyceride are present [76]. Monoolein exhibits somewhat of a cosolvent effect, as can be appreciated by the larger glycerol contents in the oleic phase – this is probably due to the hydrogen bonding potential of the monoolein, and can only be captured correctly with an EoS such as the GC-PPCSAFT, that explicitly accounts for these forces as shown **Figure 21**.

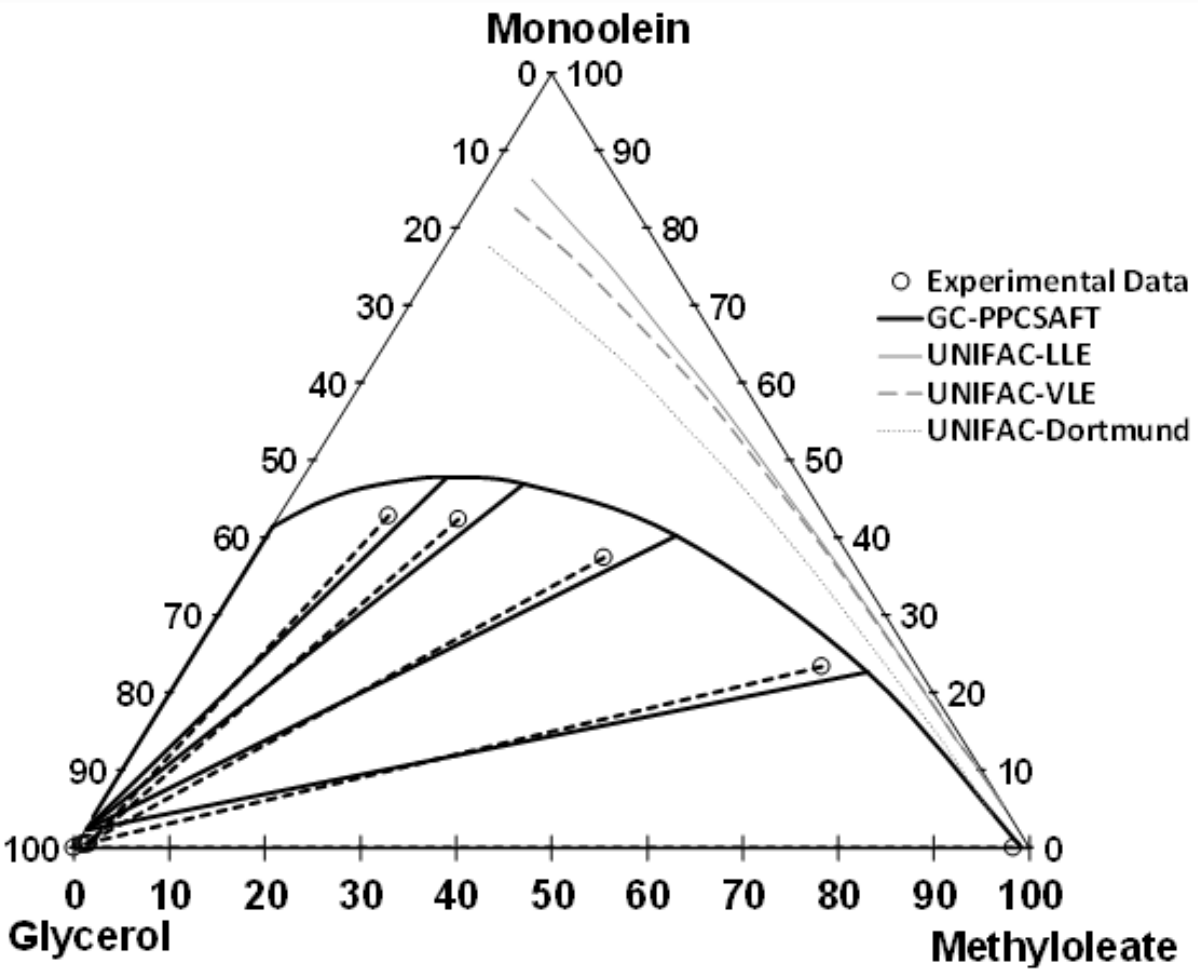

Figure 21 Liquid-liquid equilibrium of monoolein - glycerol – methyl oleate at 135 °C and 1 atm in molar fraction as measured by Negi et al [76].

5.3.3 Carbon Dioxide - Ethanol – Triglyceride

A ternary mixture of carbon dioxide, ethanol and rapeseed oil was modelled using parameters from **Table 3** and the procedure described in section **5.2.1** for rapeseed oil. The binary interaction parameter between the triglyceride and ethanol was set to zero, making these diagrams effectively a pure prediction based on previous calculations of systems containing carbon dioxide as calculated in section **5.2.1** and the binary interaction coefficient calculated by NguyenHuynh et al. [97] for CO_2 and alcohols. As can be seen in **Figure 22**, there is good agreement between the model and experimental data, with an increased error towards the higher isobars. Comparable results were obtained by Geana and Steiner [72] by fitting multiple parameters directly to this ternary system using a cubic EoS. The prediction error in the current work was estimated to be 10% in mole fraction.

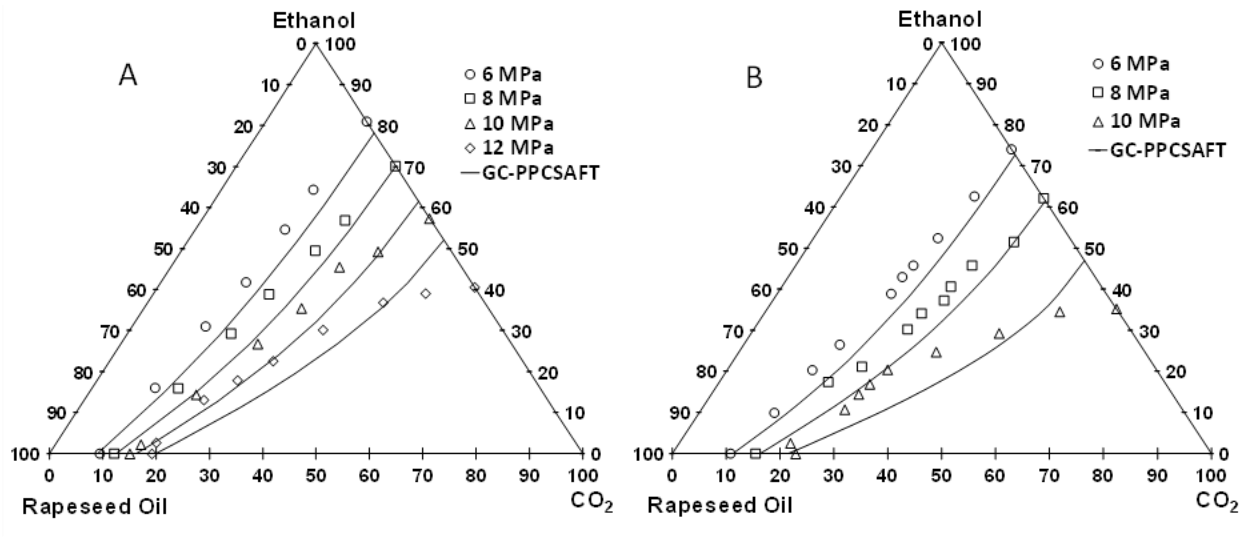

Figure 22 Phase equilibria modelling of CO_2 - ethanol – rapeseed oil at A) 353.15 K and B) 333.15 K in mass fraction as measured by Geana and Steiner [72].

6.0 Predicting the optimal conditions for CO_2-enhanced transesterification of triglycerides with methanol to form biodiesel using a polar version of PC-SAFT [invited paper submitted to *I&EC Research* as part of the special issue honoring Charles Eckert, June, 2019]

6.1 Phase equilibria of CO_2 - Methanol -Triolein (TO)

Phase separation in the triolein + methanol + carbon dioxide ternary occurs in one of two ways depending upon the pressure. "Low-pressure" phase separation exhibits a ternary LLVE at high CO_2 and methanol concentrations which produces (1) a CO_2 -rich vapor phase (a "dense" vapor phase when CO_2 is above its critical temperature), (2) a liquid-CO_2-expanded methanol-rich phase, and (3) a triolein-rich phase swollen by both CO_2 and methanol (see **Figure 23**). At low CO_2 concentrations and high methanol concentrations, a liquid-liquid split exists instead, consistent with previous experimental findings registering a phase split amongst the reactants in traditional biodiesel transesterification [27], [34], [35]. In the ternary mixture, the initial immiscibility of the short-chain alcohol with the triolein is mitigated by progressively adding carbon dioxide while keeping pressure and temperature constant. At lower concentrations of methanol and high concentrations of carbon dioxide a liquid-vapor phase split can be observed, corresponding with the maximum CO_2 uptake to the liquid phase and consequently triglyceride concentration in this phase as well; this behavior has been reported by many experimentalists [67], [70], [74], [75]. High-pressure phase diagrams exhibit only the previously mentioned liquid-liquid phase split, which is itself governed by the generally unfavorable alcohol-triglyceride interactions and the liquid-(SC)vapor phase separation related to the CO_2 + Triglyceride binary system. The

change in the sign of the slope of tie-lines in the triangular diagram signals a transition from one regime to the other (see tie line in **Figure 23.B** near 80% CO_2). The closer the phase boundary is to the lower right vertex of the triangular diagram, the higher content of methanol in the triglyceride-rich phase, favoring a higher ratio of methanol to triolein in this phase.

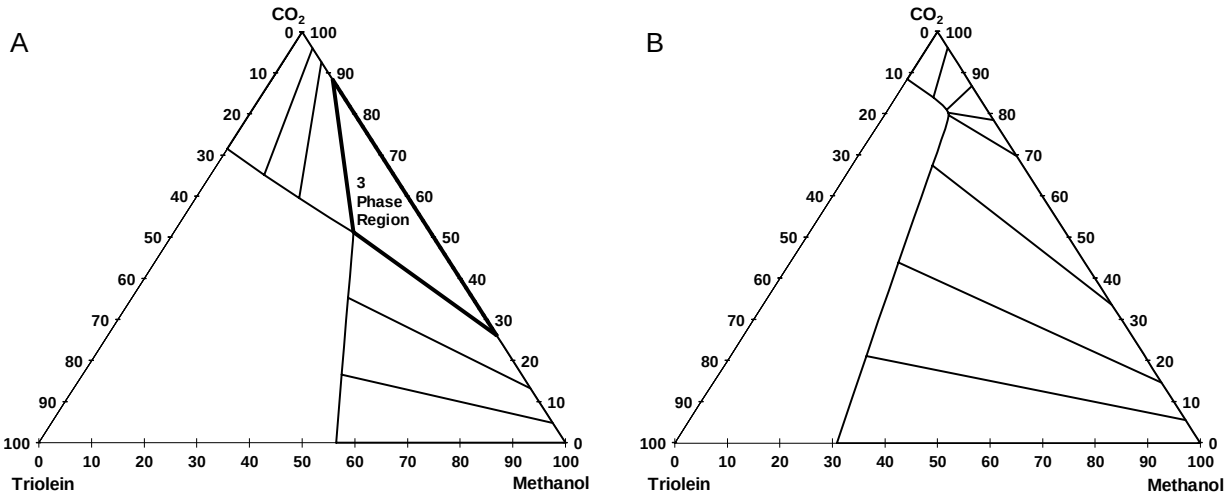

Figure 23 Phase envelopes of CO_2-methanol-triolein mixtures at 10 MPa and (A) 393.15 K and (B) 313.15 K.

The presence or absence of the LLVE phase split is controlled by CO_2-methanol binary interactions (the content of triglyceride in the light phase is always negligible). Thus a triphasic equilibrium will exist at the same P-T conditions where a CO_2-methanol phase split occurs, as can be seen in the measurements collected by different experimentalists.[160]–[162] In general, higher prediction errors are predicted to happen near the lower left vertex of the triangular diagrams (100% triolein) as explained previously, owing to errors in prediction of the triglyceride vapor pressure. Prediction error is expected to be smaller towards the center of the diagrams, due to the good correlation obtained by the model in the CO_2-methanol binary system, and should be

progressively diminished by increasing pressure values as verified during the fitting procedures of binary interaction coefficients [163].

The effect of pressure and temperature on phase behavior can be seen in **Figure 24**. Not surprisingly, increasing pressure favors miscibility of all components present in the mixture and progressively narrows the triphasic area of the diagram until it vanishes completely;

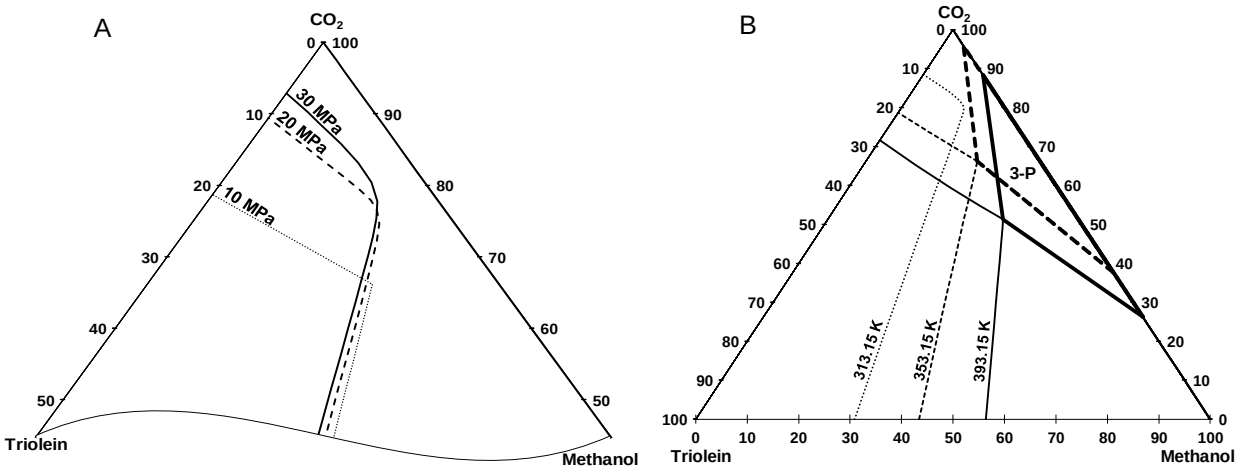

Figure 24 Oleic phase composition of the CO_2-methnaol-triolein systems at 353.15 K and different pressure values (A), and at 10 MPa and different temperature values (B).

Figure 24.A shows the transition from a LLVE at 313.15 K and 10 MPa (only the left side composition is depicted) to LLE at higher pressures. On the other hand, increasing the temperature enlarges the area of LLVE coexistence, rendering the liquid-liquid regime unstable at lower concentrations of carbon dioxide, it also lowers the CO_2 concentration transition from LLVE to LVE. **Figure 24.B** shows this transition from LLE at 313.15 K and 10 MPa to a LLVE at higher temperatures. Another expected effect that can be observed with increasing temperature is an

increase in the initial miscibility of methanol and triolein and therefore a shift of the concentration of the oleic-rich phase towards the lower right vertex of the triangular diagram.

6.2 Optimal composition for miscibility enhancement

One of the main obstacles to efficient biodiesel synthesis is the initial phase separation of the reactants (methanol and most commonly used triglycerides are not miscible). Given that CO_2 behaves as a co-solvent for the triglyceride-methanol mixture, we investigated the variation of molar ratio of methanol to triolein in the oleic-rich phase (defined for this work as Φ, shown in equation **6-1**) as a function of CO_2 total mole fraction – this should provide a measure of the enhancement that carbon dioxide can provide to mitigate the above-mentioned difficulties. Ideally, we are seeking the greatest improvement in methanol-to-oil ratio through addition of CO_2.

$$\Phi = \left.\frac{x_{Methanol}}{x_{Triolein}}\right|_{oil-rich\ phase} \qquad 6\text{-}1$$

Every pressure-temperature pair supports generation of a particular ternary phase diagram, similar to the ones noted in the previous section. The upper left-hand side of each of the depicted triangular diagrams is an undesirable operational space, since in this region there are large amounts of triolein in the oleic phase but almost no methanol despite there being a large amount of CO_2 in the system. Increasing the CO_2 concentration in this region lowers the value of Φ since the carbon dioxide in the vapor phase effectively "extracts" the methanol from the lower phase owing to entropic considerations. By contrast, if the system remains two-phase (LLE), adding carbon dioxide enhances the ratio of methanol-to-oil in the heaviest liquid phase. ***The contrasting effects that the overall concentration of CO_2 has over the mixture leads to the presence of a***

mathematical maximum in the methanol to oil ratio in the oleic-rich phase (Φ) as a function of CO_2 molar content, as depicted in Figure 3 for two different P-T conditions. This remains viable so long as the trial composition lies far from the single-phase region (near the lower right vertex of the triangular diagrams).

To predict the behavior of the ratio (Φ) as T-P-x conditions change, a search was conducted along a constant methanol to oil total molar fraction (dashed line in **Figure 25.A** and **Figure 25.C** where the total ratio is 5:1) from 0% to 100 % CO_2 total mole fraction. At each CO_2 increment, at least two stable phases are found, whose concentrations are then described with tie-lines. The ratio Φ is then obtained using equation **6-1** for the phase that contains the majority of the triolein. In the first case, (**Figure 25.A** and **Figure 25.B**) the ratio continues to increase with increasing CO_2 content until the tri-phase equilibrium occurs. At this point, the equilibrium composition remains unchanged for all trials that lie inside the LLVE area, thus Φ remains unchanged as well inside that region. CO_2 total mole fractions that lie towards the top vertex (100% CO_2) yield equilibriums that have lower values of Φ since the oil phase composition shifts away from the methanol vertex. Therefore, the optimal CO_2 content is given by all the composition trials included between the highlighted gray dots and, in this case, all solutions inside the LLVE area. Similarly, for the second case the same constant methanol oil total fraction is used (dashed line value 5:1), and tie lines that cross the dashed line are the equilibrium solutions for that given CO_2 total fraction. For systems like the ones in **Figure 25.C** and **Figure 25.D** the ratio Φ continues to increase with increasing values of CO_2 total molar fraction until a sudden drop that occurs due to the transition from LLE to LVE behavior (highlighted point).

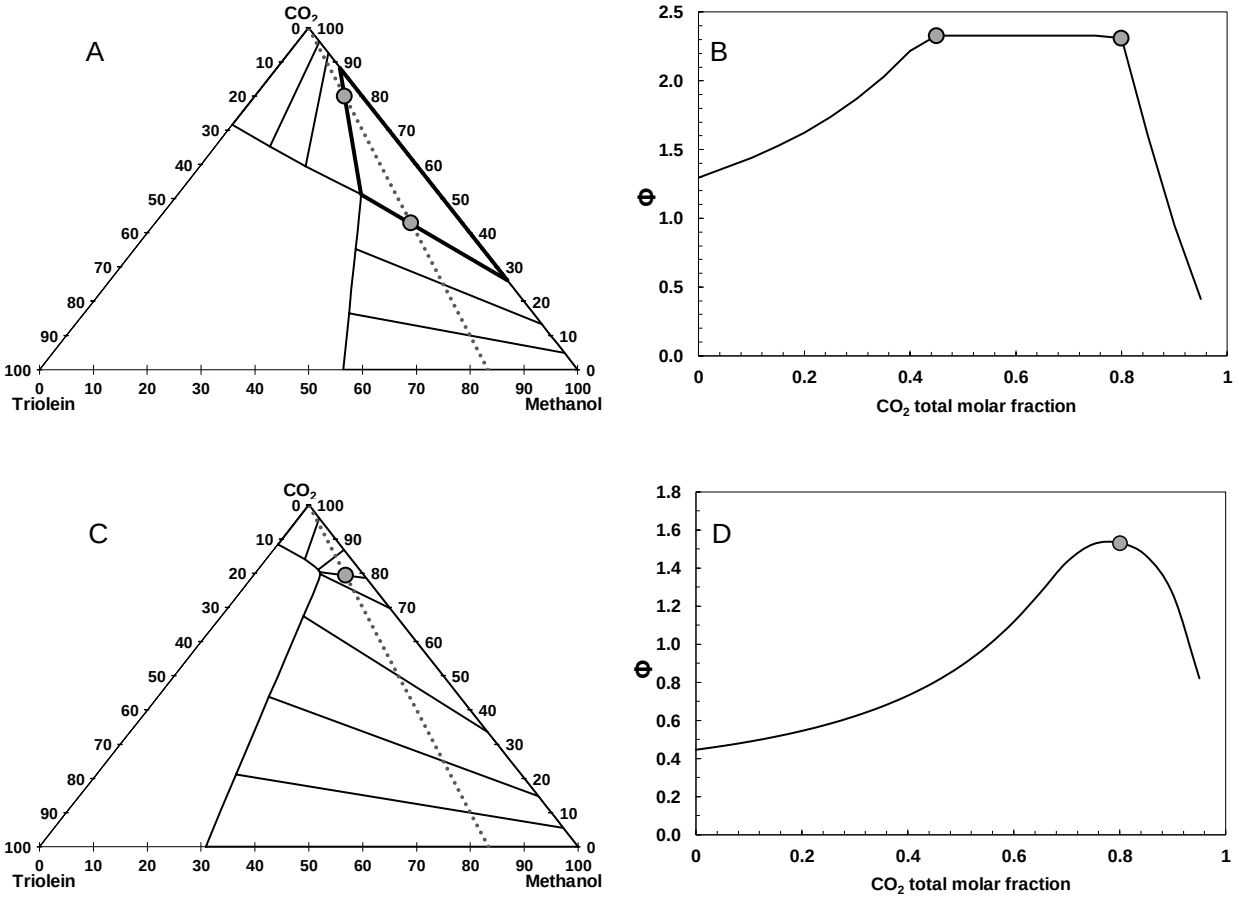

Figure 25 Phase separation for systems at 393.15 K and 10 MPa exhibiting LLVE (A), and for systems and 313.15 and 10 MPa always in biphasic regime (C). Methanol to triolein in the oil rich phase value search along a total methanol to oil fraction 5:1 (B and D).

Pressure and temperature conditions that exhibit LLVE always exhibit their maximum methanol to oil ratios within the triphasic region, and as expected, there are several CO_2 fractions (all the ones contained inside the LLVE area) that will yield the optimal Φ values. Also, P-T conditions where the phase split of the mixture shifts from LLE to LVE without a tri-phase area being observed have a unique optimal value for CO_2 concentration defined by the equilibrium tie-line where there is an imminent transition to LV regime. Beyond this point addition of carbon dioxide results effectively in extraction of methanol from the oleic-rich phase and therefore, is counter-productive. At the optimal condition the molar CO_2 concentration is nearly equal in both liquid phases and any ratio of methanol to oil total fraction will result in the same phase split as long as there is enough methanol to be in a biphasic regime.

6.3 Pressure and temperature effect on optimal loci

Higher pressure shrinks the 3-phase region to a point where it ultimately vanishes completely, and hence such conditions consistently show higher values for Φ than P-T conditions that induce 3-phase LLVE behavior. This result is expected since the vapor phase is mainly composed of CO_2 and methanol, thus reducing the amount of the latter in all other phases present. At any given temperature the pressure increase has a stronger effect on Φ than when LLVE is present. Further increasing the pressure above the minimum required to suppress the formation of the 3-phase split has a linearly positive effect on the desired ratio. The dependence of Φ on pressure is more pronounced at higher temperatures; for example, at temperatures below 353 K increases to pressure show only modest increases to the methanol-to-oil ratio (a doubling of pressure leads to only an 18% increase in Φ).

Figure 25 can be constructed for any combination of temperature and pressure, and hence the maximum value of Φ can be determined as a function of temperature and pressure; this leads to the curves shown in **Figure 26.A**. Here, every point on each of the curves is a maximum value of Φ, found using the search procedure outline for **Figure 25.B** and **Figure 25.D.** The gray-shaded region shown in **Figure 26.A** is the approximate boundary between 3-phase (LLV) and 2-phase (LL) equilibria; the 2-phase region occurs to the right of the shaded region in **Figure 26.A**. The pressure that transforms a 3-phase mixture to a 2-phase split was calculated with a $\pm$0.2 MPa value. As explained in section **6.1**, the transition pressure matches the trend of the CO_2 - Methanol binary system's critical values.

As depicted in **Figure 26.A**, the maximum value of Φ increases significantly as the temperature is increased. The modeling shows that one can surpass the minimum required stoichiometric ratio of methanol to triglyceride (3:1) in the oil-rich phase at temperatures of 358 K and above, and pressures of 20 MPa and higher. This is desirable for different reasons, including further shifting the equilibrium towards the products, and supplying enough methanol in the reactive phase to account for the loss of methanol into a glycerol-rich phase ultimately formed as a result of the transesterification. These findings are consistent with experiments from Soh et al. [44] who obtained high conversions at short times operating at temperatures near 80 °C in a multiphase reactor.

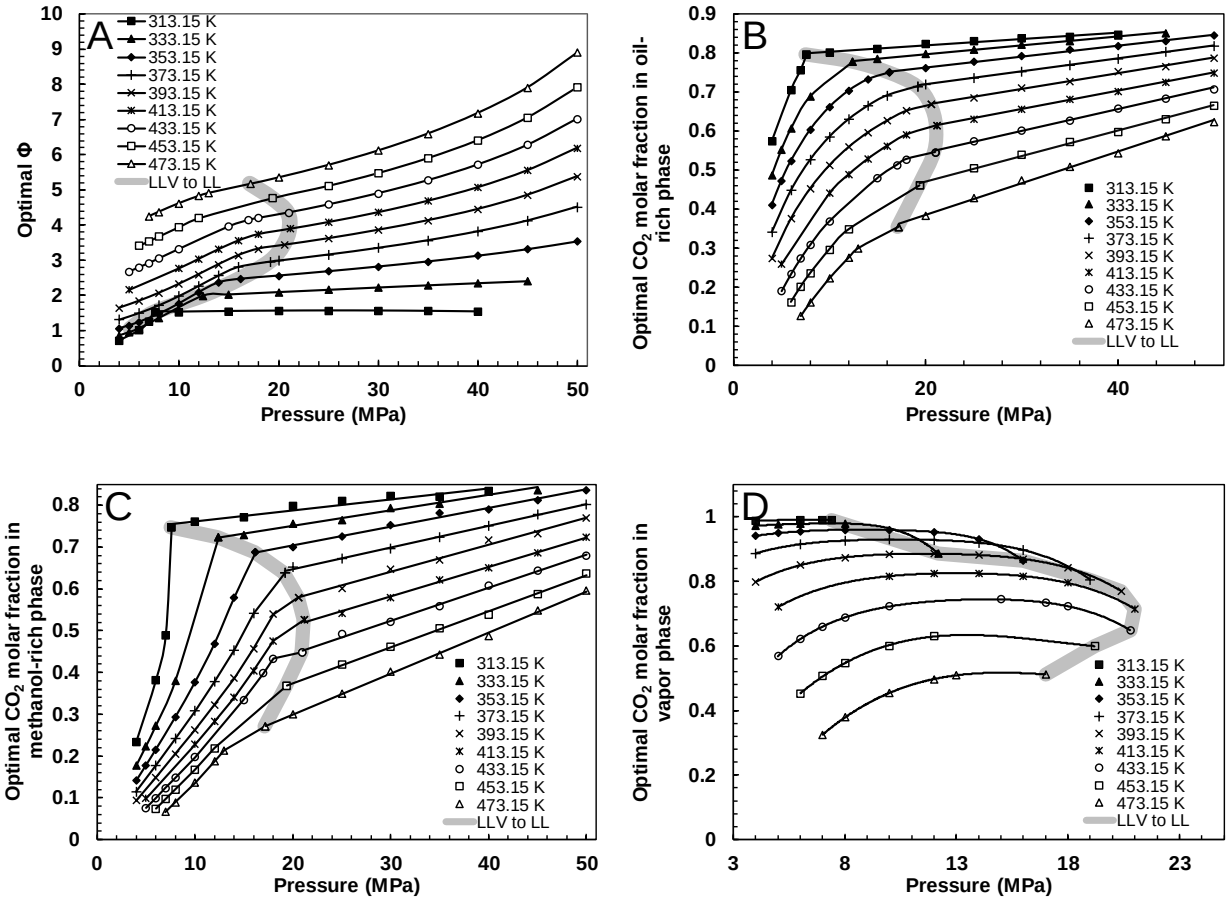

Figure 26 Optimization results for: Methanol to triolein ratio in the oil-rich phase (A), CO2 molar fraction in the liquid oil-rich phase (B) liquid methanol-rich phase (C) and vapor phase (D) (lines are polynomial interpolations to guide the eye).

The results in **Figure 26.A** show that the transition from a three-phase to a two-phase system exhibits a maximum in the neighborhood of 413K, which can be attributed to predictions of critical point loci for the carbon dioxide + methanol system, this temperature is close to midway between the pure components critical conditions when plotted in P-T space, thus when the gray-shaded area in **Figure 26** shows a maximal value of temperature as a function of pressure is also a maximum value of the critical temperature for the CO_2-methanol binary system [164]. In regards of the pressure values obtained they are effectively around 25% higher than the experimental values of critical pressure the CO_2- methanol pressure envelope probably due both the presence of triolein of the system, and a systematic overestimation of the critical conditions observed for this version of PC-SAFT for such binary systems as shown in NguyenHuynh et al [97]**.**

At temperatures below 353.15 K, there is only a weak dependence of Φ on temperature; in this regime the increase of methanol to oil ratio is mainly a pressure effect. The two phases in equilibrium at the optimal conditions have similar values of the CO_2 mole fraction, this is expected since the transition to LV happens when the tie lines in the triangular diagrams are very flat, and the optimal value is achieved near this transition.

At each point in **Figure 26.A** (maximum values of Φ at given temperature and pressure) one can employ the individual ternary phase diagram for each P-T pair to derive the mole fraction CO_2 in the triolein-rich, the methanol-rich, and, if present (3-phase splits), the CO_2-rich phases. These results are shown in **Figure 26.B** through **Figure 26.D**. Typically, the mole fraction of triolein is negligible in the methanol-rich and CO_2-rich phases, and hence in the first approximation the methanol mole fraction in these two phases is 1.0 minus the CO_2 concentration shown in **Figure 26.C** and **Figure 26.D**. Again, the gray-shaded area in **Figure 26.B** through **Figure 2624.D** shows the pressure at which the system transitions from LLV (left of the shaded area) to LL

equilibrium (right of the shaded area). Needless to say, this is why there are no points to the right of the gray-shaded area in **Figure 26.D**, as this represents the CO_2 mole fraction in the CO_2-rich "vapor-like' phase, which vanishes at pressures to the right of the shaded area.

Figure 26 contains all of the required information to estimate the CO_2 total concentration necessary for a given biodiesel system to run at optimal initial miscibility (Φ) provided that the P-T conditions and a total methanol to oil ratio (defined here as R) have been chosen. Pressure and temperature selection allow one to derive the CO_2 mole fraction in each of the potential phases from **Figure 26.B** to **Figure 26.D**, plus the value of the optimal ratio Φ from **Figure 26.A**. We construct a material balance for the system as shown in equations **6-2** to **6-5**:

$$z_{CO_2} = \beta_1 \cdot x_{CO_2}^{p_1} + \beta_2 \cdot x_{CO_2}^{p_2} + (1 - \beta_1 - \beta_2) \cdot x_{CO_2}^{p_3} \quad \text{6-2}$$

$$z_{Methanol} = \frac{\beta_1 \cdot \Phi}{(1+\Phi)} \cdot \left(1 - x_{CO_2}^{p_1}\right) + \beta_2 \cdot \left(1 - x_{CO_2}^{p_2}\right) + (1 - \beta_1 - \beta_2) \cdot \left(1 - x_{CO_2}^{p_3}\right) \quad \text{6-3}$$

$$z_{TO} = \frac{\beta_1}{(1+\Phi)} \cdot \left(1 - x_{CO_2}^{p_1}\right) \quad \text{6-4}$$

$$z_{Methanol}/z_{TO} = R \quad \text{6-5}$$

Here z_i refers to the total system mole fraction of the i[th] component, x_w^{pi} stands for the composition of component "w" in phase "i", and β_i is the total mole fraction of phase "i". All x_{CO_2} and Φ are known variables from the plots (**Figure 26**) at selected pressures and temperatures. Naturally, the case where the system contains only two phases is a subset of the above system where $\beta_1 + \beta_2 = 1$ – this effectively renders the third term of equation **6-3** zero, yielding a unique mathematical solution for the optimal CO_2 concentration. The ratio R (total moles of methanol to those of triglyceride in the system) is usually greater than 3.0 (the minimum amount for complete conversion to biodiesel), and often much greater than 3 (9 to 40) to try to account for losses of methanol to one or more of the phases that form initially and during reaction. If operation occurs

at conditions where 3 phases are present, the systems of equations represented by equations **6-2** to **6-5** is under-specified; this corresponds to the multiple possible solutions obtained for triphasic systems inside the LLVE area, as explained in section **6.2** and shown in **Figure 25.A** and **Figure 25.B**. Hence, in summary, one would choose a value of R, the temperature and pressure – and then calculate all z_i and β_i from the equations above to find the "correct" amount of CO_2 to add to the system to optimize the phase behavior for the reaction.

7.0 Predicting the optimal phase equilibria conditions for CO_2-enhanced biodiesel transesterification with polar PC-SAFT. [to be submitted to FUEL]

In section **6.0** it was shown that the concentration of carbon dioxide can be critical to enhance the miscibility of the initial biodiesel reactants. A second important issue regarding the phase equilibria for triglycerides transesterification rises when significant amounts of glycerol are present on the reactor. The strong association between glycerol and methanol effectively deprives the reaction of the necessary methanol reactant thus potentially lowering yields and increasing reaction times. Modelling phase equilibria with GC-PPCSAFT can be used to quantify the methanol distribution amongst each phase, which is key to the reaction process, and analyze potential improvements when carbon dioxide is used as a co-solvent in the reaction.

Glisic and Skala measured the behavior of a 3-phase multicomponent system containing methanol, glycerol, FAMEs, mono-, di- and triglycerides [47], they ran a transesterification reaction for ten thousand minutes without any catalyst to show the evolution of the phase equilibria as the reaction progresses. GC-PPC-SAFT, as described in chapter **6.0** was used for the pure component parameters of the glycerides and FAMES and the binary interaction parameters of the various pairs in this system. This data represents a challenging task from the modelling perspective because the experiments were conducted at high methanol contents, where small changes in molar concentration can generate large shifts in the overall phase behavior. **Figure 27** compares the obtained modelled molar fraction in each phase (**Figure 27.A** and **Figure 27.B**) with the experimental data (**Figure 27.C** and **Figure 27.D**). Good results in terms of the overall character of each phase were obtained, where the greatest error lies in a larger amount of methanol in the liquid phases, and consequentially a slightly higher solubility of glycerol in the oleic phase.

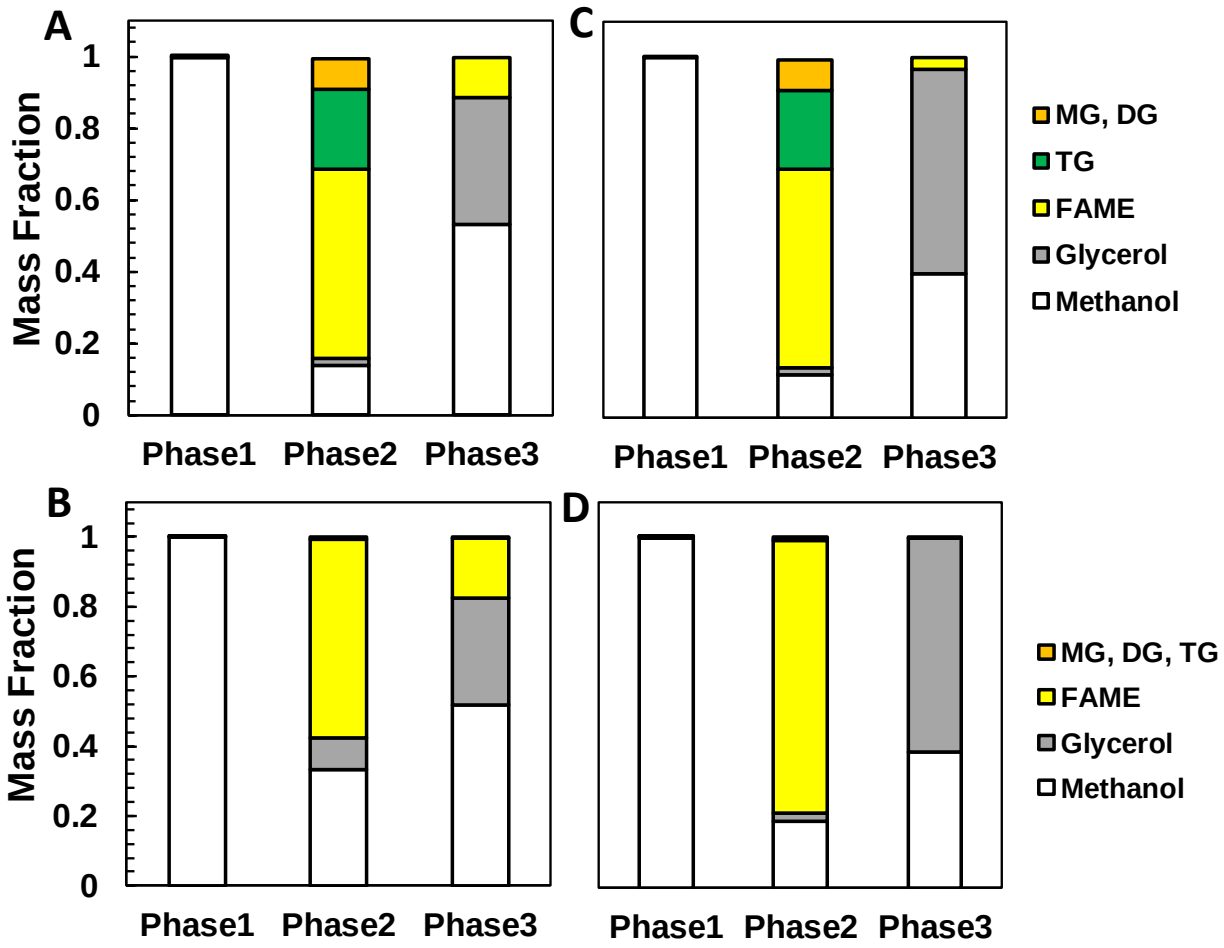

Figure 27 Three phase systems for multicomponent system modelled using PPC-SAFT (A and B) compared to experimental measurements from Glisic and Skala. at 2000 min and 10000 min of experiment (C and D) [47].

7.1 Phase equilibria of the CO_2 + methanol + glycerol + methyl oleate system.

Using the parameters derived from chapter **4.0** and **5.0**, predictions of the phase equilibria of the CO2 + methanol + glycerol + methyl oleate (MO) quaternary system have been performed to resolve how the methanol partition behaves with changing thermodynamic conditions. At sufficiently low values of pressure and temperature the phase equilibria transitions from LLE to a LLVE or to a single-phase system depending on increasing amounts of CO_2 or methanol respectively. The structural differences between FAMEs and glycerol generate two very distinct immiscible phases amongst which methanol distributes, likely favoring the glycerol phase due to strong hydrogen bonding and polar forces. Loss of methanol to a glycerol-rich phase effectively robs the glycerides of the key reactant needed to create biodiesel (FAME's). This trend can be mitigated by adding carbon dioxide, as shown in **Figure 28**. Due to stoichiometry of triglycerides (versus FAME's and glycerol) during transesterification, only 3:1 ratios of FAME to glycerol (and above) are worth studying unless reaction products are artificially added to reaction beforehand, such ratio is depicted in the straight line in **Figure 28**.

The CO_2 co-solvent effect can be observed in the reduction of the slope of the tie-lines in **Figure 28**, when plotted in a carbon free basis to make the molar fraction of the other three compounds comparable. The flattening of the tie-lines indicates that the molar ratio of methanol to methyl oleate has increased in the oil-rich phase (defined as Φ for this work and shown in eq **6-1** and the molar ratio of methanol to glycerol in the glycerol-rich phase has decreased (defined as Ψ for this work and shown in eq **7-1**).

$$\Psi = \frac{x_{methanol}}{x_{glycerol}}\Bigg|_{glycerol-rich\ phase} \qquad 7\text{-}1$$

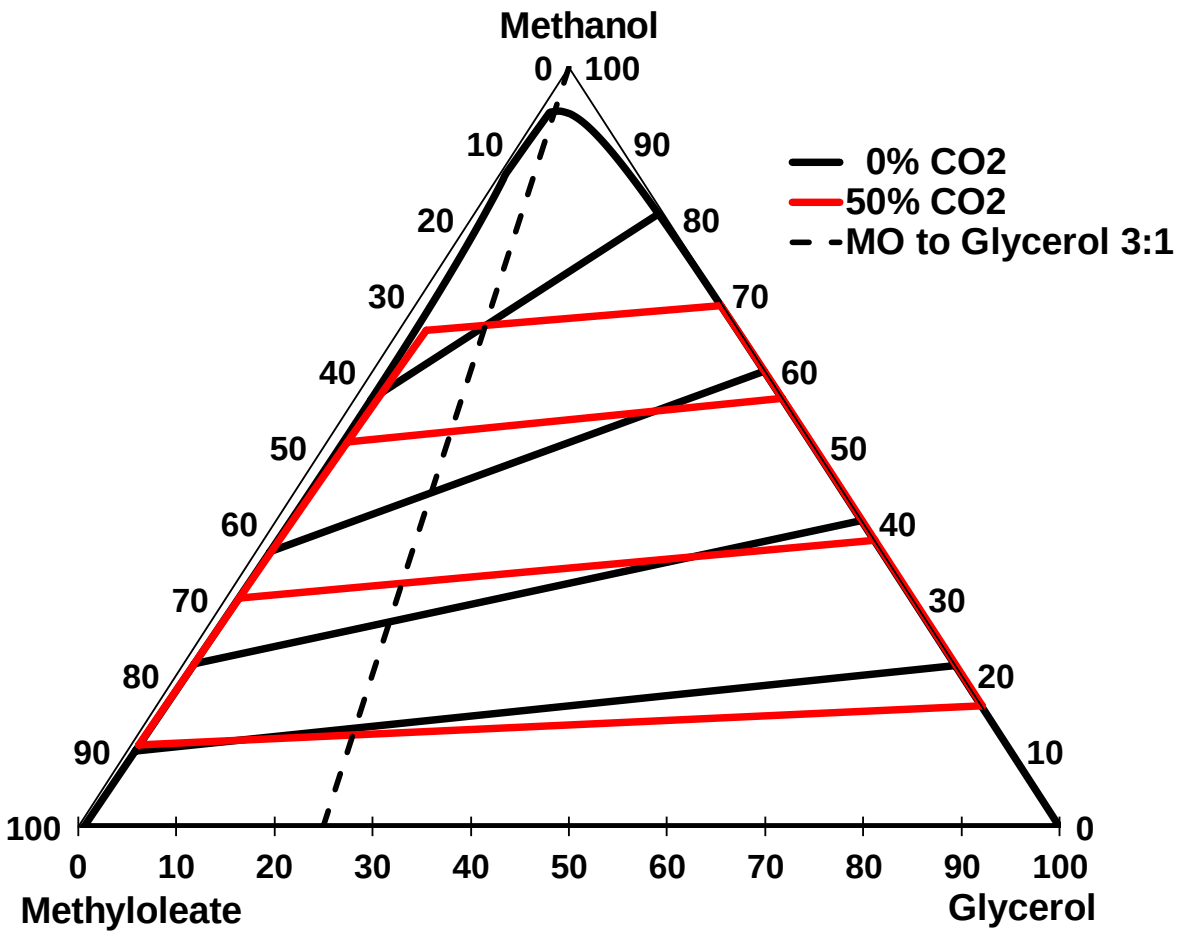

Figure 28 LLE of the methanol – glycerol – MO system with and without carbon dioxide at 353.15 K, 10 MPa and 3:1 MO to glycerol ratio.

7.2 Optimal CO_2 content for the CO_2 + methanol + glycerol + MO system.

The CO_2 + methanol + glycerol + MO quaternary can be fully represented in a three-dimensional space once pressure and temperature conditions are set. **Figure 28** represents a chosen slice or planar projection of the tetrahedron shown in **Figure 29**. Four projections of the quaternary system mole fraction surfaces are shown to further expand on the variation of the phase equilibria due to varying amounts of methanol and carbon dioxide. The addition of methanol only affects the immiscibility of glycerol and FAME at very high concentrations, as has been reported by various authors operating the transesterification in a single-phase reactor [16], [66]. Carbon dioxide has only a marginal effect on the immiscibility of the glycerol-FAME system, but does enhance the methanol-alkyl ester miscibility, therefore increasing Φ. Such effects can be better observed in the drop of methanol content in the glycerol phase, as seen on the projection of **Figure 29.A** and in the variation of the slope of the tie-lines in **Figure 29.B**. This effect is reversed when a third dense-vapor-phase becomes thermodynamically stable (since studied P-T conditions make CO_2 a supercritical fluid even though the rest of the mixture still lies below the critical value). Once the LLVE is established, the carbon dioxide phase solubilizes methanol, effectively depriving the rest of the phases of methanol -- this can be better appreciated by the drop of methanol content depicted in the tetrahedron projection on **Figure 29.C** for the data points connected with solid lines (triphasic equilibria). **Figure 29.D** is a planar projection showing the triple phase equilibrium formation at high carbon dioxide content.

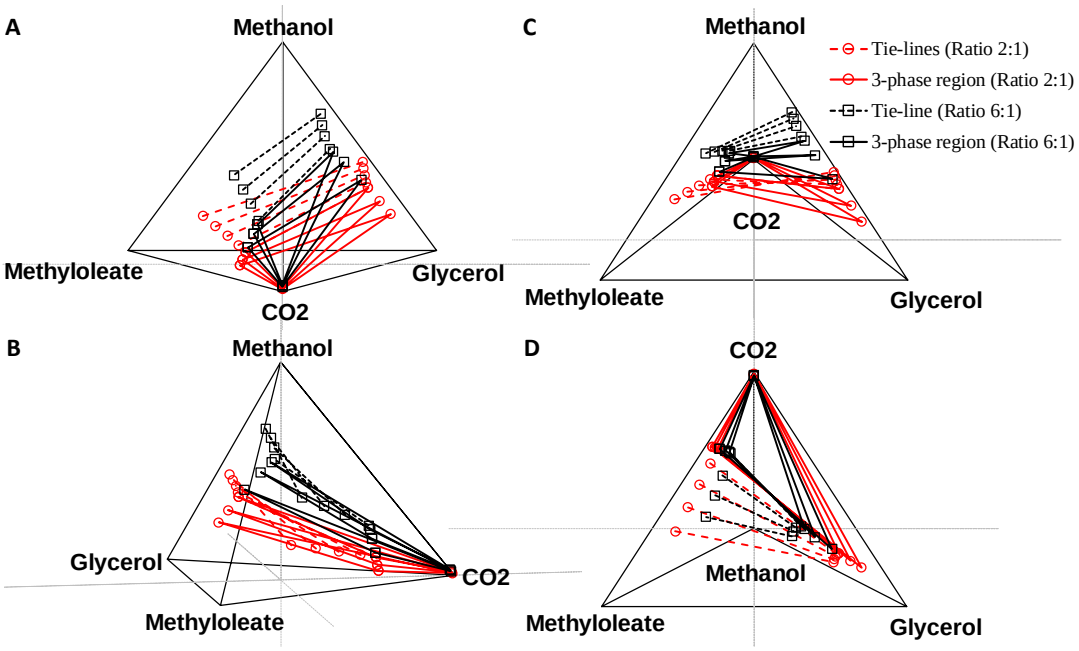

Figure 29 Multiple angles of the phase equilibria of CO_2 – methanol – glycerol – MO quaternary system showing the tie-lines for different CO_2 contents at 353.15 K, 10 MPa, 3:1 MO to glycerol ratio and two different methanol to glycerol ratios.

Similar results were established in a previous work for the CO_2 + Methanol + Trioleate systems, where increasing amount of carbon dioxide led to enhancement of the biodiesel reactants mutual solubility until the formation of a third stable vapor phase appears as shown section **6.2**. ***The opposing effects of adding carbon dioxide on enhancing methanol-FAME solubility while also reducing methanol content in both liquid phases when LLVE is established, leads to the presence of a mathematical optimum in terms of methanol content in the oil rich phase***. The optimal value is shown in **Figure 30.A** for the above defined molar ratios Φ, Ψ, and a diagram of the phase behavior is depicted on **Figure 30.B** highlighting the migration of methanol between the liquid phases in the presence of carbon dioxide and the depletion of methanol from all liquid phases when the vapor phase is formed.

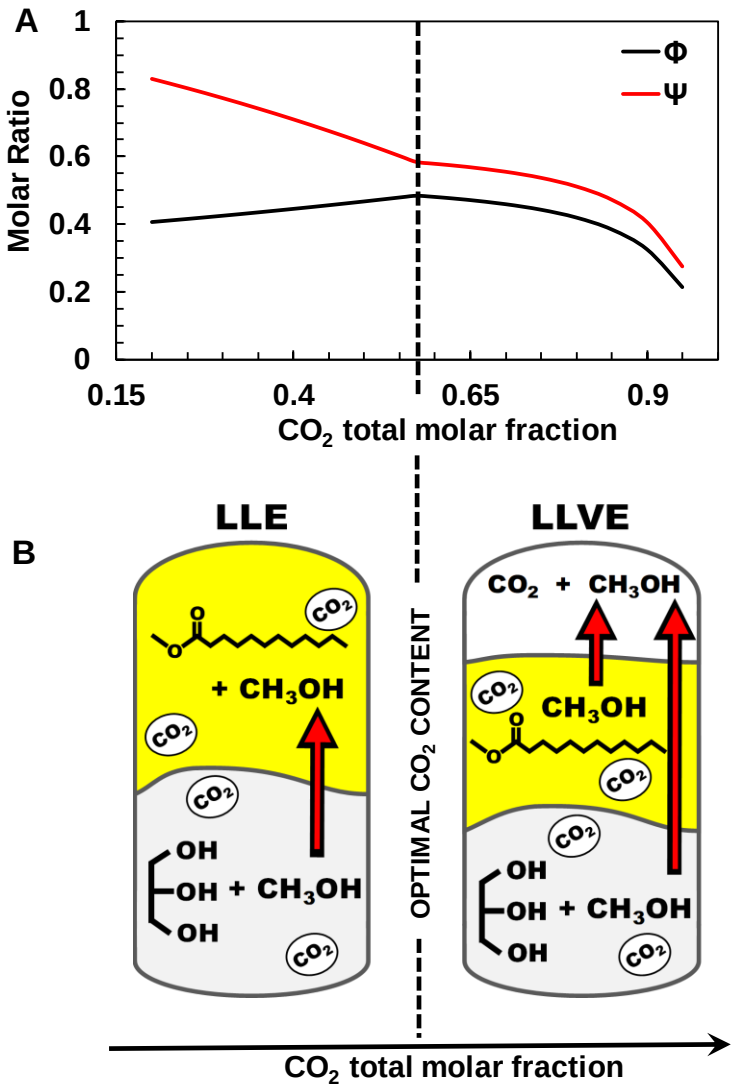

Figure 30 Presence of an optimal value of Φ at varying CO2 content for the studied system at 353.15 K, 10 MPa, 2:1 methanol to glycerol ratio and 3:1 MO to glycerol ratio (A). Picture of the multiple phases present before and after the optimal value is reached (B).

7.3 P, T and total methanol to glycerol molar ratio effect on optimal loci.

The same procedure mentioned above can be applied to a range of pressure and temperature conditions to explore how the optimal CO_2 loci varies. Increasing values of both P and/or T has proven beneficial to increment Φ as shown in **Figure 31**. Since the addition of CO_2 is beneficial, as long as carbon dioxide remains in the liquid phases, the thermodynamic effect for each case can be explained in terms of the formation of LLE or LLVE for each set of P-T conditions. Holding the temperature constant and increasing the value of pressure allows for higher solubility of carbon dioxide in both glycerol and methyl oleate phases, therefore favoring a higher ratio of methanol on methyl oleate as explained in the previous section (see **Figure 31.A**). Increasing the temperature of the mixture while holding the pressure constant renders all components less soluble in terms of a lighter vapor phase formation, consequentially the optimal value of Φ occurs at lower values of carbon dioxide total molar content since less CO_2 can be dissolved in each phase at higher T. However, there are two effects present: a temperature deactivation of the dispersive forces and hydrogen bonding that affects primarily the glycerol-methanol miscibility, thus increasing Φ (as well captured by PC-SAFT's association strength term dependence on temperature); and at the same time increasing temperatures can render the CO_2 – methanol mixture to fall in the sub-subcritical region making the vapor phase lighter and driving more methanol out of the liquid phase, therefore decreasing Φ (See CO_2 + methanol phase behavior in the critical region [67], [70], [74], [75]). The combination of these effect generates a reduction of the value of Φ, as long as the P-T conditions are supercritical for CO_2 – methanol and then a sequential increase of Φ as shown in **Figure 31.B**.

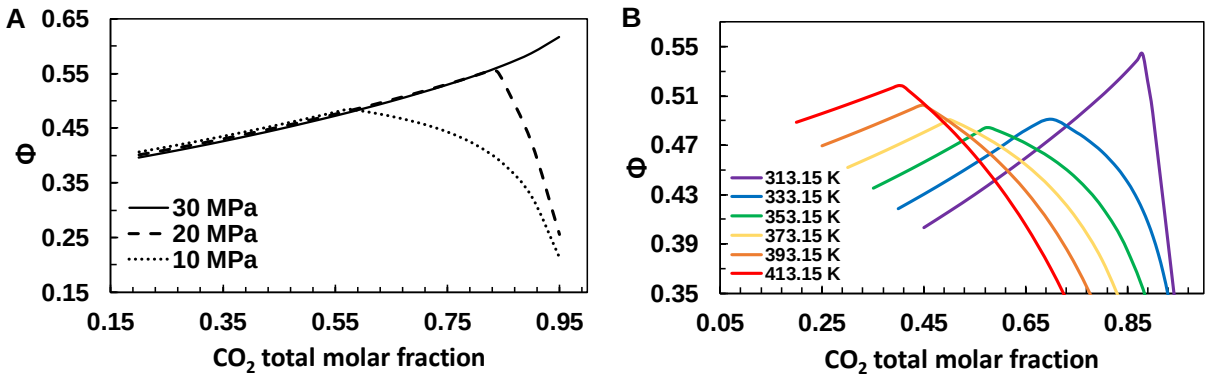

Figure 31 Effect of pressure on optimal Φ loci at 353.15 K, 2:1 methanol to glycerol and 3:1 MO to glycerol (A). Effect of temperature on optimal Φ loci at 10 MPa, 2:1 methanol to glycerol and 3:1 MO to glycerol (B).

The above-mentioned effects can be also appreciated in **Figure 30** showing the value of optimal Φ and optimal CO_2 content at different pressures and temperatures in a 3D surface for a specific methanol content (2:1 methanol to glycerol ratio). **Figure 32.A** shows the value of Φ can be generally improved by increasing P and T; however, **Figure 32.B** shows that the required amounts of CO_2 to reach the optimal values might be unrealistic for a biodiesel reactor (occasionally even 99% CO_2 is required at certain conditions). Therefore, a full investigation of the phase behavior can provide relevant information in terms of process conditions using carbon dioxide for biodiesel production.

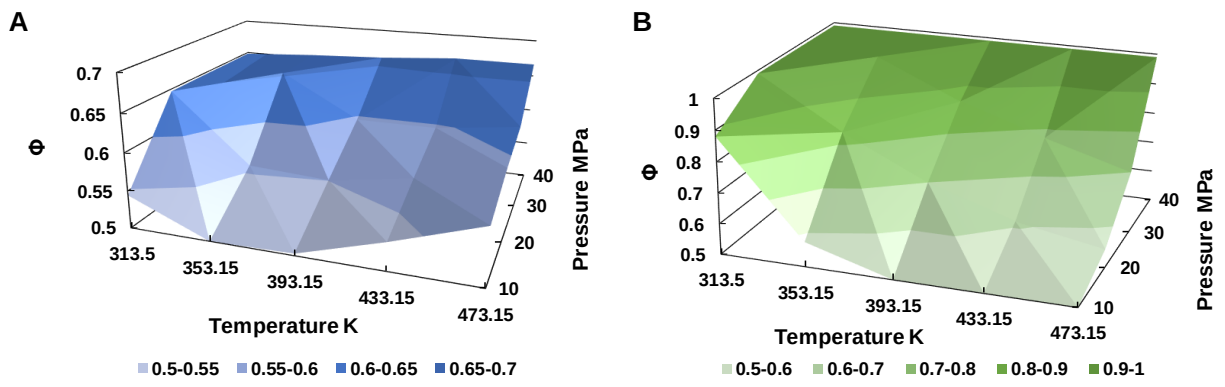

Figure 32 Effect of P – T conditions on optimal Φ (A) and optimal CO_2 content (B) at 2:1 methanol to glycerol and 3:1 MO to glycerol (B).

Variations of the methanol to oil ratio are frequently evaluated in experimental reactors to understand the impact of such ratios on the kinetics of the transesterification. However, as shown in section **7.1** this ratio also affects the phase behavior favoring a higher content of methanol in the oil rich phase. As shown in **Figure 33.A** there is significant spacing between the Φ value for each methanol to glycerol total molar ratio considered. This effect is expected since the methanol fraction is effectively increasing in all phases because the methanol total molar fraction is higher. Finally, CO_2 lowers the methanol to oil ratio required to generate a single-phase system -- in such cases a dramatic increase of Φ is expected and well reported in the literature for transesterifications operating in single phase systems at very high methanol to oil ratios. **Figure 33.B** shows the transition from a LLE system to a single phase system for 30:1 methanol to MO ratio and a range of CO_2 molar content that varies from 20 – 40%. After these conditions increasing amounts of carbon dioxide will generate a third phase that progressively subtracts methanol from the liquid phase thus lowering the Φ ratio.

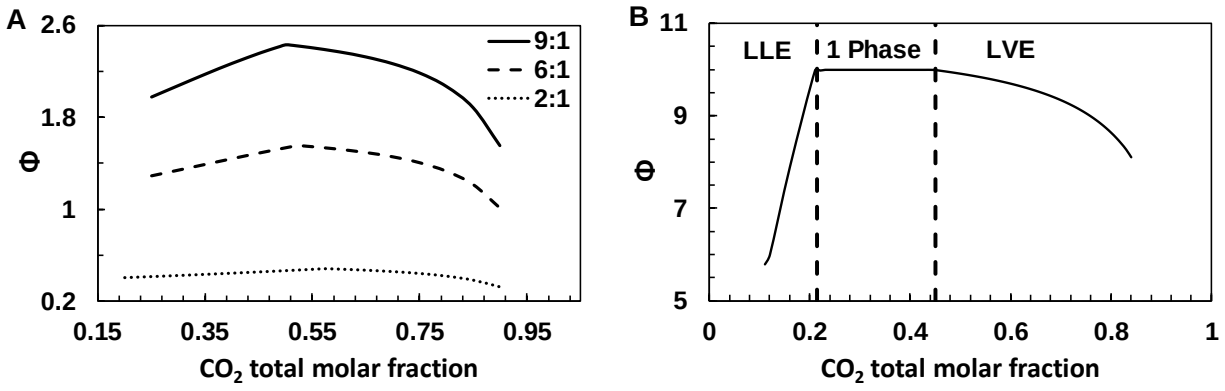

Figure 33 Effect of methanol to glycerol ratio on optimal Φ loci at 353.15 K, 10 MPa and 3:1 MO to glycerol (A). Φ value at varying CO2 content at 353.15 K, 10 MPa, 30:1 methanol to glycerol ratio and 3:1 MO to glycerol ratio (B).

8.0 Conclusions

A systematic basis to model multicomponent biodiesel related mixtures that include CO_2 was evaluated using PPC-SAFT and GC-PPC-SAFT. Similar errors were obtained for phase behavior prediction in relation to those found in literature using both PC-SAFT and other EoS regarding isolated binaries or ternary biodiesel related systems. The polar term inclusion lowers the error in phase behavior prediction involving highly polar components, particularly glycerol containing systems. Low temperature independent binary interaction coefficients that can be easily extended to different types of FAME and FAEE were obtained suggesting good predictability of the model and providing a basis to estimate relevant conditions for biodiesel production with carbon dioxide as a co-solvent.

The PC-SAFT model modified with a polar term was also employed to evaluate the phase behavior of various tri-, di- and monoglycerides mixed with those small molecules relevant to biodiesel reactions where CO_2 is used as a cosolvent. As expected, the model handles well the binary interaction of the glycerides with other components but is not nearly as accurate when predicting the pure component properties of the triglycerides themselves, which leads to larger errors in binary systems at very high molar concentration of glycerides. Because little data regarding binary mixtures of monoglycerides with small molecules are available, experimental results on the MG-methanol-CO_2 ternary were acquired and used to extract the binary interaction coefficient between MG's and methanol. In general, errors in predicted phase envelope loci for these glyceride systems were higher than for analogous binary and ternary mixtures containing the fatty acid methyl esters (FAMES), likely owing to higher errors in predicting pure component glyceride properties than for the FAMES. However, the model was able to provide good

descriptions of ternary systems that incorporate the key components of a biodiesel-oriented esterification reaction where CO_2 is employed as a cosolvent.

The derived model using PPC-SAFT, GC-PPC-SAFT and binary interaction coefficients fitted to experimental data was used as a tool for prediction of the optimal conditions under which to operate a transesterification reaction of a triglyceride with methanol to form biodiesel (fatty acid methyl esters of the triglyceride). CO_2 is typically added to a biodiesel system (methanol + triglyceride) to enhance the mutual miscibility of the two reactants, which is otherwise poor. As such, the methanol to triolein ratio in the oil-rich phase (Φ) has been investigated as an indicator of the degree to which added CO_2 (as a function of temperature and pressure) improves the situation, as higher methanol-to-oil ratio initially should lead to faster rates. Using the model, it was found the phase behavior of the CO_2 + methanol + triolein system exhibits, for all pressure and temperature conditions, an optimal value of composition (added CO_2) at which the methanol to oil ratio is maximized. It was found that this optimal value was effectively at the point where the system transitions from 3 phases to 2. A full map depicting the influence of P-T conditions at optimal composition was provided using PPC-SAFT.

PPC-SAFT and GC-PPC-SAFT, along with binary calculations performed with available data, were used to predict the phase separation of the quaternary system CO_2 -methanol- glycerol-FAME. The phase equilibria calculations reveal that carbon dioxide addition to the biodiesel transesterification process could provide tangible benefits regarding the miscibility of methanol in the oleic phase by reducing methanol depletion due to the formation of the glycerol byproduct. Pressure, temperature and the methanol to oil ratio have a relevant influence in the phase separation and can be tuned based on theoretical calculations to modify the phase equilibria of a transesterification process running at sub-critical conditions. Also, it was confirmed that the

presence of CO_2 can reduce the required pressure and temperature to generate a single-phase system, proving beneficial even if used for supercritical transesterification. Carbon dioxide optimal composition were consistently found at the point where the formation of a third (LLVE) or second phase (LVE) is imminent, thus providing a path for designing transesterification processes using CO_2 as a co-solvent and experimentally searching for optimal conditions.

9.0 Future work

The parameters calculated in chapters **4.0** and **5.0** complete the necessary basis to perform phase behavior predictions of methanolysis and ethanolysis of triglyceride reactive systems. Also, they provide a valuable virtual source to calculate optimal thermodynamic conditions to increase the solubility of the transesterification reactants when carbon dioxide is employed as a co-solvent in the reaction. Moreover, they allow one to investigate the behavior of all reactants, products and intermediaries of the biodiesel reaction throughout the reaction process and can be used to show how CO_2 can modify phase behavior when operating at sub-critical mixture conditions. In order to expand the model, other substances commonly present in the feed during biodiesel transesterification can be incorporated (i.e. water, free fatty acids). Such substances can alter the phase equilibria significantly provided they are present in high enough concentrations, but their inclusion requires analyzing pure component, binary and ternary data to obtain PPC-SAFT parameters and binary interaction coefficients to make the phase equilibria as "realistic" as possible.

Optimal values for maximum solubility of biodiesel reactants were consistently found in the transition of a LLE or a LLVE to a simpler LVE when using carbon dioxide in chapter **6.0**, this method can be extended to investigate the dependence of optimal conditions on the FAME's molecular weight and number of unsaturations. Similarly, when the transesterification reaction has progressed carbon dioxide showed a positive effect in avoiding methanol depletion into the glycerol phase, but the composition of the present FAME, carbon chain length and number of unsaturation can alter this effect since there is a strong influence of this parameters with the FAMES vapor pressure. Therefore, using the method developed in chapter **7.0** by searching for

the formation of the LVE equilibria can be used to build a dependence of the optimal loci with these parameters.

Section **7.3** showed very briefly that at very high contents of methanol and CO_2 a single phase can be formed, dramatically increasing the value of Φ. Even though such conditions are in reality closely related to supercritical transesterification, since the two most abundant components (methanol and CO_2) are close or above critical conditions, however the thermodynamic model is able to provide with trends for the dependence of optimal Φ with pressure, temperature and methanol to oil ratio in order to achieve a single phase system.

Optimal values of miscibility are dependent on all present substances in a transesterification reaction: the influence that commonly present "impurities" of the biodiesel reaction (i.e. free fatty acids, water, etc.) have on the phase equilibria of the system and the sensitivity of the optimal values on the content of these substances has yet to be explored.

Ultimately the goal of biodiesel research focuses on attaining high purity FAMES or FAEES that can be used in diesel engines by lowering the cost of production. The modification of the phase behavior of the reactive system based on thermodynamic predictions is a promising mean to obtain improvements in this process. However, once the phase equilibria has been optimized to warrant maximum solubility of reactants or the desired products, the improvement over transesterification reaction times and yield can only be investigated by coupling the thermodynamic predictions with a kinetic model or by experimentally observing the improvement obtained with the thermodynamic predictions.

Appendix A **Polar PC-SAFT and Group Contribution PC-SAFT**

Chapman et al. expressed the chosen reference fluid to be monomeric clusters of chainlike molecules and Every thermodynamic potential and derived property can be calculated based on three segment parameters: the number of segments *m*, and the Lennard Jones parameters for the segment: diameter σ (Å) and potential depth ε (K). The reference fluid was later modified by Gross and Sadowski in the development of PC-SAFT to be hard chain molecules, and expressed the Helmholtz free energy of the reference fluid as follows [85]:

$$A^{hc} = RT\left(\overline{m}A^{hs} + \sum_i x_i(1-m_i)\cdot ln(g_{ii}(d_{ii})^{hs})\right) \quad \text{A-1}$$

$$\overline{m} = \sum_i x_i m_i \quad \text{A-2}$$

Where m is the number of segments in the chain and $(g_{ii}(d_{ii})^{hs})$ is the radial distribution function of a mixture of hard sphere derived by Reed and Gubbins [165]:

$$g_{ij}(d_{ij})^{seg} = \frac{1}{1-\zeta_3} + 3\left[\frac{d_{ii}d_{jj}}{d_{ii}+d_{jj}}\right]\frac{\zeta_2}{(1-\zeta_3)^2} + 2\left[\frac{d_{ii}d_{jj}}{d_{ii}+d_{jj}}\right]^2\frac{{\zeta_2}^2}{(1-\zeta_3)^3} \quad \text{A-3}$$

Where ζ_k is given by:

$$\zeta_k = \frac{\pi N_{av}}{6}\cdot\rho\cdot\sum_i x_i m_i {d_{ii}}^k \quad \text{A-4}$$

And d is an effective temperature diameter linearly dependent of the Lennard-Jones hard sphere diameter and a function of the reduced temperature and the number of segments present in the chain that accounts for soft repulsion:

$$d_i = \sigma\left(1-0.12e^{-\frac{3\varepsilon_i}{kT}}\right) \quad \text{A-5}$$

The Association forces contribution to Helmholtz free energy was re-used from Chapman et al. [112] since bonding association was approximated with a square well potential happening amongst specific sites in monomers present in a mixture of polymer chains.

$$A^{assoc} = RT\left(\sum_i x_i\left[\frac{m_i}{2} + \sum_{A_i} ln\left(X^{A_i}\right) - \frac{X^{A_i}}{2}\right]\right) \quad \text{A-6}$$

Where X^{A_i} is the fraction of the of molecules not bonded to a given site A in one segment of the chain molecule and is given by:

$$X^{A_i} = \left(1 + \sum_j \sum_B \rho_j \cdot X^{B_j} \cdot \Delta^{A_i B_j}\right)^{-1} \quad \text{A-7}$$

Where ρ_j is the density of the fluid and $\Delta^{A_i B_j}$ is the association strength given by:

$$\Delta^{A_i B_j} = d_{ij}^3 g_{ij}\left(d_{ij}\right)^{seg} \kappa^{A_i B_j}\left(e^{\frac{\varepsilon^{A_i B_j}}{kT}} - 1\right) \quad \text{A-8}$$

Two more pure components parameters are hereby introduced: κ^{AB} represents a volumetric overlap characterization of site AB and a given unique value of energy potential for bonding occurrence ε^{AB}. [Sub-indexes *i* and *j* refer to bonding sites in segments of different chains]

The final Perturbation term is a chain to chain interaction to account for dispersion forces of Lennard-Jones spheres in mixtures of spheres expressed as a second order perturbation as proposed by Barker and Henderson [117] and extended for chains with Gross and Sadowski's approximation.

$$A^{disp} = A_1 + A_2 \quad \text{A-9}$$

$$A_1 = -RT2\pi\rho I_1(\eta, \bar{m}) \sum_i \sum_j x_i x_j m_i m_j \left(\frac{\varepsilon_{ij}}{kT}\right) {\sigma_{ij}}^3 \quad \text{A-10}$$

$$A_2 = -(RT\rho)^2\pi\bar{m}\left(RT\rho + \frac{\partial A^{hc}}{\partial\rho} + \rho\frac{\partial^2 A^{hc}}{\partial\rho^2}\right)^{-1} I_2(\eta,\bar{m})\sum_i\sum_j x_i x_j m_i m_j \left(\frac{\varepsilon_{ij}}{kT}\right)^2 {\sigma_{ij}}^3 \quad \text{A-11}$$

Where the interaction integrals are polynomials of the packing fraction:

$$I_1(\zeta_4,\bar{m}) = \sum_{i=0}^{6} a_i {\zeta_4}^i \quad \text{A-12}$$

$$I_2(\zeta_4,\bar{m}) = \sum_{i=0}^{6} b_i {\zeta_4}^i \quad \text{A-13}$$

And the constants are dependent on average segment number and fitted constants that have been generalized using alkanes phase equilibria data following the nearest neighbor approximation suggested by Stell and Cummings [166], [167]:

$$a_i(m) = a_{0i} + \frac{\bar{m}-1}{\bar{m}}a_{1i} + \frac{\bar{m}-1}{\bar{m}}\frac{\bar{m}-2}{\bar{m}}a_{2i} \quad \text{A-14}$$

$$b_i(m) = b_{0i} + \frac{\bar{m}-1}{\bar{m}}b_{1i} + \frac{\bar{m}-1}{\bar{m}}\frac{\bar{m}-2}{\bar{m}}b_{2i} \quad \text{A-15}$$

Substance parameters involving a pair of unlike parameters are estimated using combining rules as shown below:

$$\sigma_{ij} = \frac{\sigma_{ii}+\sigma_{jj}}{2} \quad \text{A-16}$$

$$\varepsilon_{ij} = \sqrt{\varepsilon_{ii}\varepsilon_{jj}}\cdot(1-k_{ij}) \quad \text{A-17}$$

$$\varepsilon^{A_iB_j} = \varepsilon^{A_jB_i} = \frac{\varepsilon^{A_iB_i}+\varepsilon^{A_jB_j}}{2} \quad \text{A-18}$$

$$\kappa^{A_iB_j} = \sqrt{\kappa^{A_iB_i}\cdot\kappa^{A_jB_j}} \quad \text{A-19}$$

Where k_{ij} is the binary interaction coefficient required to adjust for oversimplifications done throughout the development of the equation of state.

Twu et al. suggested a segment localized polar contribution term based on a padé approximation of a third order perturbation theory expressed as [87]–[89]:

$$A^{pol} = A_2 \left[\frac{1}{1 - \frac{A_3}{A_2}} \right] \quad \text{A-20}$$

Where A_2 and A_3 are a sums of binary and ternary polar interaction contribution to the free energy respectively:

$$A_2 = A_2^{mult}(112) + 2A_2^{mult}(123) + A_2^{mult}(224) \quad \text{A-21}$$

$$A_3 = A_{3A} + A_{3B} \quad \text{A-22}$$

Each term is the contribution of a binary or ternary interaction of polar segments imbedded in the chains:

$$A_{3A} = 3A_{3A}^{mult}(112,112,224) + 6A_{3A}^{mult}(112,123,213) + 6A_{3A}^{mult}(123,123,224) + A_{3A}^{mult}(224,224,224) \quad \text{A-23}$$

$$A_{3B} = 3A_{3B}^{mult}(112,112,112) + 6A_{3B}^{mult}(112,123,123) + 6A_{3B}^{mult}(123,123,224) + A_{3B}^{mult}(224,224,224) \quad \text{A-24}$$

As used by Nguyen et al. [111] The equations for each contribution have been adjusted to deal with chain molecules instead of segments by incorporating a polar fraction of the chain x_{pi}^{μ} for molecules with dipole moment or x_{pi}^{Q} for molecules with quadrupolar moment and the equations are given by:

$$A_2(112) = -\frac{2}{3}\frac{\pi N_{av}\rho}{kT}\sum_i\sum_j x_i x_j x_{pi}^{\mu} x_{pj}^{\mu} m_i m_j \frac{\mu_i^2\mu_j^2}{d_{ij}^3} J_{ij}^{(6)} \quad \text{A-25}$$

$$A_2(123) = -\frac{\pi N_{av}\rho}{kT}\sum_i\sum_j x_i x_j x_{pi}^{\mu} x_{pj}^{Q} m_i m_j \frac{\mu_i^2 Q_j^2}{d_{ij}^3} J_{ij}^{(8)} \quad \text{A-26}$$

$$A_2(224) = -\frac{14}{5}\frac{\pi N_{av}\rho}{kT}\sum_i\sum_j x_i x_j x_{pi}^{Q} x_{pj}^{Q} m_i m_j \frac{Q_i^2 Q_j^2}{d_{ij}^3} J_{ij}^{(10)} \quad \text{A-27}$$

As proposed by Nguyen et al. [121] the only relevant term for a Ternary polar interaction when three polar segments are localized in two molecules is the $\mathrm{A}_{3\mathrm{A}}(224{,}224{,}224)$ term. Since for this approximation all molecules have only one dipolar or a quadrupolar moment, consequentially the term $3\mathrm{A}_{3\mathrm{A}}^{\mathrm{mult}}(112{,}112{,}224) + 6\mathrm{A}_{3\mathrm{A}}^{\mathrm{mult}}(112{,}123{,}213) + 6\mathrm{A}_{3\mathrm{A}}^{\mathrm{mult}}(123{,}123{,}224)$ will always drop to zero.

$$A_{3A}(224{,}224{,}224) = -\frac{144}{245}\frac{\pi N_{av}\rho}{(kT)^2}\sum_i\sum_j x_i x_j x_{pi}^{Q} x_{pj}^{Q} m_i m_j \frac{Q_i^3 Q_j^3}{d_{ij}^3} J_{ij}^{(15)} \quad \text{A-28}$$

$A_{3b}(112{,}112{,}112)$

$$= -\frac{32}{135}\left(\frac{14\pi}{5}\right)^{0.5}\frac{N_{av}\rho^2}{(kT)^2}\sum_i\sum_j\sum_k x_i x_j x_k x_{pi}^{\mu} x_{pj}^{\mu} x_{pk}^{\mu} m_i m_j m_k \frac{\mu_i^2\mu_j^2\mu_k^2}{d_{ij}d_{ik}d_{jk}} K_{ijk}^{(222,333)} \quad \text{A-29}$$

$A_{3b}(112{,}123{,}123)$

$$= -\frac{64\pi^3}{315}(3\pi)^{0.5}\frac{N_{av}\rho^2}{(kT)^2}\sum_i\sum_j\sum_k x_i x_j x_k x_{pi}^{\mu} x_{pj}^{\mu} x_{pk}^{Q} m_i m_j m_k \frac{\mu_i^2\mu_j^2 Q_k^2}{d_{ij}d_{ik}^2 d_{jk}^2} K_{ijk}^{(233,344)} \quad \text{A-30}$$

$A_{3b}(123{,}123{,}224)$

$$= -\frac{32\pi^3}{45}\left(\frac{22\pi}{63}\right)^{0.5}\frac{N_{av}\rho^2}{(kT)^2}\sum_i\sum_j\sum_k x_i x_j x_k x_{pi}^{\mu} x_{pj}^{Q} x_{pk}^{Q} m_i m_j m_k \frac{\mu_i^2 Q_j^2 Q_k^2}{d_{ij}^2 d_{ik}^2 d_{jk}^2} K_{ijk}^{(334,445)} \quad \text{A-31}$$

$A_{3b}(224,224,224)$

$$= -\frac{32\pi^3}{2025}(2002\pi)^{0.5}\frac{N_{av}\rho^2}{(kT)^2}\sum_i\sum_j\sum_k x_i x_j x_k x_{pi}^{\mu} x_{pj}^{Q} x_{pk}^{Q} m_i m_j m_k \frac{Q_i^2 Q_j^2 Q_k^2}{d_{ij}^3 d_{ik}^3 d_{jk}^3} K_{ijk}^{(444,555)} \qquad \text{A-32}$$

This approach assumes well localized dipolar and quadrupolar moments and it neglects induction forces. Each molecule polar contribution is characterized by a dipolar or Quadrupolar moment (*D* or *Q* respectively) and a number of segments of the chain ($x_p m$) where the polar forces are localized. The

Dipolar and quadrupolar experimental values can be used directly however the fraction of polar segments in the chain is generally considered a fitting parameter.[111] Even if the number of polar segments in a chain is well known the dipolar forces are not entirely localized. Therefore, some degree of flexibility is allowed for the $x_p m$ parameter.

The J and K integrals are correlation functions for a pure Lennard-Jones reference fluid. And are an expansion dependent on reduced density and Temperature given by

$$log\left|J^{(n)}\right| = A_n\rho^{*2} ln\,(T^*) + B_n\rho^{*2} + C_n\rho^* ln\,(T^*) + D_n\rho^* + E_n ln\,(T^*) + F_n \qquad \text{A-33}$$

And the constants A_n, B_n, C_n, D_n, E_n and F_n are fitted constants given In Twu and Gubbins [88].

Appendix B **Temperature dependent binary coefficient for the CO_2 glycerol system**

Binary interaction for the CO_2 – glycerol parameters will be calculated using available L-V equilibrium data [61]. A temperature dependent binary coefficient as proposed by Chen et al. [168] was herby tested as shown equation **B-1**, as opposed as the simple constant value for the binary coefficient ($k1_{ij} \neq 0$ and $k2_{ij} = 0$) used throughout the rest of this work.

$$k_{ij} = k_{1ij} + \frac{k_{2ij}}{T[K]} \qquad \text{B-1}$$

Obtained results were still not significantly better than the ones obtained with the simpler approach. Results are shown in **Table 13.**

Table 13 Binary interaction coefficients for best set of glycerol with CO_2 modelling

	Npts	Parameters				Average errors			
		SET V / SET IV		SET I*/ SET II*		SET V / SET IV		SET I*/ SET II*	
Assoc Sites		K_{1ij}	K_{2ij}	K_{1ij}	K_{2ij}	P	X	P	X
4 sites	12	0.3877	-94.558	0.198	-79.336	22.5%	18.1%	19.3%	20.4%
6 sites		0.329	-66.248	0.1606	-73.377	20.2%	15.9%	22.7%	20.9%

*Data sets from Barreau et al. [98]

Appendix C **Optimized parameters for triglycerides subgroup to use with the GC-PPCSAFT**

Eight triglycerides were considered for the parametrization of an optimized trimester core for triglycerides. However, no substantial improvements were found in any of the binary or ternary systems considered in chapter **5.0**. Parameters results and graphical representation are shown in **Table 14** and **Figure 34** below.

Table 14 Sub group parameter calculated for triglycerides

Subgroup	Assoc.	*m*	*σ (Å)*	*ε/k (K)*
-CH_2- (TG)		0.39898	3.851987	282.5454
-$C_3H_5O_3$<	3Sites	2.151871	3.277518	374.3759

The Parameters on **Table 14** were calculated while reusing the same parameters for the CH3- group described in section **4.1** and the same criteria for polar parameters described in section **5.1**.

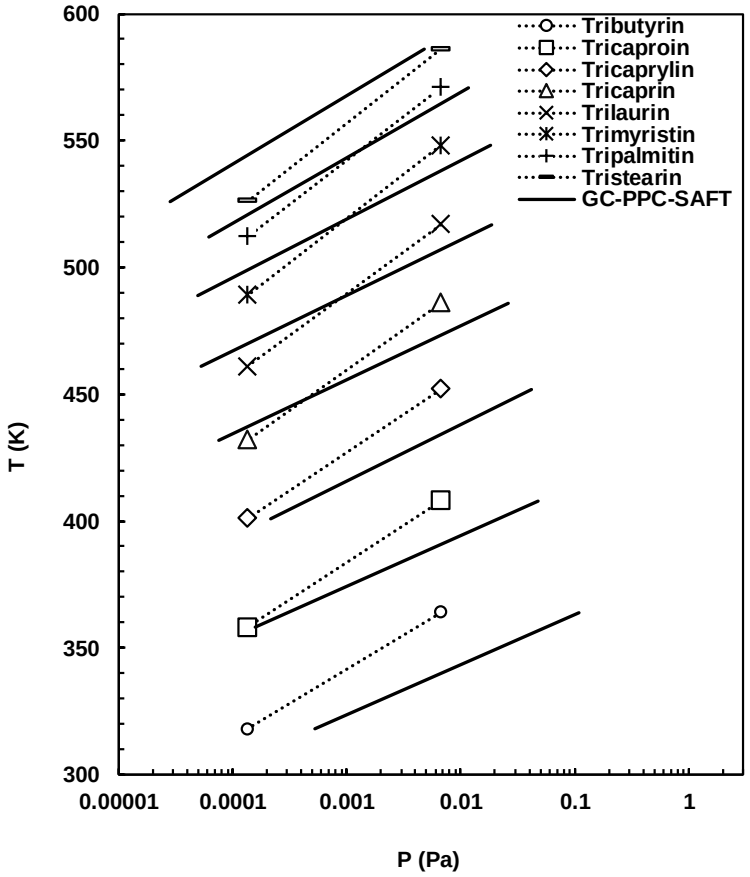

Figure 34 Experimental data from Perry et al. [99] and and pure component parametrization of vapor pressure for eight triglycerides using GC-PPCSAFT

Appendix D **Calibration experiments for phase equilibria measurements**

Curves for CO_2 with methanol were measured at different temperatures and compared with available literature data shown in **Figure 35** Methanol Phase equilibria measurements and literature data [162], [169]–[171].. Good agreement with data measured in literature was obtained, thus showing correct experimental setup for the rest of the required phase-equilibria measurements from section **5.2.2** .

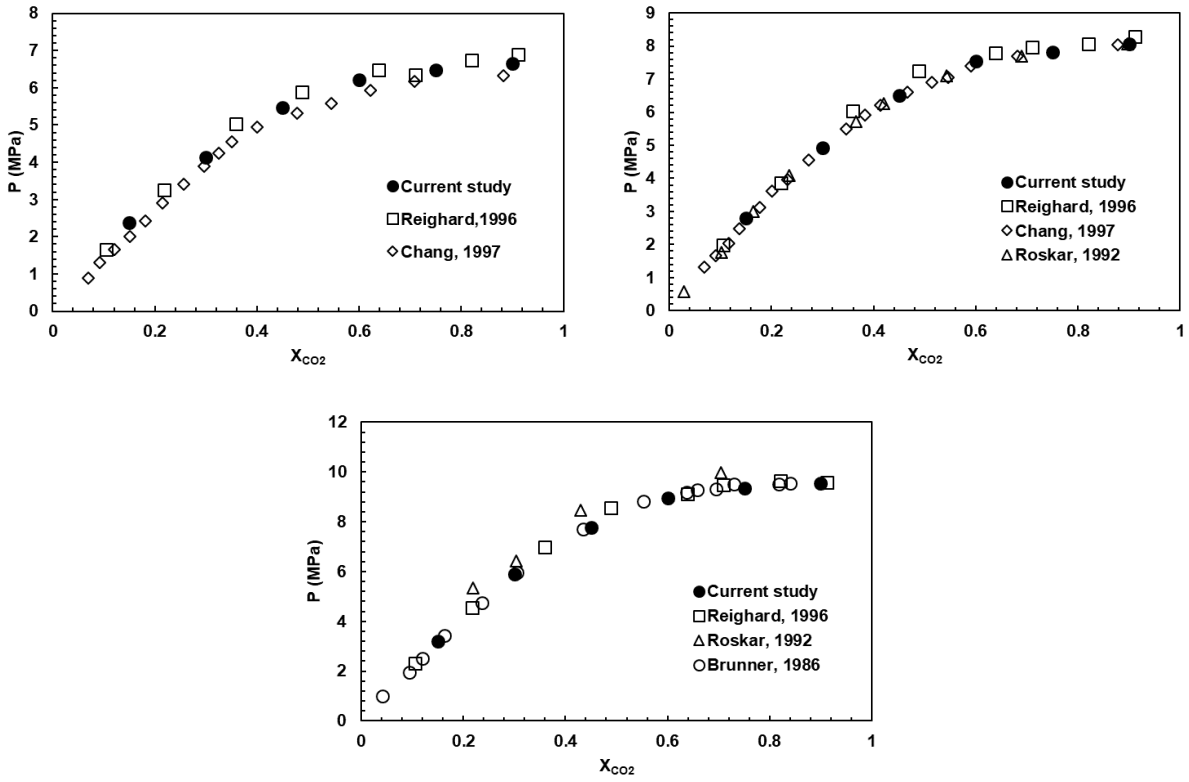

Figure 35 Methanol Phase equilibria measurements and literature data [162], [169]–[171]**.**

Bibliography

[1] J. Hill, E. Nelson, D. Tilman, S. Polasky, and D. Tiffany, "Environmental, economic, and energetic costs and benefits of biodiesel and ethanol biofuels.," *Proc. Natl. Acad. Sci. U. S. A.*, vol. 103, no. 30, pp. 11206–10, 2006.

[2] Z. Hu, P. Tan, X. Yan, and D. Lou, "Life cycle energy, environment and economic assessment of soybean-based biodiesel as an alternative automotive fuel in China," *Energy*, vol. 33, no. 11, pp. 1654–1658, 2008.

[3] T. Pinnarat and P. E. Savage, "Assessment of noncatalytic biodiesel synthesis using supercritical reaction conditions," *Ind. Eng. Chem. Res.*, vol. 47, no. 18, pp. 6801–6808, 2008.

[4] J. Sheehan, V. Camobreco, J. Duffield, M. Graboski, and H. Shapouri, "An overview of biodiesel and petroleum diesel life cycles," *U.S.Department Agric. U.S Dep. Energy*, no. May, pp. 1–60, 1998.

[5] S. Saka and D. Kusdiana, "Biodiesel fuel from rapeseed oil as prepared in supercritical methanol," *Fuel*, vol. 80, no. 2, pp. 225–231, 2001.

[6] C. R. Coronado, J. A. de Carvalho, and J. L. Silveira, "Biodiesel CO2 emissions: A comparison with the main fuels in the Brazilian market," *Fuel Process. Technol.*, vol. 90, no. 2, pp. 204–211, 2009.

[7] U.S. Energy Information Administration, "Monthly biodiesel production report," 2019. [Online]. Available: http://www.eia.gov/biofuels/biodiesel/production/.

[8] A. A. Mayvan, "Current biodiesel production technologies : a comparative review . Energy Convers Manag," vol. 63, no. AUGUST, pp. 138–148, 2012.

[9] B. Karmakar and G. Halder, "Progress and future of biodiesel synthesis: Advancements in oil extraction and conversion technologies," *Energy Convers. Manag.*, vol. 182, no. September 2018, pp. 307–339, 2019.

[10] P. Hegel, A. Andreatta, S. Pereda, S. Bottini, and E. A. Brignole, "High pressure phase equilibria of supercritical alcohols with triglycerides, fatty esters and cosolvents," *Fluid Phase Equilib.*, vol. 266, no. 1–2, pp. 31–37, 2008.

[11] Z. Tang, Z. Du, E. Min, L. Gao, T. Jiang, and B. Han, "Phase equilibria of methanol – triolein system at elevated temperature and pressure," vol. 239, pp. 8–11, 2006.

[12] A. Demirbas, "Biodiesel Production via Rapid Transesterification," *Energy Sources , Part A Recover. , Util. , Environ. Eff.*, vol. 7036, no. March 2015, pp. 37–41, 2008.

[13] R. Sawangkeaw, K. Bunyakiat, and S. Ngamprasertsith, “A review of laboratory-scale research on lipid conversion to biodiesel with supercritical methanol (2001-2009),” *J. Supercrit. Fluids*, vol. 55, no. 1, pp. 1–13, 2010.

[14] G. Madras, C. Kolluru, and R. Kumar, “Synthesis of biodiesel in supercritical fluids,” *Fuel*, vol. 83, no. 14-15 SPEC. ISS., pp. 2029–2033, 2004.

[15] H. He, T. Wang, and S. Zhu, “Continuous production of biodiesel fuel from vegetable oil using supercritical methanol process,” *Fuel*, vol. 86, no. 3, pp. 442–447, 2007.

[16] H. He, S. Sun, T. Wang, and S. Zhu, “Transesterification kinetics of soybean oil for production of biodiesel in supercritical methanol,” *JAOCS, J. Am. Oil Chem. Soc.*, vol. 84, no. 4, pp. 399–404, 2007.

[17] A. Demirbas, “Biodiesel from vegetable oils via transesterification in supercritical methanol,” *Energy Convers. Manag.*, vol. 43, pp. 2349–2356, 2002.

[18] a. Demirbas, “Biodiesel from Vegetable Oils with MgO Catalytic Transesterification in Supercritical Methanol,” *Energy Sources, Part A Recover. Util. Environ. Eff.*, vol. 30, no. 17, pp. 1645–1651, 2008.

[19] W. Cao, H. Han, and J. Zhang, “Preparation of biodiesel from soybean oil using supercritical methanol and co-solvent,” *Fuel*, vol. 84, pp. 347–351, 2005.

[20] G. Vicente, M. Martínez, and J. Aracil, “Integrated biodiesel production: A comparison of different homogeneous catalysts systems,” *Bioresour. Technol.*, vol. 92, no. 3, pp. 297–305, 2004.

[21] M. Balat, “Biodiesel Fuel Production from Vegetable Oils via Supercritical Ethanol Transesterification,” *Energy Sources, Part A Recover. Util. Environ. Eff.*, vol. 30, no. 5, pp. 429–440, 2008.

[22] A. H. West, D. Posarac, and N. Ellis, “Assessment of four biodiesel production processes using HYSYS.Plant,” *Bioresour. Technol.*, vol. 99, no. 14, pp. 6587–6601, 2008.

[23] U. Schuchardt, R. M. Vargas, and G. Gelbard, “Transesterification of soybean oil catalyzed by alkylguanidines heterogenized on different substituted polystyrenes,” *J. Mol. Catal. A Chem.*, vol. 109, no. 1, pp. 37–44, 1996.

[24] K. G. Georgogianni, A. K. Katsoulidis, P. J. Pomonis, G. Manos, and M. G. Kontominas, “Transesterification of rapeseed oil for the production of biodiesel using homogeneous and heterogeneous catalysis,” *Fuel Process. Technol.*, vol. 90, no. 7–8, pp. 1016–1022, 2009.

[25] S. Gryglewicz, “Rapeseed oil methyl esters preparation using heterogeneous catalysts,” vol. 70, no. February, 1999.

[26] N. Shibasaki-Kitakawa, H. Honda, H. Kuribayashi, T. Toda, T. Fukumura, and T. Yonemoto, "Biodiesel production using anionic ion-exchange resin as heterogeneous catalyst," *Bioresour. Technol.*, vol. 98, no. 2, pp. 416–421, 2007.

[27] S. N. Csernica and J. T. Hsu, "The phase behavior effect on the kinetics of transesterification reactions for biodiesel production," *Ind. Eng. Chem. Res.*, vol. 51, no. 18, pp. 6340–6349, 2012.

[28] H. Noureddini and D. Zhu, "Kinetics of Transesterification of Soybean Oil," vol. 74, no. 11, pp. 1457–1463, 1997.

[29] O. S. Stamenkovic, M. L. Lazic, Z. B. Todorovic, V. B. Veljkovic, and D. U. Skala, "The effect of agitation intensity on alkali-catalyzed methanolysis of sunflower oil," vol. 98, pp. 2688–2699, 2007.

[30] K. Huang, Q. Xu, S. Zhang, Z. Ren, and Y. Yan, "Multi-Step controlled kinetics of the transesterification of crude soybean oil with methanol by Mg(OCH3)2," *Chem. Eng. Technol.*, vol. 32, no. 10, pp. 1595–1604, 2009.

[31] X. Liu, X. Piao, Y. Wang, and S. Zhu, "Model study on transesterification of soybean oil to biodiesel with methanol using solid base catalyst," *J. Phys. Chem. A*, vol. 114, no. 11, pp. 3750–3755, 2010.

[32] G. Vicente, M. Martínez, J. Aracil, and A. Esteban, "Kinetics of sunflower oil methanolysis," *Ind. Eng. Chem. Res.*, vol. 44, no. 15, pp. 5447–5454, 2005.

[33] S. B. Glisic and A. M. Orlovic, "Modelling of non-catalytic biodiesel synthesis under sub and supercritical conditions: The influence of phase distribution," *J. Supercrit. Fluids*, vol. 65, pp. 61–70, 2012.

[34] D. G. B. Boocock, S. K. Konar, V. Mao, and H. Sidi, "FAST ONE-PHASE OIL-RICH PROCESSES FOR THE PREPARATION OF VEGETABLE OIL METHYL ESTERS," vol. 11, no. 1, 1996.

[35] D. G. B. Boocock, S. K. Konar, V. Mao, C. Lee, and S. Buligan, "Fast formation of high-purity methyl esters from vegetable oils," *JAOCS, J. Am. Oil Chem. Soc.*, vol. 75, no. 9, pp. 1167–1172, 1998.

[36] D. E. Lopez, J. G. Goodwin Jr, D. A. Bruce, and E. Lotero, "Transesterification of triacetin with methanol on solid acid and base catalysts," vol. 295, pp. 97–105, 2005.

[37] D. Kusdiana and S. Saka, "Kinetics of transesterification in rapeseed oil to biodiesel fuel as treated in supercritical methanol," *Fuel*, vol. 80, no. 5, pp. 693–698, 2001.

[38] P. D. Patil, V. G. Gude, and S. Deng, "Transesterification of Camelina Sativa Oil using Supercritical and Subcritical Methanol with Cosolvents," no. 12, pp. 746–751, 2010.

[39] I. A. Mohammed-Dabo, M. S. Ahmad, A. Hamza, K. Muazu, and A. Aliyu, “Cosolvent transesterification of Jatropha curcas seed oil,” *J. Pet. Technol. Altern. Fuels*, vol. 3, no. 4, pp. 42–51, 2012.

[40] Y. Alhassan, N. Kumar, I. M. Bugaje, H. S. Pali, and P. Kathkar, “Co-solvents transesterification of cotton seed oil into biodiesel: Effects of reaction conditions on quality of fatty acids methyl esters,” *Energy Convers. Manag.*, vol. 84, pp. 640–648, 2014.

[41] H. Kuramochi, K. Maeda, M. Osako, K. Nakamura, and S. I. Sakai, “Superfast transesterification of triolein using dimethyl ether and a method for high-yield transesterification,” *Ind. Eng. Chem. Res.*, vol. 47, no. 24, pp. 10076–10079, 2008.

[42] J. Maçaira, A. Santana, F. Recasens, and M. Angeles Larrayoz, “Biodiesel production using supercritical methanol/carbon dioxide mixtures in a continuous reactor,” *Fuel*, vol. 90, no. 6, pp. 2280–2288, 2011.

[43] M. B. García-Jarana, J. Sánchez-Oneto, J. R. Portela, L. Casas, C. Mantell, and E. Martínez de la Ossa, “Use of supercritical methanol/carbon dioxide mixtures for biodiesel production,” *Korean J. Chem. Eng.*, vol. 33, no. 8, pp. 2342–2349, 2016.

[44] L. Soh, J. Curry, E. J. Beckman, and J. B. Zimmerman, “Effect of System Conditions for Biodiesel Production via Transesterification Using Carbon Dioxide-Methanol Mixtures in the Presence of a Heterogeneous Catalyst,” *ACS Sustain. Chem. Eng.*, no. 2, pp. 387–395, 2014.

[45] B. Freedman, R. O. Butterfield, and E. H. Pryde, “Reaction Conditions Employed in Kinetic Studies,” *Anal. Soybean Oil by CGC*, vol. 63, no. 10, pp. 1375–1380, 1986.

[46] Y. Maeda *et al.*, “New technology for the production of biodiesel fuel,” *Green Chem.*, vol. 13, no. 5, pp. 1124–1128, 2011.

[47] S. B. Glišić and D. U. Skala, “Phase transition at subcritical and supercritical conditions of triglycerides methanolysis,” *J. Supercrit. Fluids*, vol. 54, no. 1, pp. 71–80, 2010.

[48] J. Yin, M. Xiao, and J. Song, “Biodiesel from soybean oil in supercritical methanol with co-solvent,” vol. 49, pp. 908–912, 2008.

[49] M. A. Ribeiro, “Solubilities of Triolein in Supercritical,” pp. 1188–1192, 1995.

[50] P. Maheshwari, Z. L. Nikolov, T. M. White, and R. Hartel, “Solubility of Fatty Acids in Supercritical Carbon Dioxide,” vol. 69, no. 11, pp. 1069–1076, 1992.

[51] W. B. Nilsson, E. J. Gauglitz, and J. K. Hudson, “Solubilities of Methyl Oleate , Oleic Acid , Oleyl Glycerols , and Oleyl Glycerol Mixtures in Supercritical Carbon Dioxide,” vol. 68, no. 2, pp. 87–91, 1991.

[52] I. Ashour and H. Hammam, “Equilibrium Solubility of Pure Mono-, Di-, and Trilaurin in Supercritical Carbon Dioxide-Experimental Measurements and Model Prediction,” pp. 3–8, 1993.

[53] T. Bamberger, J. C. Erickson, C. L. Cooney, and S. K. Kumar, “Measurement and model prediction of solubilities of pure fatty acids, pure triglycerides, and mixtures of triglycerides in supercritical carbon dioxide,” *J. Chem. Eng. Data*, vol. 33, no. 3, pp. 327–333, 1988.

[54] H. Inomata, T. Kondo, S. Hirohama, K. Arai, Y. Suzuki, and M. Konno, “Vapour-Liquid Equilibria for Binary Mixtures of Carbon Dioxide and Fatty acid Methil Esters,” *Fluid Phase Equilib.*, vol. 46, pp. 41–52, 1989.

[55] M. Zou, Z. R. Yu, P. Kashulines, and S. S. H. Rizvi, “Fluid-Liquid Phase Equilibria of Fatty Acids and Fatty Acid Methyl Esters in Supercritical Carbon Dioxide,” pp. 23–28, 1990.

[56] C.-M. J. Chang, M.-S. Lee, B.-C. Li, and P.-Y. Chen, “Vapor-liquid equilibria and densities of CO2 with four unsaturated fatty acid esters at elevated pressures,” *Fluid Phase Equilib.*, vol. 233, no. 1, pp. 56–65, 2005.

[57] R. Bharath, H. Inomata, and K. Arai, “Vapor-liquid equilibria for binary mixtures of carbon dioxide and fatty acid ethyl esters,” *Fluid Phase Equilib.*, vol. 50, pp. 315–327, 1989.

[58] W. H. Hwu, J. S. Cheng, K. W. Cheng, and Y. P. Chen, “Vapor-liquid equilibrium of carbon dioxide with ethyl caproate, ethyl caprylate and ethyl caprate at elevated pressures,” *J. Supercrit. Fluids*, vol. 28, no. 1, pp. 1–9, 2004.

[59] C. J. Chang, K.-L. Chiu, and C.-Y. Day, “A new apparatus for the determination of P–x–y diagrams and Henry’s constants in high pressure alcohols with critical carbon dioxide,” *J. Supercrit. Fluids*, vol. 12, pp. 223–237, 1998.

[60] A. V. M. Nunes, G. V. S. M. Carrera, V. Najdanovic-Visak, and M. Nunes Da Ponte, “Solubility of CO2 in glycerol at high pressures,” *Fluid Phase Equilib.*, vol. 358, pp. 105–107, 2013.

[61] Y. Medina-Gonzalez, T. Tassaing, S. Camy, and J.-S. Condoret, “Phase equilibrium of the CO2/glycerol system: Experimental data by in situ FT-IR spectroscopy and thermodynamic modeling,” *J. Supercrit. Fluids*, vol. 73, pp. 97–107, 2013.

[62] C. A. Lockemann, “Interfacial tensions of the binary systems carbon dioxide-oleic acid, carbon dioxide-methyl myristate, and carbon dioxide-methyl palmitate and of the ternary system carbon dioxide-methyl myristate-methyl palmitate at high pressures,” *Chem. Eng. Process.*, vol. 33, no. 4, pp. 193–198, 1994.

[63] S. Glisic, O. Montoya, A. Orlovic, and D. Sakala, “Vapor – liquid equilibria of triglycerides – methanol mixtures and their influence on the biodiesel synthesis under supercritical conditions of methanol,” vol. 72, no. 1, pp. 13–27, 2007.

[64] C. Silva, L. Soh, A. Barberio, J. Zimmerman, and W. D. Seider, “Phase equilibria of triolein to biodiesel reactor systems,” *Fluid Phase Equilib.*, vol. 409, pp. 171–192, 2016.

[65] J. Chrastill, “Solubility of Solids and Liquids in Supercritical Gases,” *J. Chem. Phys.*, vol. 86, no. 15, pp. 3016–3021, 1982.

[66] P. Hegel, G. Mabe, S. Pereda, and E. A. Brignole, “Phase Transitions in a Biodiesel Reactor Using Supercritical Methanol,” pp. 6360–6365, 2007.

[67] L. J. Florusse, T. Fornari, S. B. Bottini, and C. J. Peters, “Phase behavior of carbon dioxide - Low-molecular weight triglycerides binary systems: Measurements and thermodynamic modeling,” *J. Supercrit. Fluids*, vol. 31, no. 2, pp. 123–132, 2004.

[68] R. Bharath, S. Yamane, H. Inomata, T. Adschiri, and K. Arai, “Phase Equilibria of Supercritical CO2 - Fatty oil Component,” vol. 83, pp. 183–192, 1993.

[69] C. Borch-Jensen and J. Mollerup, “Phase equilibria of carbon dioxide and tricaprylin,” *J. Supercrit. Fluids*, vol. 10, pp. 87–93, 1997.

[70] C.-C. Chen, C. Chang, and P. Yang, “Vapor-liquid equilibria of carbon dioxide with linoleic acid, [alpha]-tocopherol and triolein at elevated pressures,” *Fluid Phase Equilib.*, vol. 175, no. 1–2, pp. 107–115, 2000.

[71] R. Bharath, H. Inomata, T. Adschiri, and K. Arai, “Phase equilibrium study for the separation and fractionation of fatty oil components using supercritical carbon dioxide,” *Fluid Phase Equilib.*, vol. 81, pp. 307–320, 1992.

[72] D. Geana and R. Steiner, “Calculation of phase equilibrium in supercritical extraction of C54 triglyceride (rapeseed oil),” *J. Supercrit. Fluids*, vol. 8, no. 2, pp. 107–118, 1995.

[73] M. P. Fernández-Ronco, M. Cismondi, I. Gracia, A. De Lucas, and J. F. Rodríguez, “High-pressure phase equilibria of binary and ternary mixtures of carbon dioxide, triglycerides and free fatty acids: Measurement and modeling with the GC-EOS,” *Fluid Phase Equilib.*, vol. 295, no. 1, pp. 1–8, 2010.

[74] W. Weber, S. Petkov, and G. Brunner, “Vapour – liquid-equilibria and calculations using the Redlich – Kwong-Aspen-equation of state for tristearin , tripalmitin , and triolein in CO 2 and propane,” pp. 695–706, 1999.

[75] P. Münüklü, F. Wubbolts, T. W. De Loos, and P. J. Jansens, “The phase behavior of systems of supercritical CO2 or propane with edible fats and a wax,” *J. Supercrit. Fluids*, vol. 39, no. 1, pp. 1–5, 2006.

[76] D. S. Negi, F. Sobotka, T. Kimmel, and R. Schoma, “Liquid - Liquid Phase Equilibrium in Glycerol - Methanol - Methyl Oleate and Glycerol - Monoolein - Methyl Oleate Ternary Systems,” *Ind. Eng. Chem. Resour.*, vol. 45, pp. 3693–3696, 2006.

[77] S. Shiozawa, A. J. A. Meirelles, and E. A. C. Batista, “Liquid-liquid equilibrium data for systems important in biodiesel production, involving vegetable oils + ethyl esters + monoacylglycerols and diacylglycerols + anhydrous ethanol, at 303.15 and 318.15 K,” *Fuel*, vol. 180, pp. 333–342, 2016.

[78] M. C. Ferreira, L. C. B. A. Bessa, S. Shiozawa, A. J. A. Meirelles, and E. A. C. Batista, “Liquid-liquid equilibrium of systems containing triacylglycerols (canola and corn oils), diacylglycerols, monoacylglycerols, fatty acids, ester and ethanol at T/K=303.15 and 318.15,” *Fluid Phase Equilib.*, vol. 404, pp. 32–41, 2015.

[79] P. Raveendran and S. L. Wallen, “Cooperative C-H0 ⋯ O hydrogen bonding in CO2-Lewis base complexes: Implications for solvation in supercritical CO2,” *J. Am. Chem. Soc.*, vol. 124, no. 42, pp. 12590–12599, 2002.

[80] H. Nishiumi, T. Arai, and K. Takeuchi, “Generalization of the binary interaction parameter of the Peng-Robinson equation of state by component family,” *Fluid Phase Equilib.*, vol. 42, no. C, pp. 43–62, 1988.

[81] O. Ferreira, E. A. Brignole, and E. A. Macedo, “Modelling of phase equilibria for associating mixtures using an equation of state,” *J. Chem. Thermodyn.*, vol. 36, no. 12, pp. 1105–1117, 2004.

[82] A. E. Andreatta, L. M. Casa, P. Hegel, S. B. Bottini, and E. A. Brignole, “Phase Equilibria in Ternary Mixtures of Methyl Oleate , Glycerol , and Methanol,” pp. 5157–5164, 2008.

[83] M. B. Oliveira, A. R. R. Teles, A. J. Queimada, and J. A. P. Coutinho, “Phase equilibria of glycerol containing systems and their description with the Cubic-Plus-Association (CPA) Equation of State,” *Fluid Phase Equilib.*, vol. 280, no. 1–2, pp. 22–29, 2009.

[84] M. B. Oliveira, S. I. Miguel, A. J. Queimada, and J. A. P. Coutinho, “Phase equilibria of ester + alcohol systems and their description with the cubic-plus-association equation of state,” *Ind. Eng. Chem. Res.*, vol. 49, no. 7, pp. 3452–3458, 2010.

[85] J. Gross and G. Sadowski, “Perturbed-Chain SAFT: An Equation of State Based on a Pertubation Theory of Chain Molecules,” *Ind. Eng. Chem. Res*, no. 40, pp. 1244–1260, 2001.

[86] F. Tumakaka, J. Gross, and G. Sadowski, “Modeling of polymer phase equilibria using Perturbed-Chain SAFT,” *Fluid Phase Equilib.*, vol. 194–197, pp. 541–551, 2002.

[87] K. E. Gubbins and C. H. Twu, “Thermodynamics of polyatomic fluid mixtures—I theory,” *Chem. Eng. Sci.*, vol. 33, no. 7, pp. 863–878, 1978.

[88] C. H. Twu and K. E. Gubbins, “Thermodynamics of Polyatomic Fluids Mixtures-II,” *Chem. Eng. Sci.*, vol. 33, no. 2, pp. 879–887, 1977.

[89] C. H. Twu, K. E. Gubbins, and C. G. Gray, “Thermodynamics of mixtures of nonspherical molecules. III. Fluid phase equilibria and critical loci,” *J. Chem. Phys.*, vol. 64, no. 12, pp. 5186–5197, 1976.

[90] J. Vrabec and J. Gross, “Vapor - Liquid Equilibria Simulation and an Equation of State Contribution for Dipole - Quadrupole Interactions,” pp. 51–60, 2008.

[91] P. K. Jog, W. G. Chapman, “Application of Wertheim’s thermodynamic perturbation theory to dipolar hard sphere chains,” *Mol. Phys.*, vol. 97, no. 3, pp. 307–319, 1999.

[92] M. L. Corazza, W. A. Fouad, and W. G. Chapman, “PC-SAFT predictions of VLE and LLE of systems related to biodiesel production,” *Fluid Phase Equilib.*, vol. 416, pp. 130–137, 2016.

[93] D. Nguyen-Huynh, J.-P. Passarello, P. Tobaly, and J.-C. de Hemptinne, “Modeling Phase Equilibria of Asymmetric Mixtures Using a Group-Contribution SAFT (GC-SAFT) with a k ij Correlation Method Based on London’s Theory. 1. Application to CO 2 + n -Alkane, Methane + n -Alkane, and Ethane + n -Alkane Systems,” *Ind. Eng. Chem. Res.*, vol. 47, no. 22, pp. 8847–8858, 2008.

[94] D. Nguyen Huynh, T. Nguyen Thi, and S. T. Van Dinh, “Predicting the temperature / pressure dependent density of biodieselfuels,” *Petrovietnam*, vol. 10, pp. 46–58, 2012.

[95] E. K. Karakatsani and I. G. Economou, “Perturbed chain-statistical associating fluid theory extended to dipolar and quadrupolar molecular fluids,” *J. Phys. Chem. B*, vol. 110, no. 18, pp. 9252–9261, 2006.

[96] D. NguyenHuynh, A. Falaix, J. P. Passarello, P. Tobaly, and J. C. de Hemptinne, “Predicting VLE of heavy esters and their mixtures using GC-SAFT,” *Fluid Phase Equilib.*, vol. 264, no. 1–2, pp. 184–200, 2008.

[97] D. NguyenHuynh, J. P. Passarello, J. C. de Hemptinne, F. Volle, and P. Tobaly, “Simultaneous modeling of VLE, LLE and VLLE of CO2 and 1, 2, 3 and 4 alkanol containing mixtures using GC-PPC-SAFT EOS,” *J. Supercrit. Fluids*, vol. 95, pp. 146–157, 2014.

[98] A. Barreau, I. Brunella, J. C. De Hemptinne, V. Coupard, X. Canet, and F. Rivollet, “Measurements of liquid-liquid equilibria for a methanol + glycerol + methyl oleate system and prediction using group contribution statistical associating fluid theory,” *Ind. Eng. Chem. Res.*, vol. 49, no. 12, pp. 5800–5807, 2010.

[99] E. S. Perry, W. H. Weber, and B. F. Daubert, “Vapor Pressures of Phlegmatic Liquids. I. Simple and Mixed Triglycerides,” 1949.

[100] R. Ceriani and A. J. A. Meirelles, “Predicting vapor-liquid equilibria of fatty systems,” *Fluid Phase Equilib.*, vol. 215, no. 2, pp. 227–236, 2004.

[101] L. Zong, S. Ramanathan, and C. Chen, "Fragment-Based Approach for Estimating Thermophysical Properties of Fats and Vegetable Oils for Modeling Biodiesel Production Processes," *Ind. Eng. Chem. Res*, vol. 49, pp. 876–886, 2010.

[102] I. Gracia, M. T. García, J. F. Rodríguez, M. P. Fernández, and A. de Lucas, "Modelling of the phase behaviour for vegetable oils at supercritical conditions," *J. Supercrit. Fluids*, vol. 48, no. 3, pp. 189–194, 2009.

[103] A. M. Almagrbi, S. B. Glisic, and A. M. Orlovic, "The phase equilibrium of triglycerides and ethanol at high pressure and temperature: The influence on kinetics of ethanolysis," *J. Supercrit. Fluids*, vol. 61, pp. 2–8, 2012.

[104] S. B. Bottini, T. Fornari, and E. A. Brignole, "Phase equilibrium modelling of triglycerides with near critical solvents," *Fluid Phase Equilib.*, vol. 158–160, pp. 211–218, 1999.

[105] T. Fornari, D. Tenllado, C. Torres, and G. Reglero, "Supercritical Phase Equilibria Modeling of Glyceride Mixtures and Carbon Dioxide Using the Group Contribution EoS," *J. Thermodyn.*, vol. 2011, pp. 1–9, 2011.

[106] S. Espinosa, T. Fornari, S. B. Bottini, and E. A. Brignole, "Phase equilibria in mixtures of fatty oils and derivatives with near critical fluids using the GC-EOS model," *J. Supercrit. Fluids*, vol. 23, no. 2, pp. 91–102, 2002.

[107] E. J. Hernández, P. Luna, E. Ibáñez, R. P. Stateva, and T. Fornari, "Solubility of a Multicomponent Glyceride Mixture in SC-CO 2 : Experimental Determination and Correlation."

[108] A. Dominik and W. G. Chapman, "Thermodynamic model for branched polyolefins using the PC-SAFT equation of state," *Macromolecules*, vol. 38, no. 26, pp. 10836–10843, 2005.

[109] F. M. Vargas Arreola, "Modeling of Asphaltene Precipitation and Arterial Deposition," Rice University, 2009.

[110] Y. Peng, K. D. Goff, M. C. Dos Ramos, and C. McCabe, "Predicting the phase behavior of polymer systems with the GC-SAFT-VR approach," *Ind. Eng. Chem. Res.*, vol. 49, no. 3, pp. 1378–1394, 2010.

[111] D. NguyenHuynh, J. P. Passarello, J. C. de Hemptinne, and P. Tobaly, "Extension of polar GC-SAFT to systems containing some oxygenated compounds: Application to ethers, aldehydes and ketones," *Fluid Phase Equilib.*, vol. 307, no. 2, pp. 142–159, 2011.

[112] W. G. Chapman, K. E. Gubbins, G. Jackson, and M. Radosz, "New reference equation of state for associating liquids," *Ind. Eng. Chem. Res.*, vol. 29, no. 8, pp. 1709–1721, 1990.

[113] M. S. Wertheim, "Fluids with Highly Directional Attractive Forces . I . Statistical Thermodynamics," vol. 35, no. 1, pp. 19–34, 1984.

[114] M. S. Wertheim, “Fluids with Highly Directional Attractive Forces . II . Thermodynamic Perturbation Theory and Integral Equations,” vol. 35, pp. 35–47, 1984.

[115] M. S. Wertheim, “Fluids with Highly Directional Attractive Forces . III . Multiple Attraction Sites,” vol. 42, pp. 459–476, 1986.

[116] M. S. Wertheim, “Fluids with Highly Directional Attractive Forces . IV . Equilibrium Polymerization,” *J. Stat. Phys.*, vol. 42, pp. 477–492, 1986.

[117] J. A. Barker and D. Henderson, “Perturbation Theory and Equation of State for Fluids. II. A Successful Theory of Liquids,” *J. Chem. Phys.*, vol. 47, no. 4714, 1967.

[118] P. K. Jog, S. G. Sauer, J. Blaesing, and W. G. Chapman, “Application of Dipolar Chain Theory to the Phase Behavior of Polar Fluids and Mixtures,” *Ind. Eng. Chem. Res.*, vol. 40, no. 21, pp. 4641–4648, 2001.

[119] J. Gross, “An Equation-of-State Contribution for Polar Components : Quadrupolar Molecules,” *AIChE J.*, vol. 51, no. 9, pp. 2556–2568, 2005.

[120] J. Gross, “An Equation-of-State Contribution for Polar Components : Dipolar Molecules,” vol. 52, no. 3, 2006.

[121] D. NguyenHuynh, J. P. Passarello, P. Tobaly, and J. C. de Hemptinne, “Application of GC-SAFT EOS to polar systems using a segment approach,” *Fluid Phase Equilib.*, vol. 264, no. 1–2, pp. 62–75, 2008.

[122] S. Tamouza, J.-P. Passarello, P. Tobaly, and J.-C. de Hemptinne, “Group contribution method with SAFT EOS applied to vapor liquid equilibria of various hydrocarbon series,” *Fluid Phase Equilib.*, vol. 222–223, no. 0, pp. 67–76, 2004.

[123] E. J. Henley, *Material and energy balance computations [by] Ernest J. Henley [and] Edward M. Rosen*. New York: Wiley, 1969.

[124] M. L. Michelsen, “The isothermal flash problem. Part I. Stability,” *Fluid Phase Equilib.*, vol. 9, no. 1, pp. 1–19, 1982.

[125] M. Ma, S. Chen, and J. Abedi, “Predicting the multiphase equilibrium and density of bitumen with C 2 H 6 , C 3 H 8 and CO 2 using the simplified PC-SAFT Equation of State,” vol. 181, pp. 652–659, 2016.

[126] M. L. Michelsen, “The isothermal flash problem. Part II. Phase split calculation.,” *Fluid Phase Equilib.*, vol. 9, pp. 21–40, 1982.

[127] M. L. Michelsen, “Saturation Point Calculations,” *Fluid Phase Equilib.*, vol. 23, pp. 181–192, 1985.

[128] T. A. Hoefling, R. M. Enick, and E. J. Beckman, “Microemulsions in near-critical and supercritical carbon dioxide,” *J. Phys. Chem.*, vol. 95, no. 19, pp. 7127–7129, 1991.

[129] L. F. Pinto, P. M. Ndiaye, L. P. Ramos, and M. L. Corazza, "Phase equilibrium data of the system CO2+glycerol+methanol at high pressures," *J. Supercrit. Fluids*, vol. 59, pp. 1–7, 2011.

[130] L. F. Pinto, D. I. S. da Silva, F. Rosa da Silva, L. P. Ramos, P. M. Ndiaye, and M. L. Corazza, "Phase equilibrium data and thermodynamic modeling of the system (CO2+biodiesel+methanol) at high pressures," *J. Chem. Thermodyn.*, vol. 44, no. 1, pp. 57–65, 2012.

[131] O. A. S. Araujo, P. M. Ndiaye, L. P. Ramos, and M. L. Corazza, "Phase behavior measurement for the system CO 2 + glycerol + ethanol at high pressures," *J. Supercrit. Fluids*, vol. 62, pp. 41–46, 2012.

[132] H. H. Ku, "Notes on the use of propagation of error formulas," *J. Res. Natl. Bur. Stand. Sect. C Eng. Instrum.*, vol. 70C, no. 4, p. 263, 1966.

[133] M. Mourah, D. NguyenHuynh, J. P. Passarello, J. C. de Hemptinne, and P. Tobaly, "Modelling LLE and VLE of methanol+n-alkane series using GC-PC-SAFT with a group contribution kij," *Fluid Phase Equilib.*, vol. 298, no. 1, pp. 154–168, 2010.

[134] S. H. Huang and M. Radosz, "Equation of state for small, large, polydisperse and associating molecules," *Ind. Eng. Chem. Res.*, vol. 29, pp. 2284–2294, 1990.

[135] J. P. Wolbach and S. I. Sandler, "Using Molecular Orbital Calculations To Describe the Phase Behavior of Hydrogen-Bonding Fluids †," *Ind. Eng. Chem. Res.*, vol. 36, no. 10, pp. 4041–4051, 1997.

[136] M. Yarrison and W. G. Chapman, "A systematic study of methanol + n-alkane vapor-liquid and liquid-liquid equilibria using the CK-SAFT and PC-SAFT equations of state," *Fluid Phase Equilib.*, vol. 226, no. 1–2, pp. 195–205, 2004.

[137] P. C. V. Tybjerg, G. M. Kontogeorgis, M. L. Michelsen, and E. H. Stenby, "Phase equilibria modeling of methanol-containing systems with the CPA and sPC-SAFT equations of state," *Fluid Phase Equilib.*, vol. 288, no. 1–2, pp. 128–138, 2010.

[138] J. C. De Hemptinne, P. Mougin, A. Barreau, and L. Ruffine, "Application to Petroleum Engineering of Statistical Thermodynamics – Based Equations of State," vol. 61, no. 3, pp. 363–386, 2006.

[139] A. Barreau, I. Brunella, J. De Hemptinne, V. Coupard, X. Canet, and F. Rivollet, "Measurements of Liquid - Liquid Equilibria for a Methanol + Glycerol + Methyl Oleate System and Prediction Using Group Contribution Statistical Associating Fluid Theory," *Ind. Eng. Chem. Res.*, pp. 5800–5807, 2010.

[140] AIChE, "DIPPR." [Online]. Available: https://www.aiche.org/dippr/events-products/801-database.

[141] J. J. McDuffie, G. E.; Forbes, J. W.; Madigosky, W. M.; Von Bretzel, "Density and Compressibility of Four Higher Alcohols for Pressures to 2800 Kg . per Sq . Cm .," *J. Chem. Eng. Data*, pp. 176–180, 1968.

[142] Y. Shimoyama, T. Abeta, L. Zhao, and Y. Iwai, "Measurement and calculation of vapor-liquid equilibria for methanol + glycerol and ethanol + glycerol systems at 493-573 K," *Fluid Phase Equilib.*, vol. 284, no. 1, pp. 64–69, 2009.

[143] J. G. Veneral *et al.*, "Thermophysical properties of biodiesel and related systems. Part I. Vapour-liquid equilibrium at low pressures of binary and ternary systems involving methanol, ethanol, glycerol, water and NaCl," *J. Chem. Thermodyn.*, vol. 58, pp. 398–404, 2013.

[144] M. L. Corazza, W. A. Fouad, and W. G. Chapman, "Application of molecular modeling to the vapor – liquid equilibrium of alkyl esters (biodiesel) and alcohols systems," vol. 161, pp. 34–42, 2015.

[145] L. F. Zubeir, C. Held, G. Sadowski, and M. C. Kroon, "PC-SAFT Modeling of CO_2 Solubilities in Deep Eutectic Solvents," *J. Phys. Chem. B*, vol. 120, no. 9, pp. 2300–2310, 2016.

[146] C. A. Perakis, E. C. Voutsas, K. G. Magoulas, and D. P. Tassios, "Thermodynamic modeling of the water + acetic acid + CO2system: The importance of the number of association sites of water and of the nonassociation contribution for the CPA and SAFT-type models," *Ind. Eng. Chem. Res.*, vol. 46, no. 3, pp. 932–938, 2007.

[147] O. A. S. ARAÚJO, "Equilíbrio De Fases Dos Sistemas Co2 + Biodiesel + Etanol E Co2 + Glicerol + Etanol a Altas Pressões," *Univ. Fed. DO PARANÁ,CURITIBA*, pp. 1–74, 2012.

[148] Y. Shimoyama, Y. Iwai, B. S. Jin, T. Hirayama, and Y. Arai, "Measurement and correlation of vapor-liquid equilibria for methanol + methyl laurate and methanol + methyl myristate systems near critical temperature of methanol," *Fluid Phase Equilib.*, vol. 257, no. 2, pp. 217–222, 2007.

[149] Y. Shimoyama, Y. Iwai, T. Abeta, and Y. Arai, "Measurement and correlation of vapor – liquid equilibria for ethanol + ethyl laurate and ethanol + ethyl myristate systems near critical temperature of ethanol," vol. 264, pp. 228–234, 2008.

[150] R. Coelho, P. G. Dos Santos, M. R. Mafra, L. Cardozo-Filho, and M. L. Corazza, "(Vapor + liquid) equilibrium for the binary systems {water + glycerol} and {ethanol + glycerol, ethyl stearate, and ethyl palmitate} at low pressures," *J. Chem. Thermodyn.*, vol. 43, no. 12, pp. 1870–1876, 2011.

[151] N. Garrido, O. Ferreira, R. Lugo, J.-C. Hemptinne, M. E Macedo, and S. Bottini, "A-UNIFAC Modeling of Binary and Multicomponent Phase Equilibria of Fatty Esters+Water+Methanol+Glycerol," 2018.

[152] E. F. Andrade, L. Igarashi-Mafra, M. R. Mafra, and M. L. Corazza, "(Liquid + liquid) equilibrium for the system {ethyl stearate(1) + ethanol(2) + glycerol(3)}," *J. Chem. Thermodyn.*, vol. 47, pp. 213–218, 2012.

[153] G. R. Paranjpe and D. J. Davar, "DIELECTRIC PROPERTIES OF SOME ORGANIC SUBSTANCES," Bombay, 1938.

[154] W. Johnson, "Final Report on the Safety Assessment of Trilaurin , Triarachidin , Tribehenin , Tricaprin , Tricaprylin , Ricinoleate , and Glyceryl Stearate Diacetate," Washington DC, 2001.

[155] J. I. García, H. García-Marín, and E. Pires, "Glycerol based solvents: Synthesis, properties and applications," *Green Chem.*, vol. 16, no. 3, pp. 1007–1033, 2014.

[156] eThermo_Research_team, "Ethermo Thermodynamic & Transport Properties Caculation Platform," 2009. [Online]. Available: http://www.ethermo.us/.

[157] R. Stenutz, "STENUTZ," 2015. [Online]. Available: http://www.stenutz.eu/.

[158] G. Rodriguez and E. J. Beckman, "Modelling phase behavior of biodiesel related systems with CO2 using a polar version of PC-SAFT," *Fluid Phase Equilib.*, vol. 485, pp. 32–43, 2019.

[159] T. B. Nguyen, "THÈSE DE DOCTORAT DE L ' UNIVERSITÉ PIERRE ET MARIE CURIE NGUYEN Thanh Binh Représentation des charges oxygénées associées à la valorisation de la biomasse : définition de descripteurs (Representation of oxygenated fluids associated with biomass valorisa," *These Dr. Luniversite Pierre Marie Curie*, no. Ed 388, 2013.

[160] E. Brunner, "Fluid mixtures at high pressures I. Phase separation and critical phenomena of 10 binary mixtures of (a gas + methanol)," *J. Chem. Thermodyn.*, vol. 17, no. 7, pp. 671–679, Jul. 1985.

[161] A. Leu, S. Y. K. Chung, and D. B. Robinson, "The equilibrium phase properties of (carbon dioxide + methanol)," pp. 979–985, 1991.

[162] C. J. Chang, C.-Y. Day, C.-M. Ko, and K.-L. Chiu, "Densities and P-x-y diagrams for carbon dioxide dissolution in methanol, ethanol, and acetone mixtures," *Fluid Phase Equilib.*, vol. 131, pp. 243–258, 1997.

[163] G. Rodriguez and E. J. Beckman, "Modelling phase behavior of triglycerides, diglycerides and monoglycerides related to biodiesel transesterification in mixtures of alcohols and CO2 using a polar version of PC-SAFT," Manuscript submitted for publication, 2019.

[164] C. Secuianu, V. Feroiu, and D. Geană, "High-pressure phase equilibria for the carbon dioxide + methanol and carbon dioxide + isopropanol systems," *Rev. Chim.*, vol. 54, no. 11, 2003.

[165] T. M. Reed and K. E. Gubbins, “Applied statistical mechanics: thermodynamic and transport properties of fluids .” McGraw-Hill , New York , 1973.

[166] P. T. Cummings and G. Stell, “Statistical mechanical models of chemical reactions,” *Mol. Phys.*, vol. 51, no. 2, pp. 253–287, Feb. 1984.

[167] P. T. Cummings and G. Stell, “Statistical mechanical models of chemical reactions,” *Mol. Phys.*, vol. 55, no. 1, pp. 33–48, May 1985.

[168] Y. Chen and F. Mutelet, “Modeling the Solubility of Carbon Dioxide in Imidazolium-Based Ionic Liquids with the PC-SAFT Equation of State,” 2012.

[169] T. S. Reighard, S. T. Lee, and S. V. Olesik, “Determination of methanol/CO2 and acetonitrile/CO2 vapor-liquid phase equilibria using a variable-volume view cell,” *Fluid Phase Equilib.*, vol. 123, pp. 215–230, 1996.

[170] V. Roškar, R. A. Dombro, G. A. Prentice, C. R. Westgate, and M. A. McHugh, “Comparison of the dielectric behavior of mixtures of methanol with carbon dioxide and ethane in the mixture-critical and liquid regions,” *Fluid Phase Equilib.*, vol. 77, no. C, pp. 241–259, 1992.

[171] E. Brunner, W. Hultenschmidt, and G. Schlichtharle, “Fluid mixtures at high pressures IV . Isothermal phase equilibria in binary mixtures consisting of (methanol + hydrogen or nitrogen or methane or carbon monoxide or carbon dioxide),” 1987.